DIVIDE AND CONQUER: AN OSCILLATORY DIVISION OF LABOUR IN SERVICE OF EPISODIC MEMORY

by

BENJAMIN JAMES GRIFFITHS

A thesis submitted to the University of Birmingham

for the degree of

DOCTOR OF PHILOSOPHY

School of Psychology

College of Life and Environmental Sciences

The University of Birmingham

December 2019

ABSTRACT

Both oscillatory synchronisation and oscillatory desynchronisation underpin the formation and retrieval of episodic memories. This paradox begs the question: how can two polar opposite neural phenomena produce the same outcome? Here, we investigate this conundrum by presenting a series of empirical experiments that test the hypothesis that these two phenomena reflect a division of labour in service of episodic memory. We demonstrate that neocortical desynchrony correlates with enhanced information representation, while hippocampal synchrony stiches this information together into a coherent memory trace. Critically, we demonstrate that these processes interact. Neocortical desynchrony precedes and predicts hippocampal synchrony during episodic memory formation, while hippocampal synchrony precedes and predicts neocortical desynchrony during episodic memory retrieval. This thesis suggests that the interaction between neocortical desynchrony and hippocampal synchrony sits at the heart of the formation and retrieval of episodic memories, providing empirical resolution to the so-called synchronisation/desynchronisation conundrum.

ACKNOWLEDGEMENTS

This work could never have come to be without the support of magnificent network of people. I do not think I could ever find the words to express how grateful I am to have you all in my life. But still, one must try…

Firstly, many thanks to Simon Hanslmayr. I cannot imagine a better supervisor. Thank you for providing me with so many opportunities over the last five years. It has been a whole lot of fun, whether it was figuring out how to address a never-ending list of paper revisions, or those quiet mornings spent surfing in Huntington Beach. I also owe great thanks to Maria Wimber for your ever-insightful and thought-provoking suggestions. Every comment added a little extra shine to these works.

Thanks to Rodika Sokoliuk and Catarina Ferreira. You are two of the most incredible people I have ever I had the pleasure of knowing. The depth of your kindness and support continue to astound me to this day. A part of me did not want to finish this thesis simply so that I could spend more time in Birmingham with you.

Thanks to Charlotte Poulisse, Isotta Rigoni, Giulio Degano, Federica Meconi, Ross Wilson, Geoff Brookshire, Remi Gau, Kelly Garner and Chris Nolan for those countless hours spent climbing and/or lindy hopping. It was always the perfect way to escape the world of science.

Thanks to Marit Petzka, Casper Kerrén, Juan Linde-Domingo, Julia Lifanov, Sophie Watson, Consuelo Vidal, Verena Braun and many more I've met in the School of Psychology. It was wonderful to work (and more importantly, go to the pub) with such an amazing group of people whose mere presence would bring a smile to my face.

Thanks to my parents for the support you have given me throughout this endeavour. Heading back home for a curry on a Saturday evening never got old.

Lastly, thanks to the European Research Council and to those many participants and patients who consented to take part in these experiments. Without you, none of this work would have come to be.

TABLE OF CONTENTS

PUBLICATIONS AND CONTRIBUTIONS

A substantial portion of this thesis contains material that has been published in academic journals/books, presented at conferences, or posted on preprint servers. The text of these works has, on occasion, been adjusted to provide the thesis with a coherent narrative.

Chapter 1: Exerts of this chapter have been taken from a paper published by Lluís Fuentemilla and myself, and a book chapter in preparation by Sebastian Michelmann, Simon Hanslmayr and myself. The exerts that have been taken from these publications and included in this thesis were written by myself, with my co-authors providing feedback.

Chapter 2: Data was collected and analysed by myself. Simon Hanslmayr and Maria Wimber supervised all aspects of the project. Stephen Mayhew and Karen Mullinger supervised the collection of the EEG-fMRI recordings, and supervised the idiosyncrasies of EEG-fMRI analysis. João Jorge provided scripts to help analyse the EEG recordings. Ian Charest supervised the multivariate analysis of the fMRI data.

Chapter 3 and 4: Data was collected by Frederic Roux, Sebastian Michelmann, Mircea van der Plas, Luca Kolibius, and myself. Analysis of the video-word associate task was conducted by myself. Analysis of the face-place associate task was conducted by George Parish. Ramesh Chelvarajah, David T. Rollings, Vijay Sawlani, Hajo Hamer, Stephanie Gollwitzer, Gernot Kreiselmeyer cared for the patients. Simon Hanslmayr, Maria Wimber and Bernhard Staresina supervised.

Chapter 5: Data was collected by myself. María Carmen Martín-Buro pre-processed the data. All subsequent analysis was conducted by myself. Simon Hanslmayr and Bernhard Staresina supervised.

Journal Articles

Griffiths, B. J., Fuentemilla, L. (2019). Event conjunction: How the hippocampus integrates episodic memories across event boundaries. *Hippocampus*. doi: 10.1002/hipo.23161.

Griffiths, B. J., Parish, G., Roux, F., Michelmann, S., van der Plas, M., Kolibius, L. D., Rollings, D., Sawlani, D., Chelvarajah, R., Gollwitzer, S., Kreiselmeyer, G., Hamer, H., Staresina, B., Wimber, M., & Hanslmayr, S. (2019). Directional coupling of slow and fast hippocampal gamma with neocortical alpha/beta oscillations in human episodic memory. *Proceedings of the National Academy of Sciences*. doi: 10.1101/305698

Griffiths, B. J., Mayhew, S. D., Mullinger, K. J., Jorge, J., Charest, I., Wimber, M., & Hanslmayr, S. (accepted). Alpha/beta power decreases track the fidelity of stimulus-specific information. *eLife*.

Griffiths, B. J., Martín-Buro, M. C., Staresina, B. P., & Hanslmayr, S. (*in preparation*). Disentangling the roles of neocortical alpha/beta and hippocampal theta/gamma activity in human episodic memory

Book Chapters

Michelmann, S., Griffiths, B. J., & Hanslmayr, S. (*in preparation*). The role of alpha and beta oscillations in the human EEG during perception and memory processes. The Oxford Handbook on Time-Frequency Analyses.

Media

Griffiths, B. J., & Hanslmayr, S. (2019, October 22). How memories are formed and retrieved by the brain revealed in a new study. *The Conversation*. Retrieved from https://theconversation.com/.

Conference Proceedings

Griffiths, B. J., et al. (2019). Cognitive Computational Neuroscience. Berlin, Germany

Griffiths, B. J., et al. (2019). Royal Society Meeting on Memory Reactivation. Chicheley Hall, UK.

Griffiths, B. J., et al. (2018). Society for Neuroscience. San Diego, USA.

Griffiths, B. J., et al. (2018). Replay at Cardiff. Cardiff, UK.

Griffiths, B. J., et al. (2018). Learning and Memory. Huntington Beach, USA.

Griffiths, B. J., Hanslmayr S. (2017). International Conference for Cognitive Neuroscience. Amsterdam, The Netherlands.

Griffiths, B. J., et al. (2017). International Conference for Cognitive Neuroscience. Amsterdam, The Netherlands.

Griffiths, B. J., et al. (2017). Cutting EEG. Glasgow, UK.

Griffiths, B. J., et al. (2017). Neural Oscillations in Speech and Language Processing. Berlin, Germany.

Griffiths, B. J., et al. (2017). Memory Reactivation Workshop. Cardiff, UK.

Griffiths, B. J., et al. (2017). British Neuroscience Association. Birmingham, UK.

Griffiths, B. J., et al. (2017). Event Representations in Episodic and Semantic Memory Workshop. York, UK.

Griffiths, B. J., et al. (2016). Society for Neuroscience. San Diego, USA.

LIST OF FIGURES

LIST OF TABLES

LIST OF ABBREVIATIONS

ANOVA	analysis of variance
ATL	anterior temporal lobe
BCG	ballistocardiogram
BEM	boundary element model
BF	Bayes factor
BOLD	blood-oxygen level dependent
BUIC	Birmingham University Imaging Centre
CA1	cornu ammonis 1
CA3	cornu ammonis 3
CBU	Cognition and Brain Sciences Unit
cHPI	continuous head position indicator
CVM	cross-validated Mahalanobis
DBS	deep brain stimulation
ECG	electrocardiogram
EEG	electroencephalography
EOG	electrooculogram
EPI	echo-planar imaging
ERP	event-related potential
FDR	false discovery rate
FIR	finite impulse response
fMRI	functional magnetic resonance imaging
FWE	family-wise error
FWHM	full-width half-maximum
GLM	general linear model
HPI	head position indicator
HRF	hemodynamic response function
Hz	hertz
IED	inter-epileptical discharges
iEEG	intracranial electroencephalography
IIR	infinite impulse response
IRASA	irregular-resampling auto-spectral analysis
LCMV	linearly constrained minimum variance
LFP	local field potential
LTD	long-term depression
LTP	long-term potentiation
MEC	medial entorhinal cortex
MEG	magnetoencephalography
MNI	Montreal Neurological Institute
MRC	medical research council
MVPA	multivariate pattern analysis
NHS	National Health Service
NIBS	non-invasive brain stimulation
PSD	power spectral density
PTSD	post-traumatic stress disorder
RF	radiofrequency
ROI	region of interest
RSA	representational similarity analysis
RSE	retrieval success effect
SDF	sync./desync. framework
SENSE	sensitivity encoding
SME	subsequent memory effect
SPM	statistical parametric mapping
STDP	spike-timing dependent plasticity
tACS	transcranial alternating stimulation
TE	echo time
TMS	transcranial magnetic stimulation
TR	repetition time

CHAPTER 1: THE OSCILLATORY UNDERPINNINGS OF HUMAN EPISODIC MEMORY FORMATION AND RETRIEVAL – AN OVERVIEW

An episodic memory is a highly-detailed memory of a personally-experienced event, anchored to a unique point in both time and space. In order to successful form and later retrieve such a memory, the brain must be capable of (i) representing a large amount of information regarding the to-be-encoded event, and (ii) associating different elements of the event together to form a coherent memory trace. A large body of neuroscientific research has suggested that these two processes relate to the neocortex and the hippocampus respectively. However, it remains unclear how these regions underpin such processes. The rhythmic fluctuations of neural activity (known as neural oscillations) may provide an answer. Here, I discuss how neocortical alpha/beta oscillatory desynchronisation may facilitate information representation, and how hippocampal theta/gamma oscillatory synchronisation may facilitate representational association. At the end of the chapter, I highlight the current gaps in knowledge surrounding these ideas, and how these gaps will be empirically addressed in this thesis.

Published in:

Griffiths, B. J., & Fuentemilla, F. (2019). Event conjunction: How the hippocampus integrates episodic memories across event boundaries. Hippocampus. https://doi.org/10.1002/hipo.23161

and in preparation for:

Michelmann, S., Griffiths, B. J., & Hanslmayr, S. (in preparation). The role of alpha and beta oscillations in the human EEG during perception and memory processes. The Oxford Handbook on Time-Frequency Analyses.

1.1. Episodic memory: The briefest of primers

As human beings, we possess the incredible ability to mentally re-live our personally experienced past. For example, you may reflect on your last birthday and be vividly and rapidly instilled with the sights, sounds and smells of that dimly lit bar where you spent the evening with friends. Lay knowledge would label this a "memory", but more specifically, it reflects the subcategory "episodic memory" (Tulving, 1972). Episodic memories can be distinguished from other forms of memory based on a number of criteria: (i) episodic memories can last a lifetime, unlike short-term (or, working) memories which last for less than a minute; (ii) episodic memories can be easily verbalised and communicated, unlike implicit memories such as motor movements (e.g. tying a shoelace); and (iii) episodic memories are anchored to a unique point in space and time (i.e. the dimly lit bar on my 26th birthday), unlike semantic memories which relate to decontextualised facts (e.g. the name of the bar, or the date of my birthday). While additional criteria exist (see Conway, 2009), these three aspects describe the key tenets of episodic memory.

On a neuroanatomical level, episodic memories rely on a wide range of structures. Two structures with central importance are (i) the hippocampus and (ii) the sensory neocortex (from here on simply referred to as the neocortex). The neocortex is seen to house incredibly rich and complex sensory representations that are highly stable over time. The hippocampus, in contrast, is thought to code abstracted and simple representations of current experience and rapidly associate these representations together (Marr, 1971; Teyler & Rudy, 2007). In isolation, neither system is optimised to encode or retrieve episodic memories: the neocortex lacks the ability to rapidly associate representations, preventing the encoding of any novel and unique experience, while the hippocampus lacks the representational complexity required to encode and retrieve the highly-detailed information that is a trademark of episodic memory. When working together however, these two regions become 'complementary learning systems' – a highly specialised network capable of creating and recalling episodic memories (McClelland, McNaughton, & O'Reilly, 1995). Under this framework (see figure 1.1), sensory information about an ongoing event is processed by the neocortex, before being

abstracted and passed to the hippocampus, where different strands of sensory information become associated and encoded as an episodic memory trace. When a cue is later encountered, the memory trace is reinstated in the hippocampus and then passed to the neocortex, where the original sensory representations are reactivated to provide a vivid recollection of the event.

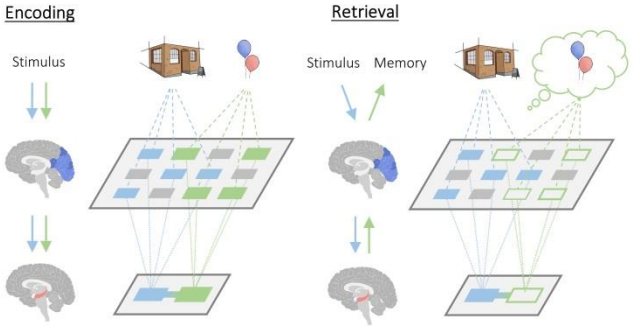

Figure 1.1. The division of labour between the sensory neocortex and the hippocampus in service of episodic memory. During encoding (left), the visual information of two co-occurring stimuli (i.e. a bar and balloons) are processed in detail by the occipital lobe (a part of the sensory neocortex responsible for the representation of visual information). These details are then simplified and passed onto the hippocampus, where they become associated. During retrieval (right), a visual cue (i.e. the bar) is passed to the hippocampus via the occipital lobe, where it reactivates the memory trace. This memory trace is passed back to the occipital lobe, where details of the trace that are not present in current environment (i.e. the balloons) are reinstated.

1.2. The oscillating brain

Neuronal activity rhythmically fluctuates over time. Neurons fire in synchrony and are then collectively silenced. The summed electrical potential of synchronised neurons, therefore, produces a wave-like pattern known as a *neural oscillation* (see figure 1.2a for oscillatory activity from my occipital cortex). In some of the earliest human electrophysiological recordings, Hans Berger observed that electrophysiological signals oscillate at around 10Hz – a rhythm he termed the 'alpha oscillation' (Berger & Gloor, 1969). As electrophysiological research bloomed, recordings uncovered a wide range of neural oscillations that resonated at frequencies from 0.05Hz to 500Hz (Buzsaki & Draguhn, 2004). To aid interpretation, researchers have discretised these oscillations into approximate frequency bands, including the theta (θ; 3-7Hz), alpha (α; 8-12Hz), beta (β; 13-30Hz) and gamma (γ; 30-100Hz) bands (see figure 1.2b).

The most direct method to identify neural oscillations is to record individual neurons and assess the degree to which they synchronise. This is a common approach in animal research, where hundreds of electrodes can be implanted within a healthy brain and recorded from simultaneously. In humans, however, this is an ethical impossibility. Instead, macroscopic measures are used to infer the underlying synchronisation of neuronal firing. When neurons fire together, their electric potentials sum together to generate a measurable oscillation in the local field potential (LFP). While an increase

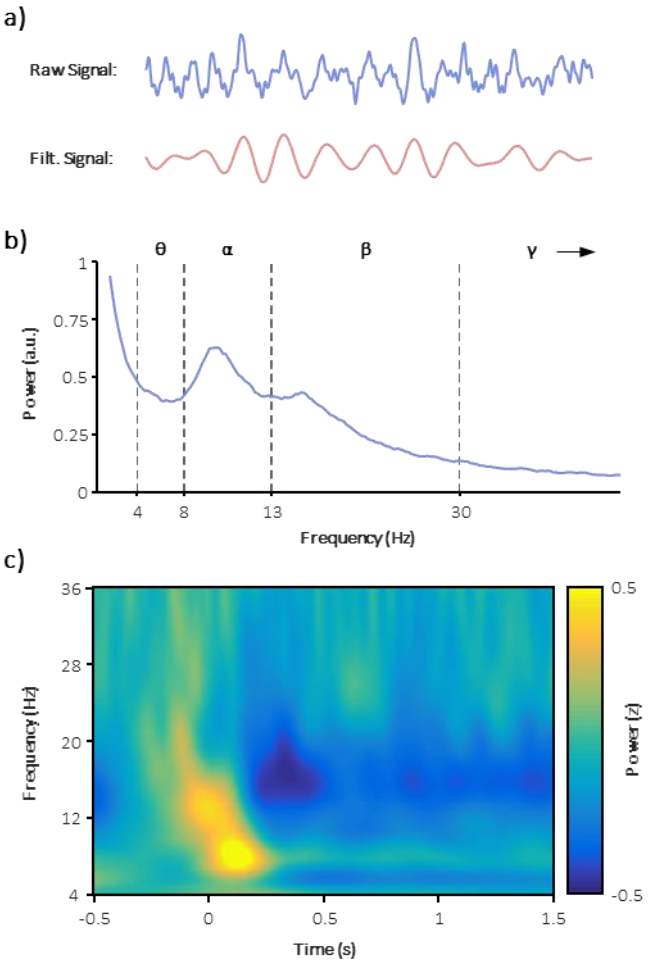

Figure 1.2. Neural oscillations in the authors brain. (a) an alpha oscillation recorded using an MEG sensor placed over the occipital lobe. A periodic increase and decrease in amplitude can be observed (top). This oscillation becomes clearer after filtering the signal to the alpha frequencies (i.e. 8 and 13Hz; bottom). **(b)** a power spectrum computed over several trials using the same sensor placement as above. The plotted result is the sum of two characteristics: exponentially decreasing power as frequency increases, and bumps (or, peaks) at approximately 10Hz and 16Hz. The former represents the 1/f curve found in biological systems and the latter is often interpreted as evidence for neural oscillations. In this plot, there would appear to be oscillations in the alpha (α) and beta bands (β), but none in the theta (θ) or gamma (γ) bands. **(c)** a time-frequency plot computed over several trials using the same sensor placement as above. The plot details instantaneous power at a range of different times and frequencies. When t=0, a visual stimulus is presented on the screen, which evokes a large increase in power in the theta band (~6Hz) and a slightly later decrease in power in the beta band (~12-20Hz). As the theta response is spectrally broad (~6-20Hz) and temporally brief (~100ms), it is unlikely to be oscillatory and may be better attributed to the event-related potential (ERP) evoked by the visual stimulus. In contrast, the spectrally-narrow (~12-20Hz) and temporally-extended (~250ms-1500ms) beta power decrease is more likely to reflect a change in oscillatory activity.

in the amplitude of an oscillation within the LFP does not perfectly equate to an increase in the underlying synchrony of neurons, it nonetheless provides a reliable proxy for the synchronisation and desynchronisation of neural activity (Buzsáki, Anastassiou, & Koch, 2012).

Electroencephalography (EEG) records this local field potential using electrodes attached to the scalp. Scalp EEG is the most prominent method for electrophysiological research in humans owning to its cost-effectiveness and versatility (such as its ability to be recorded concurrently with functional magnetic resonance imaging; fMRI). That said, as these electric potentials must pass through the skull to be detected by the electrodes, signals can be distorted which impedes our ability to localise a signal to a specific brain region (particularly when the signal comes from a source deep within the brain). Intracranial EEG (iEEG) overcomes this issue by directly placing electrodes within brain tissue.

Therefore, the location from where a signal is generated can be identified with a substantially better degree of accuracy. However, opportunities are rare. Due to ethical constraints, these recordings can only be acquired from individuals who have the electrodes implanted for medical treatment (e.g. the detection of epileptic seizure foci). As a result, electrode coverage is restricted to regions where medical professionals predict the seizures arise. Therefore, data recording is restricted to a small number of potentially pathological brain regions. Bridging the gap between scalp and intracranial EEG is magnetoencephalography (MEG). MEG measures the magnetic fields generated by the neural electrical potentials. As the magnetic fields are not distorted by the skull, greater spatial focus can be determined (including deeper sources [although not to the same degree as iEEG]; Ruzich, Crespo-García, Dalal, & Schneiderman, 2019). However, MEG is a substantially more costly technique to use than EEG.

1.3. Episodic memory, alpha/beta oscillations and the neocortex

By definition, episodic memory is rich in sensory information. Therefore, it comes as no surprise to suggest that the neocortex (a hub for sensory information representation) plays a key role in the formation and retrieval of episodic memories. Extensive reviews of fMRI (Kim, 2011), ERP (Friedman & Johnson, 2000) and oscillation literature (Hanslmayr & Staudigl, 2014) support this idea by consistently linking fluctuations of neural activity in the neocortex to successful memory formation. Similarly, a wealth of fMRI (Johnson & Rugg, 2007; Nyberg, Habib, McIntosh, & Tulving, 2000; Nyberg et al., 2001; Wheeler, Petersen, & Buckner, 2000; Woodruff, Johnson, Uncapher, & Rugg, 2005) and electrophysiological research (Friedman & Johnson, 2000; Khader & Rösler, 2011; Michelmann, Bowman, & Hanslmayr, 2016; Waldhauser, Braun, & Hanslmayr, 2016) also link increased neocortical activation to successful memory retrieval. With such substantial evidence demonstrating that the neocortex is linked to episodic memory, the field no longer asks *whether* the neocortex is implicated in episodic memory, but rather *what* and *how* the neocortex contributes to episodic memory.

The complementary learning systems model (McClelland et al., 1995) proposes that the neocortex contains highly-detailed and stable representations of stimuli. Each of these sensory representations is distinguishable from every other owning to the fact that they are coded by a unique and distributed neural code (or, "*neural pattern"*). Episodic memory is thought to rely on the activation of these patterns during both memory formation (to allow sufficient detail about the event to be encoded) and memory retrieval (to allow a vivid recalling of details). Indeed, extensive work has demonstrated that, during perception, neural patterns for faces, objects, scenes and sounds can be decoded based on neocortical blood-oxygen level dependent (BOLD) activity (e.g. Bosch, Jehee, Fernández, & Doeller, 2014; Chen et al., 2016; Kriegeskorte, Formisano, Sorger, & Goebel, 2007) and electrophysiological activity (e.g. Linde-Domingo, Treder, Kerrén, & Wimber, 2019; Michelmann et al., 2016; Ng, Logothetis, & Kayser, 2013). Importantly, these patterns are found to be reinstated in the sensory cortex during retrieval (e.g. Bosch et al., 2014; Chen et al., 2016; Johnson, McDuff, Rugg, & Norman, 2009; Linde-Domingo et al., 2019; Michelmann et al., 2016; Staresina, Henson, Kriegeskorte, & Alink, 2012). This suggests that the neocortex is involved in the representation of sensory information during both perception and memory retrieval. As similar decoding was not observed in the hippocampus (Staresina et al., 2012), it would seem that the neocortex holds a special role in the representation of detailed sensory information relating to an episodic memory.

Given that information representation is a highly general cognitive process that should transcend task, sensory modality and even species, any neural mechanism facilitating the process should be equally ubiquitous. Neocortical alpha/beta oscillatory desynchronisation fits this criterion. Given that (i) alpha/beta activity is the dominant rhythm within the sensory cortices (Berger & Gloor, 1969), (ii) alpha/beta activity undergoes rapid desynchronisation when a participant engages in a task (e.g. Krause et al., 1994; Pfurtscheller, Neuper, & Mohl, 1994), and (iii) alpha/beta desynchronisation generalises across sensory cortices (Crone et al., 1998; Krause et al., 1994; Pfurtscheller et al., 1994), cognitive tasks (Hanslmayr et al., 2011; Obleser & Weisz, 2012; Pfurtscheller et al., 1994) and species (Haegens, Nacher, Luna, Romo, & Jensen, 2011; Pfurtscheller et al., 1994; Wiest & Nicolelis, 2003),

one can speculate that alpha/beta oscillations play a highly general role in brain function, such as information representation.

There are two theories that elaborate on how alpha/beta desynchronisation relates to information representation. The first is the *information via desynchronisation* hypothesis (Hanslmayr, Staudigl, & Fellner, 2012). This theory applies tenets of information theory (Shannon & Weaver, 1949) to neural oscillations, and states that synchronised states are inherently bad for information representation as neuronal activity is highly predictable (see figure 1.3). In other words, if you can predict when an event is about to occur (i.e. the firing of a neuron), you must already know something about this event and hence learn little more about it. In contrast, desynchronised states facilitate information representation as neuronal activity becomes unpredictable (i.e. you learn a lot more about an event you have never experienced before). One can therefore speculate that alpha/beta oscillatory desynchronisation may provide optimal conditions for information representation by allowing a complex and unpredictable neural code to be generated.

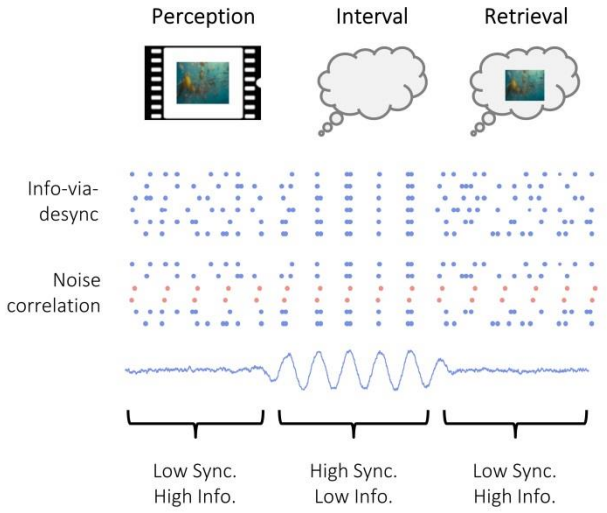

Figure 1.3. Theories of how alpha/beta desynchrony facilitates information representation. When recording from the scalp, alpha/beta oscillations fluctuate between periods of high synchrony (i.e. high amplitude oscillations) and periods of low synchrony (i.e. low amplitude oscillations). Information representation is thought to be optimal during periods of low synchrony. The information-via-desynchronisation hypothesis suggests that oscillatory desynchrony allows individual neurons to fire independently of every other, creating a highly complex and unpredictable neural code. Information theory posits that such a code is optimal for conveying highly-detailed information. The noise correlation account proposes that when many task-irrelevant neurons (in blue) fire in synchrony, they mask the relatively small signal conveyed by task-relevant neurons (in red). Only when the firing of these task-irrelevant neurons become de-correlated (marked by a drop in neural synchrony) can the signal be detected amongst the background noise.

The second theory proposes that the correlated firing of two task-irrelevant neurons can be detrimental to information representation. In sufficient numbers, these *noise correlations* mask the patterns of neural activity that represent a stimulus. Computational modelling has demonstrated that as the number of correlated task-irrelevant neurons increase, the amount of information conveyed within

the network decreases (Averbeck, Latham, & Pouget, 2006). Importantly, as the number of correlated task-irrelevant neurons increase, their summed electrical potential increases, which may be reflected in enhanced oscillatory activity in the LFP (Cui, Liu, McFarland, Pack, & Butts, 2016). Therefore, an increase in oscillatory synchronicity may be a proxy for an increase in information-limiting noise correlations. Task-induced desynchronisation of alpha/beta oscillatory activity, therefore, could be the antithesis of these detrimental noise correlations.

Several lines of evidence support the idea that neocortical alpha/beta desynchronisation reflects information representation:

1) Alpha/beta power decreases (a proxy for oscillatory desynchronisation) are restricted to task-relevant sensory regions. For example, the perception and retrieval of visual information elicits alpha/beta power decreases over the occipital lobe (e.g. Michelmann, Bowman, & Hanslmayr, 2016; Pfurtscheller et al., 1994), while the perception and retrieval of auditory information elicits alpha/beta power decreases over midfrontal regions[*] (e.g. Krause et al., 1994; Michelmann et al., 2016). The restriction of these power decreases to task-relevant sensory regions implies that they are reflective of task-relevant sensory information representation.
2) Alpha/beta power decreases scale with the depth of stimulus processing. When Hanslmayr and colleagues (2009) asked participants to either judge whether the first letter of a word preceded the last in the alphabet (a shallow, non-semantic task) or whether the word represented a living entity (a deep, semantic task), they found that the semantic task evoked greater alpha/beta power decreases than the non-semantic task. Given that the semantic task required more complex information representation, these alpha/beta power decreases were interpreted as an index for the depth of representation required in a task.

[*] While the auditory cortices are located in the temporal lobe, their dipoles are angled such that EEG electrodes placed above midfrontal regions best detect electrophysiological activity evoked by the auditory cortices.

3) Interfering with alpha/beta activity using brain stimulation affects task performance. Waldhauser and colleagues (2016) found that using transcranial magnetic stimulation (TMS) to disrupt the task-related alpha/beta power decreases that occur during episodic memory retrieval impairs the participant's ability to recall details of the memory. Hanslmayr and colleagues (2014) found complementary results when using TMS in the same manner during memory encoding. These results indicate that alpha/beta power decreases are causally relevant to episodic memory formation and retrieval.

In sum, these results indicate that alpha/beta power decreases are intimately linked to information representation in episodic memory. However, the picture is incomplete. These results do not demonstrate a direct link between alpha/beta power and an objective and parametric measure of information representation. Moreover, information representation often coincides with other processes in episodic memory (e.g. associating of stimuli) in these experiments, making it difficult to dissociate the role of alpha/beta power decreases and information representation from other cognitive and neural phenomena that are pivotal to episodic memory.

1.4. Episodic memory, theta/gamma oscillations and the hippocampus

In order to form an episodic memory, multiple neocortical sensory representations relating to the to-be-encoded event need to be bound together into a singular coherent memory trace. This task is thought to fall on the hippocampus (Konkel & Cohen, 2009; Olsen, Moses, Riggs, & Ryan, 2012; Wallenstein, Eichenbaum, & Hasselmo, 1998), and the synchronisation of theta and gamma oscillations within (Colgin, 2015b; Hanslmayr, Staresina, & Bowman, 2016; Nyhus & Curran, 2010).

The phase of the theta oscillation has been thought to dictate whether long-term potentiation (LTP; a phenomenon which strengthens connections between synapses) or long-term depression (LTD; a phenomenon which weakens connections between synapses) occurs (Hasselmo, 2005; Huerta & Lisman, 1995; Hyman, Wyble, Goyal, Rossi, & Hasselmo, 2003; Pavlides, Greenstein, Grudman, & Winson, 1988). Computational models implementing this principle demonstrate how the hippocampus

can effectively encode new associations and retrieve old associations without incurring catastrophic interference between the two processes (Schapiro, Turk-Browne, Botvinick, & Norman, 2017). Moreover, Clouter and colleagues (2017) provided empirical support for these ideas by demonstrating that two stimuli presented at the same phase of theta are more likely to be successfully encoded than two stimuli that are presented at opposing phases. These results indicate that associative memory formation varies as a function of theta phase. Similarly, Kerrén and colleagues (2018) demonstrated that neural evidence (as measured using multivariate pattern analysis; MVPA) for retrieved stimuli fluctuate at approximately 7Hz, suggesting that episodic memory retrieval is also dependent on theta phase.

As for gamma oscillations, an increase in their amplitude is thought to reflect increases in spike-timing-dependent plasticity (STDP; Axmacher, Mormann, Fernández, Elger, & Fell, 2006; Nyhus & Curran, 2010) – a form of long-term potentiation (LTP) that depends on the highly precise firing of presynaptic and postsynaptic neurons. Probing rat hippocampal neurons *in vitro*, Bi and Poo (1998) showed that the postsynaptic neuron must fire ~15-20ms (i.e. ~60Hz/gamma) after the presynaptic neuron to induce STDP. Given that these hippocampal neurons have been shown to lock to gamma-band activity (Jutras, Fries, & Buffalo, 2009) and gamma-band activity is predictive of memory formation (e.g. Long & Kahana, 2015), one could speculate that increases in the amplitude of hippocampal gamma oscillations reflect increases in STDP.

However, such an explanation does not explain why hippocampal gamma oscillations also increase in power during memory retrieval (e.g. Montgomery & Buzsáki, 2007; Staresina et al., 2016), where STDP has little-to-no functional relevance to the task at hand. Recently, an alternative hypothesis has been put forward which suggests that traditional hippocampal gamma (30-100Hz) can be divided into two distinct oscillations: a "fast" gamma (60-100Hz) originating in the medial entorhinal cortex (MEC), and a "slow" gamma (30-50Hz) originating in CA3 (Bragin et al., 1995; Colgin et al., 2009). The "fast" gamma facilitates the influx of information from the neocortex into the hippocampal subfield CA1. In contrast, the "slow" gamma helps memory traces that have been

reinstated in CA3 flow into the neocortex via CA1. Notably however, while evidence in support of this theory has been growing rapidly in the field of animal neuroscience (Bragin et al., 1995; Colgin et al., 2009; Montgomery & Buzsáki, 2007), such a phenomenon has yet to be demonstrated in humans.

While the origins and proposed functions of hippocampal theta and gamma rhythms are distinct, gamma oscillations are frequently seen to nest within the ongoing theta cycle (Colgin & Moser, 2010) – a phenomenon known as theta-gamma phase-amplitude coupling. Numerous studies have demonstrated that theta-gamma coupling correlates with successful memory formation (Heusser, Poeppel, Ezzyat, & Davachi, 2016; Staudigl & Hanslmayr, 2013; Tort, Komorowski, Manns, Kopell, & Eichenbaum, 2009). Phase-amplitude coupling is thought to provide a neural code capable of recording sequences (Lisman & Jensen, 2013). Under this framework, each gamma cycle is thought to reflect the firing of a cell population that codes for a unique element in the sequence. It is thought that the theta cycle organises these cell assembly indices into a sequence, dictating the order in which elements are encoded. Several studies have supported these ideas (Bahramisharif, Jensen, Jacobs, & Lisman, 2018; Heusser et al., 2016). For example, Bahramisharif and colleagues (2018) asked participants to retain a sequence of three letters for several seconds and examined whether gamma-band representations of these letters peaked at distinct phases of the theta cycle. Indeed, they found that gamma-band representations of the first letter peaked earlier in the theta cycle than the second letter, and representations of the second letter peaked earlier in the theta cycle than the third letter. This result demonstrates that theta-gamma phase-amplitude coupling can provide a neural framework that codes for sequences of stimuli.

The proposed neural code supported by hippocampal theta-gamma coupling may appear vastly different to the proposed roles of hippocampal theta and gamma in isolation. However, the principles can be reconciled. Gamma oscillations within a theta-gamma code ensure that cell populations coding for each element fire approximately 20ms after the preceding cell population fires for the preceding element. As discussed above, this temporally precise firing allows STDP to strengthen the synaptic connections between two cell populations and, in the case of a theta-gamma code, would create a

chain of elements (first to second element, second to third element etc.). In other words, the ability for gamma oscillations to facilitate STDP makes it ideal for creating temporally-sequenced memories. A notable limitation of this view is that, in isolation, there is no mechanism to terminate such a sequence. Theta phase-dependent plasticity remedies this: as gamma rides the peak of the theta cycle, a sequence can be generated through gamma-linked STDP (Bi & Poo, 1998) and further enhanced by theta-related LTP (Huerta & Lisman, 1995; Pavlides et al., 1988). During the trough of the theta cycle however, gamma-related increases in STDP could become negated by theta-related LTD, terminating any associative change generated by gamma oscillations. A recent computational model implementing this concept has demonstrated that the combination of theta and gamma-related LTP is an effective method to form associative memories (Parish, Hanslmayr, & Bowman, 2018). Therefore, hippocampal theta-gamma coupling may not only be the most effective method for maintaining/representing sequences (Lisman & Jensen, 2013), but also for encoding these sequences.

However, questions remain. Currently, there is no evidence of a "fast"/"slow" gamma distinction in humans, making it unclear whether such a phenomenon is a viable explanation for how gamma band activity can support STDP-based encoding and STDP-irrelevant retrieval. Moreover, as with neocortical alpha/beta power decreases and information representation, previous studies probing hippocampal synchrony and representational binding involve an overlap with other neural and cognitive phenomena. Therefore, it remains unclear whether hippocampal synchrony is specifically and uniquely linked to representational binding.

1.5. The Sync-Desync Framework

Thus far, we have seen how the formation and retrieval of episodic memories is (i) serviced by a division of labour between the hippocampus and sensory neocortex (McClelland et al., 1995); (ii) tied to neocortical alpha/beta power decreases and information representation (Hanslmayr et al., 2012); and (iii) linked to hippocampal theta/gamma coupling and representational binding (Colgin, 2015b; Nyhus & Curran, 2010). However, it remains unclear how neocortical alpha/beta power decreases and hippocampal theta/gamma increases interact to form and retrieve episodic memories.

To address this, Hanslmayr and colleagues (2016) proposed the sync-desync framework (SDF). In brief, this framework integrated the principles of the complementary learning systems model (McClelland et al., 1995) with the proposed functional roles of neocortical alpha/beta and hippocampal theta/gamma oscillations. During episodic memory encoding, the SDF predicts that neocortical alpha/beta power decreases would first facilitate the representation of incoming sensory information, and this information would then be passed onto the hippocampus where it becomes integrated into a singular, coherent memory trace through hippocampal theta/gamma coupling. The SDF goes on to predict that, during retrieval, a partial cue reactivates the hippocampal theta/gamma representation of the entire memory trace, which is then projected back into the neocortex where alpha/beta power decreases allow for the rich representation of the reinstated information.

The SDF has been developed on the back of large bodies of empirical evidence, however some gaps remain. Critically, it is unclear if neocortical desynchronisation and hippocampal synchronisation actually interact. In other words, does neocortical desynchronisation predict hippocampal synchronisation during encoding, reflecting the representation of sensory information in the neocortex and the subsequent binding of this information in the hippocampus? Similarly, does hippocampal synchronisation predict neocortical desynchronisation during retrieval, reflecting the reactivation of a memory trace in the hippocampus and the subsequent reinstatement of detailed information about the memory? Furthermore, if hippocampal synchrony can be predicted by neocortical desynchrony (and vice versa), how certain can we be that they reflect two distinct cognitive processes? Could they be better explained as two neural responses to a singular cognitive process?

1.6. Thesis Aims and Objectives

Both the formation and retrieval of episodic memories appear to be reliant on oscillatory activity in the sensory neocortex and the hippocampus. The complementary learning systems theory and its derived oscillatory framework (the SDF) propose that interactions between these two regions are pivotal to episodic memory. However, critical questions still remain:

- Do neocortical alpha/beta power decreases directly map onto information representation within the sensory neocortex?
- Do multiple hippocampal gamma oscillations exist in the human hippocampus? If so, how do they relate to memory formation and retrieval?
- How do neocortical alpha/beta power decreases and hippocampal theta/gamma coupling interact to facilitate the formation and retrieval of episodic memories?
- If the two mechanisms interact, does the former uniquely reflect information representation and the latter uniquely reflect binding?

The following four chapters address each question in turn.

In chapter 2, I ask whether alpha/beta power decreases can be used as a proxy for information representation in the sensory neocortex. Utilising simultaneous EEG-fMRI recordings, I demonstrate that the quantity of stimulus-specific information represented within the sensory neocortex parametrically increases as a function of alpha/beta power decreases on a trial-by-trial level. In other words, information representation increases as alpha/beta power decreases. I demonstrate that this phenomenon occurs during visual perception, auditory perception and visual memory retrieval, which strengthens both the replicability and generalisability of the result. These results provide a clear link between alpha/beta power decreases and the representation of information in the sensory neocortex.

In chapter 3, I investigate the theory that distinct hippocampal gamma oscillations underpin the formation and retrieval of episodic memory. Taking direct intracranial recordings from the human hippocampus, I demonstrate that increases in “fast” hippocampal gamma activity (60-80Hz) correlate with successful memory formation while increases in “slow” hippocampal gamma activity (40-50Hz) correlate with successful memory formation. These results provide a potential resolution to the idea that gamma band activity supports both STDP and memory retrieval.

In chapter 4, I investigate how these dissociable neocortical and hippocampal processes interact during episodic memory formation and retrieval. Utilising simultaneous intracranial EEG recordings

from the hippocampus and anterior temporal lobe, I demonstrate that neocortical alpha/beta power decreases precede and predict hippocampal gamma power increases during encoding, but this process reverses during retrieval such that hippocampal gamma power increases precede and predict neocortical alpha/beta power decreases. These results demonstrate that episodic memory hinges on the interaction between hippocampal synchronisation and neocortical desynchronisation.

In chapter 5, I investigate whether neocortical desynchronisation and hippocampal synchronisation are separable from one another, or whether they simply reflect two sides of the same coin. By asking participants to complete a sequence learning paradigm while undergoing MEG, I demonstrate that neocortical power decreases only arise during the perception and retrieval of these sequences (i.e. when information representation must occur). In contrast, hippocampal theta/gamma coupling only arises during the post-sequence window when participants are asked to associate the sequence elements together. This double dissociation suggests that neocortical desynchrony and hippocampal synchrony reflect two distinct processes rather than reflect two neural responses to a singular process.

In the final chapter, I bring these threads together and discuss the conclusions, implications and limitations of these results.

CHAPTER 2: ALPHA/BETA POWER DECREASES TRACK THE FIDELITY OF STIMULUS-SPECIFIC INFORMATION

Massed synchronised neuronal firing is detrimental to information representation. When networks of task-irrelevant neurons fire in unison, they mask the signal generated by task-critical neurons. On a macroscopic level, such synchronisation can contribute to alpha/beta (8-30Hz) oscillations. Reducing the amplitude of these oscillations, therefore, may enhance information representation. Here, we test this hypothesis. Twenty-one participants completed an associative memory task while undergoing simultaneous EEG-fMRI recordings. Using representational similarity analysis, we quantified the amount of stimulus-specific information represented within the BOLD signal on every trial. When correlating this metric with concurrently-recorded alpha/beta power, we found a significant negative correlation which indicated that as post-stimulus alpha/beta power decreased, stimulus-specific information increased. Critically, we found this effect in three tasks: visual perception, auditory perception, and visual memory retrieval, indicating that this phenomenon transcends both stimulus modality and cognitive task. These results suggest that alpha/beta power decreases parametrically track the fidelity of both externally-presented and internally-generated stimulus-specific information represented within the cortex.

Published in:

Griffiths, B. J., Mayhew, S. D., Mullinger, K. J., Jorge, J., Charest, I., Wimber, M., & Hanslmayr, S. (accepted). Alpha/beta power decreases track the fidelity of stimulus-specific information. *eLife.* [bioRxiv doi: 10.1101/633107].

2.1. Introduction

Neuronal activity fluctuates rhythmically over time. Often referred to as "neural oscillations", these rhythmic fluctuations can be observed throughout the brain at frequencies ranging from 0.05Hz to 500Hz (Buzsaki & Draguhn, 2004). When recording from the human scalp, it is the alpha and beta frequencies (8-12Hz; 13-30Hz) that dominate. Alpha/beta activity displays an intimate link to behaviour; engaging in a cognitive task produces a large reduction in alpha/beta power (amplitude squared). These task-induced power decreases are ubiquitous, and can be observed across species (including humans [Pfurtscheller, Neuper, & Mohl, 1994], macaques [Haegens, Nacher, Luna, Romo, & Jensen, 2011], rodents [Wiest & Nicolelis, 2003] and cats [Chatila, Milleret, Buser, & Rougeul, 1992]), sensory modalities (including visual [Pfurtscheller et al., 1994], auditory [Krause et al., 1994], and somatosensory [Crone et al., 1998] domains), and cognitive tasks (including perception [Crone et al., 1998; Krause et al., 1994; Pfurtscheller et al., 1994], memory formation/retrieval [Griffiths, Mazaheri, Debener, & Hanslmayr, 2016; Hanslmayr, Spitzer, & Bauml, 2009; Waldhauser, Braun, & Hanslmayr, 2016], and language processing [Obleser & Weisz, 2012]). Given their ubiquity, it stands to reason that these decreases reflect a highly general brain process. While numerous domain-general processes have already been ascribed to alpha/beta oscillations (e.g. idling [Pfurtscheller, Stancák, & Neuper, 1996]; inhibition [Jensen & Mazaheri, 2010; Klimesch, Sauseng, & Hanslmayr, 2007]), we provide empirical evidence in support of a new perspective: alpha/beta power decreases are a proxy for information representation.

To successfully process information about a stimulus, the brain must be capable of elevating the signal of said stimulus above the noise generated by ongoing neuronal activity (Harris & Thiele, 2011). In situations where the ongoing spiking of a large population of neurons is correlated, this is problematic (Averbeck et al., 2006). Mass synchronised spiking generates noise that conceals the comparatively small neuronal signal evoked by the stimulus (see figure 2.1a), rendering momentary changes in sensory input undetectable (Busch, Dubois, & VanRullen, 2009) and responses to temporally-extended changes unreliable (Goard & Dan, 2009). Reducing these neuronal "noise

correlations", therefore, can boost the signal-to-noise ratio of an evoked neuronal response to a stimulus. Indeed, numerous studies have demonstrated that the decorrelation of task-irrelevant neuronal firing accompanies engagement in cognitive tasks (Churchland et al., 2010; Goard & Dan, 2009; Mitchell, Sundberg, & Reynolds, 2009; Poulet & Petersen, 2008). Given that these noise correlations show a strong positive correlation with the local field potential (LFP; Cui, Liu, McFarland, Pack, & Butts, 2016), one may speculate that task-induced reductions in alpha/beta LFP (e.g. Haegens et al., 2011) are, to some degree, a marker of the reduction of noise correlations. Such a hypothesis would explain why reductions in alpha/beta power are associated with the successful execution of a wide range of cognitive tasks, from visual perception (Pfurtscheller et al., 1994) to memory retrieval (Michelmann et al., 2016).

Here, we test the hypothesis that alpha/beta power decreases are a proxy for information representation (Hanslmayr et al., 2012). Specifically, we predict that as the amount of stimulus-specific information within the cortex increases, concurrently-recorded measures of alpha/beta power will decrease. Twenty-one participants took part in an associative memory task whilst simultaneous EEG-fMRI recordings were obtained (see figure 2.1b). On each trial, participants were presented with one of four videos (and on alternating blocks, one of four melodies), followed by a noun, and asked to pair the two. Later, participants were presented with the noun and asked to recall the associated video/melody (which would lead to the reinstatement of stimulus-specific information about the video/melody; Staresina, Henson, Kriegeskorte, & Alink, 2012). We first conducted representational similarity analysis (RSA) on the acquired fMRI data to quantify the relative distance between neural patterns of matching and differing videos/melodies. This provides a data-driven and objective measure of stimulus-specific information present during a single trial. We then derived alpha/beta power from the concurrently recorded EEG and correlated the observed power with our measure of stimulus-specific information on a trial-by-trial basis. Foreshadowing the results reported below, we found that post-stimulus alpha/beta power decreases negatively correlated with the amount of stimulus-specific information observed in the cortex. Importantly, we find evidence for this during both the perception

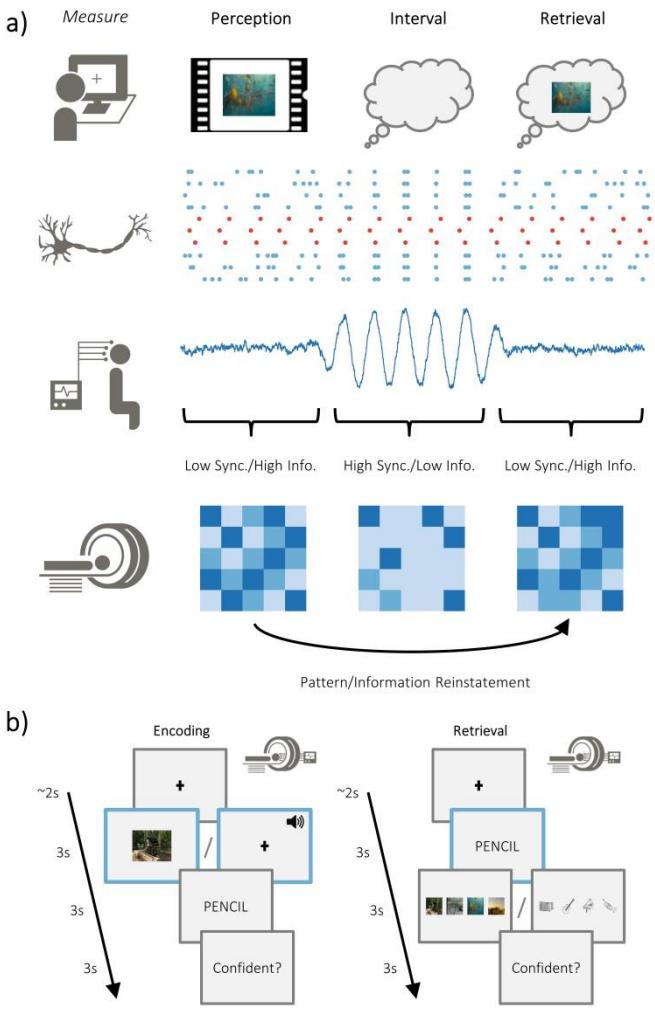

Figure 2.1. Overview of hypotheses and paradigm. (a) The brain is capable of representing stimulus-specific information through neural patterns that are consistent regardless of whether the stimulus is externally or internally generated (i.e. perceived or retrieved; top). On a neuronal level, populations that code for the stimulus (in red) need to generate signal greater than ongoing neuronal noise (in blue). When the neuronal noise correlates (i.e. arises at the same time; during the 'interval'), the signal-to-noise ratio is reduced and stimulus specific information is limited. These noise correlations may be reflected in macroscopic measures of electrophysiological activity, where periods of highly synchronised firing is accompanied by periods of high amplitude activity. Under this assumption, high amplitude activity would reflect an attenuation of the representation of stimulus-specific information. Stimulus-specific information can be measured using fMRI to look at pattern similarity during perception and pattern reinstatement during memory retrieval. **(b)** Participants completed an associative memory task while undergoing simultaneous EEG-fMRI recordings. Participants were asked to vividly associate a video/melody with a word, and then rate how plausible (i.e. believable) the imagined association was. Later, they were cued with the word and tasked with recalling the associated video/melody. After selecting the associated video/melody, they were asked to judge how confident they felt about their decision. The modality of the dynamic stimuli alternated at the end of each block (counterbalanced across participants).

and retrieval of these videos, as well as during the perception of the melodies, providing a conceptual replication of our results and supporting the modality- and task-general nature of our hypothesis.

2.2. Results

2.2.1. Detecting stimulus-specific information in BOLD patterns

Our first step was to derive a measure of stimulus-specific information (that is, information unique to each of the four repeatedly-presented videos/melodies) from the acquired fMRI data (for univariate analyses, see Appendix A, figure 7.1). To this end, we used searchlight-based representational similarity analysis (RSA) to quantify the overlap in BOLD patterns for matching videos/melodies, and contrasted this against the overlap between with the three other repeated

videos/melodies (analysis was always restricted to within a modality, at no point were visual patterns contrasted against auditory patterns). We interpret the difference in overlap between matching and differing videos/melodies as the amount of stimulus-specific information present on a single trial, under the assumption that any similarity that can only be explained by matching stimuli represents information specific to that stimulus. To evaluate whether the quantity of stimulus-specific information was meaningful within a searchlight, the observed measure of information was contrasted against the null hypothesis (i.e. that BOLD pattern overlap for matching videos is the same as BOLD pattern overlap for differing videos) in a one-sample, group-level t-test.

For the perceptual tasks, stimulus-specific information was quantified by computing the representational distance between every pair of perceptual trials. During visual perception, whole-brain searchlight analysis revealed a significant increase in stimulus-specific information relative to chance bilaterally in the occipital lobe ($p_{FWE} < 0.001$, k = 9911, peak MNI: [x = -30, y = -57, z = -2], Cohen's $d_z = 1.79$) [see figure 2.2a]. This corroborates the findings of numerous early studies (e.g. Baldassano et al., 2017; Chen et al., 2016) which indicate that the occipital lobe is critical in the representation of dynamically-unfolding visual information. A frontal central cluster ($p_{FWE} < 0.001$, k = 113, peak MNI: [x = 12, y = -16, z = 50], Cohen's $d_z = 0.28$) and a left temporal cluster ($p_{FWE} = 0.003$, k = 64, peak MNI: [x = -48, y = -1, z = 18], Cohen's $d_z = 0.81$) were also uncovered. The former may reflect goal-directed tracking of the visual stimulus (Holroyd, Ribas-Fernandes, Shahnazian, Silvetti, & Verguts, 2018), while the latter may reflect high-level semantic representations of the stimulus (Rice, Ralph, & Hoffman, 2015; Visser, Jefferies, & Lambon Ralph, 2010). During auditory perception, whole-brain searchlight analysis revealed a significant increase in stimulus-specific information relative to chance bilaterally in the temporal lobe (left temporal: $p_{FWE} < 0.001$, k = 698, peak MNI: [x = -57, y = -37, z = 10], Cohen's $d_z = 0.86$; right temporal: $p_{FWE} < 0.001$, k = 859, peak MNI: [x = 60, y = -25, z = 10], Cohen's $d_z = 1.20$) [see figure 2.2b]. These results demonstrate that stimulus-specific information is represented within the cortex during both visual and auditory

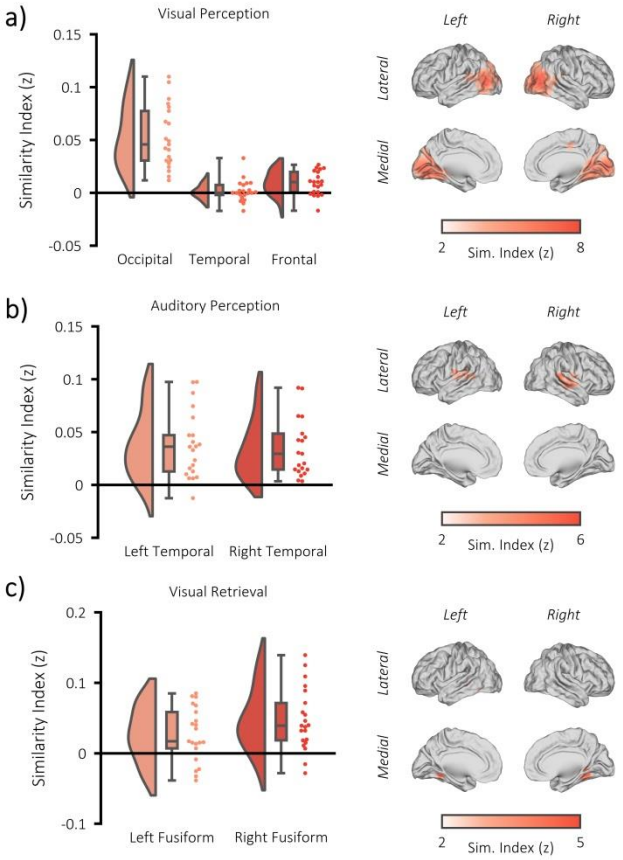

Figure 2.2. fMRI RSA searchlight analysis. **(a)** raincloud plot (left) depicting the degree to which matching and differing stimuli could be distinguished from one another during visual perception, per participant (single dots), within the significant cluster, and brain map (right) depicting the cluster where matching and differing stimuli could be distinguished from one another. **(b)** raincloud plot (left) and brain map (right) for stimulus discriminability during auditory perception. (c) raincloud plot (left) and brain map (right) for stimulus discriminability during visual memory retrieval.

perception, and identify the regions where a meaningful measure of visual/auditory stimulus-specific information can be derived for our central analysis.

For the retrieval task, stimulus-specific information was quantified by comparing every retrieval pattern with every perceptual pattern. This approach is sensitive to the reinstatement of veridical information about a successfully recalled stimulus (Staresina et al., 2012). As we would only anticipate that stimulus-specific information is present in the BOLD signal when the correct stimulus is recalled, this analysis was restricted to trials where the paired associate was successfully recalled (see Appendix A, figure 2.2). During visual memory retrieval, whole-brain searchlight analysis revealed a significant increase in reinstated stimulus-specific information relative to chance in the right fusiform gyrus ($p_{FWE} < 0.001$, k = 313, peak MNI: [x = 30, y = -46, z = -14], Cohen's $d_z = 1.07$) and left fusiform gyrus ($p_{FWE} < 0.001$, k = 456, peak MNI: [x = -45, y = -37, z = -6], Cohen's $d_z = 0.69$) [see figure 2.2c]. Notably, this effect was not driven by the presentation of video stills that followed the presentation of the retrieval cue (see Appendix A, figure 7.2). These results demonstrate that stimulus-specific information is reinstated during the retrieval of visual information, and provide a region of interest that yields a meaningful measure of stimulus-specific information for the central analysis of the memory task.

No significant cluster was identified during auditory memory retrieval (left frontal cluster: p_{FWE} = 0.153, k = 28, peak MNI: [x = -39, y = 44, z = 14], Cohen's d_z = 0.36; see Appendix A, figure 7.2). It is unclear why we could not find evidence for retrieved auditory information, but it may be explained by the fact that memory performance was substantially worse for the auditory stimuli (52.9%) when compared to visual stimuli (73.8%; t(20) = 7.13, p < 0.001). Poor memory performance meant that fewer trials could be included in the similarity analysis, limiting the statistical power of the analysis. With no measure of stimulus-specific information for retrieved auditory memories, we could not test our central hypothesis on this portion on the data.

2.2.2. Alpha/beta power decreases accompany task engagement

We then measured the degree to which alpha/beta power reduces during task engagement. As such an effect is perhaps the most ubiquitous effect in studies of task-related scalp EEG activity, it provides a strong benchmark for the quality of our EEG data (which has the potential for distortion by MRI-related artifacts; Fellner et al., 2016). For both the perceptual and retrieval trials, the time-series of every source-reconstructed virtual EEG electrode was decomposed into alpha/beta power using 6-cycle Morlet wavelets and baseline-corrected using z-transformation. Alpha/beta power was defined as power between 8 and 30Hz, as a previous experiment (Michelmann et al., 2016) using this paradigm found that this frequency range best described task-related decreases in the alpha and beta frequencies. In the first instance, post-stimulus power (500 to 1500ms) was contrasted against pre-stimulus power (-1000 to -375ms) in a cluster-based, permutation t-test. We found a significant decrease in alpha/beta power following visual stimulus presentation (p < 0.001, Cohen's d_z = 0.95; see figure 2.3a-d) and auditory stimulus presentation (p = 0.012, Cohen's d_z = 0.53) tasks. Power decreases evoked by the visual stimuli were predominately observed in the occipital lobe, while power decreases evoked by the auditory stimuli were observed in the parietal and temporal lobes (see figure 2.3d).

We then asked whether alpha/beta power decreases are not only predictive of task engagement, but also task success. In other words, is the reduction in post-stimulus alpha/beta power greater when memories are successfully recalled? As in the above paragraph, this is not a novel idea (Martín-Buro,

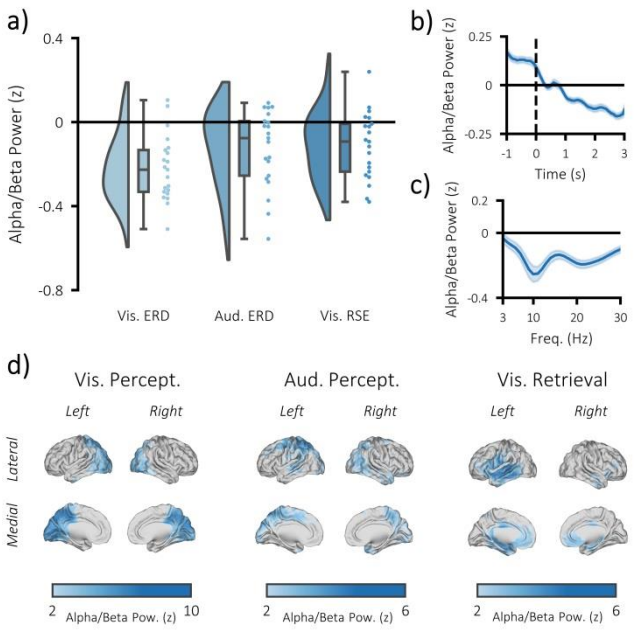

Figure 2.3. Task-induced decreases in post-stimulus alpha/beta power. (a) Raincloud plot displaying event-related decreases in power during visual perception (left) and auditory perception (middle), and memory-related decreases in power during visual retrieval (each dot represents a single subject). **(b)** time-series of alpha/beta (8-30Hz) power change over time across all three tasks (see Appendix A, figure 3, for each task individually). The dark line indicates the mean across participants; the shaded error bar represents standard error of the mean [N.B. as the electrodes were chosen because they belonged to the significant cluster, these figures are for descriptive purposes only and should not be used for statistical inference]. **(c)** frequency spectrum of post-stimulus power across all three tasks (500-1500ms; referenced to -1000 to -375ms pre-stimulus power). The dark line indicates the mean across participants; the shaded error bar represents standard error of the mean (see Appendix A, figure 3, for each task individually). **(d)** brain maps of the event-related (left/middle) and memory-related (right) differences in alpha/beta power.

Wimber, Henson, & Staresina, 2019; Michelmann et al., 2016; Staresina et al., 2016). Nevertheless, we wanted to further demonstrate the robustness of our acquired EEG data. To this end, the post-stimulus alpha/beta power (500-1500ms; 8-30Hz; matching previously-reported windows of retrieval-related memory effect; Michelmann et al., 2016) for remembered trials was contrasted with that of forgotten trials in a cluster-based, permutation t-test. Matching earlier reports, we found a significant reduction in alpha/beta power for recalled pairs, relative to forgotten pairs ($p = 0.017$, Cohen's $d_z = 0.56$; see figure 2.3 and Appendix A, figure 7.3). These power decreases were localised to the late visual ventral stream (including the region within the fusiform gyrus where stimulus-specific information could be identified), as well as other parts of the memory network (Rugg & Vilberg, 2014; including the medial temporal lobe and medial prefrontal cortex; see figure 2.3).

2.2.3. Alpha/beta power decreases track the fidelity of stimulus-specific information

We then addressed our central question: do alpha/beta power decreases parametrically track the fidelity of stimulus-specific information? For each participant, a single trial measure of stimulus-specific information was computed by comparing the trial pattern within the region of interest (i.e. the

significant clusters identified in the fMRI searchlight analysis; see figure 2.2) to patterns of matching and differing videos/melodies. For the perceptual data, this approach involved computing the representational distance for every pair of perceptual trials. These distances were then correlated with a unique model for each trial that stated representational distance for stimuli matching the stimulus presented would be zero and representational distance for stimuli differing from the stimulus presented on this trial would be one. The resulting correlation coefficient was Fisher z-transformed to provide a normally-distributed metric of stimulus-specific information for each trial. Alpha/beta power within the region that housed stimulus-specific information was calculated and averaged over virtual electrodes, frequency and time. The metric of stimulus-specific information was then correlated with post-stimulus alpha/beta power in a multiple regression for each participant (see figure 2.4a), which included two additional regressors that had been shown to correlate with alpha/beta power (BOLD amplitude and confidence rating; see methods and Appendix A, figure 7.4) and a regressor to account for changes in pre-stimulus power (e.g. Iemi, Chaumon, Crouzet, & Busch, 2017; van Dijk, Schoffelen, Oostenveld, & Jensen, 2008; Wöstmann, Waschke, & Obleser, 2019). The resulting beta weights were transformed into t-statistics to standardise the measurement across regressors and participants. These t-statistics were then contrasted against the null hypothesis (there is no correlation; $t = 0$) in a one-sample t-test across participants. During visual perception, we found a trending negative correlation ($p = 0.054$, Cohen's $d_z = 0.34$), where a reduction in alpha/beta power was accompanied by an increase in stimulus-specific information (see figure 2.4b). The additional regressors did not correlate with stimulus-specific information (see figure 2.4e; BOLD amplitude: $p = 0.917$, Cohen's $d_z = 0.02$; confidence rating: $p = 0.736$, Cohen's $d_z = 0.07$; pre-stimulus alpha/beta power: $p = 0.141$, Cohen's $d_z = 0.34$). During auditory perception, we found a larger, significant negative correlation ($p = 0.006$, Cohen's $d_z = 0.56$), where a reduction in alpha/beta power was accompanied by an increase in stimulus-specific information (see figure 2.4b). Neither BOLD amplitude ($p = 0.311$, Cohen's $d_z = 0.23$) nor pre-stimulus power ($p = 0.123$, Cohen's $d_z = 0.34$), correlated with the stimulus-specific information, though confidence rating did ($p = 0.031$, Cohen's d_z

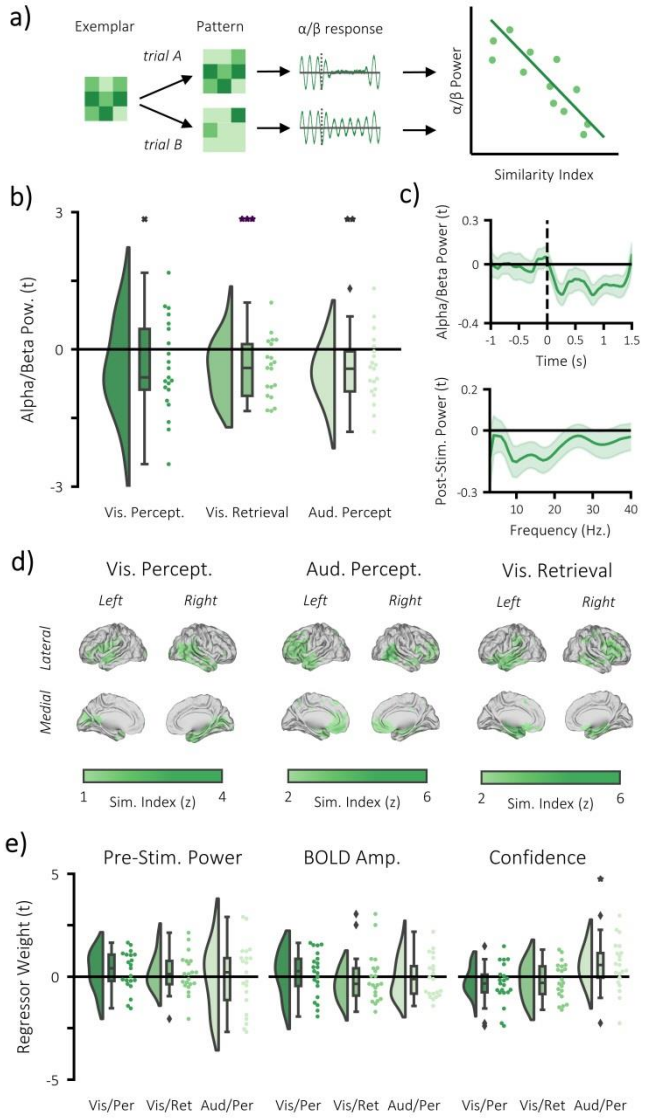

Figure 2.4. Alpha/beta power decreases track the fidelity of stimulus-specific information. (a) infographic depicting hypotheses and analytical approach. We anticipated that the more a pattern represented matching stimuli relative to differing stimuli, the greater the post-stimulus decrease in alpha/beta power would be. **(b)** Raincloud plot displaying the correlation between alpha/beta power and stimulus-specific information during visual perception, visual memory retrieval and auditory perception (each dot represents a single participant; $^{x}p = 0.054$, $^{**}p < 0.01$, $^{***}p < 0.001$). **(c)** temporal (top) and spectral (bottom) specificity of the correlation between stimulus-specific information and alpha/beta power across all tasks (see Appendix A, figure 5, for each task individually). A value below zero indicates a negative correlation between variables. The negative relationship becomes apparent after stimulus onset (time = 0) within the frequency range 8-20Hz. **(d)** brain map of the correlation between alpha/beta power at each virtual electrode with the measure of stimulus-specific information during visual perception, auditory perception and visual retrieval. **(e)** Raincloud plot displaying the correlation between stimulus-specific information and additional regressors 'pre-stimulus alpha/beta power', 'BOLD amplitude', and 'confidence rating' for each task (each dot represents a single participant; $^{*}p < 0.05$).

= 0.47). These results indicate that post-stimulus alpha/beta power decreases correlate with an increase in perceived stimulus-specific information.

We then aimed to replicate this effect in the retrieval task, working on the assumption that if alpha/beta power decreases are a proxy for information representation, the phenomenon should generalise across cognitive tasks. The correlation analysis was restricted to remembered trials to avoid a spurious correlation driven by memory-related differences in the decreases of alpha/beta power and increases of stimulus-specific information for remembered compared to forgotten trials. Representational distance was calculated between each single trial at retrieval and all trials at perception within the region of interest (i.e. the significant clusters identified in the fMRI searchlight

analysis; see figure 2.2d), and then correlated with a model that stated that representational distance for perceived stimuli matching the retrieved stimulus on this trial would be zero and representational distance for perceived stimuli differing from the retrieved stimulus on this trial would be one. The remainder of the analysis is the same as described above. In line with the previous results, we found a significant negative correlation for remembered trials ($p < 0.001$, Cohen's $d_z = 0.56$), where a reduction in post-stimulus alpha/beta power was accompanied by an increase in stimulus-specific information (see figure 2.4b-d). The additional regressors did not correlate with stimulus-specific information (BOLD amplitude: $p = 0.598$, Cohen's $d_z = 0.12$; confidence rating: $p = 0.798$, Cohen's $d_z = 0.06$; pre-stimulus alpha/beta power: $p = 0.204$, Cohen's $d_z = 0.30$).

It is worth noting that a bimodal distribution of power could explain these results (Freyer, Aquino, Robinson, Ritter, & Breakspear, 2009). To address this, we re-ran our regression analyses, this time using a median split to divide trials based on whether they had high or low alpha/beta power (approximating a bimodal split of alpha/beta power) and entering this binary regressor into the regression model in place of the continuous alpha/beta power regressor used previously. This approach found a trending link between stimulus-specific information and alpha/beta power during visual memory retrieval ($p = 0.056$, Cohen's $d_z = 0.37$; see Appendix A, figure 7.3), but not during visual perception ($p = 0.317$, Cohen's $d_z = 0.12$) or auditory perception ($p = 0.222$, Cohen's $d_z = 0.18$), suggesting that this effect cannot be consistently explained by a bimodal distribution of alpha/beta power. Furthermore, visual inspection of the distribution of alpha/beta power within each participant suggests that alpha/beta power is normally distributed around the mean, rather than bi-modally distributed (see Appendix A, figure 7.6).

It is also worth considering that functionally relevant changes in alpha/beta power needn't necessarily reflect a change in oscillatory power, but rather a change in the fractal signal (Haller et al., 2018; Miller, Sorensen, Ojemann, & Den Nijs, 2009) often referred to as the 1/f curve. In line with these ideas, we found that event-related decreases in power are a summation of decreases in oscillatory alpha/beta power and changes in the shape of the 1/f curve (see Appendix A, figure 7.7). Interestingly

however, memory-related power changes were only reflected in decreases in alpha/beta oscillatory signal. Unfortunately, we were unable to link these measures to stimulus-specific information. Quite possibly, this shortcoming is due to the fact that the 1/f curve can only be properly observed (and hence analysed) over long epochs (i.e. several seconds to several minutes; Miller et al., 2009), or when the power-spectra are averaged across trials. Indeed, we demonstrate this principle using simulated data (see Appendix A, figure 7.8). Short epochs (<5 seconds) give unreliable estimates of the 1/f curve whereas longer epochs (>30 seconds) appear much more robust. As our central analysis was event-related and conducted on the single trial level, any approach we take would be curtailed by the biologically infeasibility of getting a robust estimate of the 1/f curve in such a brief time window.

In sum, these results suggest that alpha/beta power parametrically decreases as the amount of stimulus-specific information represented within the cortex increases. While the chance of finding such an effect in the visual perception condition was marginal ($p = 0.054$), it is worth noting that its conceptual equivalents yielded more substantial support (auditory perception: $p = 0.006$; visual retrieval; $p < 0.001$). Taking all these results together, there is substantial support to suggest that post-stimulus alpha/beta power decreases correlate with stimulus-specific information.

2.2.4. Alpha/beta power decreases do not represent perceived or retrieved information

Lastly, we asked whether the observed negative correlation between alpha/beta power and stimulus-specific information could be explained by the fact that alpha/beta power, rather than providing favourable conditions for the brain to represent activity, actually represents information itself. To test this hypothesis, we conducted spatiotemporal representational similarity analysis (i.e. across virtual electrodes, time windows [500 to 1500ms, in steps of 100ms] and frequency bins [8 to 30Hz, in steps of 1Hz]) within the regions where stimulus-specific information was identified in the BOLD signal during perception and memory retrieval. By restricting analysis to regions where we had previously detected stimulus-specific information, we maximise our chance of finding an effect. Despite this extremely liberal approach, a cluster-based, permutation t-test found no evidence to suggest that alpha/beta power represents stimulus-specific information during visual perception ($p =$

0.548, Cohen's $d_z = 0.03$), auditory perception ($p = 0.773$, Cohen's $d_z = 0.17$) or visual retrieval ($p = 0.579$, Cohen's $d_z = 0.04$). Notably, the frequentist nature of this test means we cannot conclude that alpha/beta power does not represent information, but rather that there is insufficient evidence to conclude that alpha/beta power represents information. To address this limitation, we ran a Bayesian one-sample t-test to probe the nature of the evidence in favour of the null hypothesis. The continued use of the region of interest switches the test from a liberal test of the alternative hypothesis (alpha/beta represents information) to a conservative test of the null hypothesis (alpha/beta does not represent information). Bayesian one-sample t-tests revealed moderate evidence in favour of the null hypothesis for the visual perceptual ($BF_{10} = 0.230$), auditory perceptual ($BF_{10} = 0.272$), and visual retrieval tasks ($BF_{10} = 0.232$). These results suggest that the observed relationship between alpha/beta power decreases and stimulus-specific information cannot be explained by the hypothesis that alpha/beta power itself represents information. Rather these results suggest that alpha/beta power decreases are a marker of the fidelity of stimulus-specific information.

2.3. Discussion

Here, we provide empirical evidence to suggest that task-induced alpha/beta power decreases track the fidelity of stimulus-specific information represented within the cortex. We correlated simultaneously recorded alpha/beta power (as measured using scalp EEG) with a metric of stimulus-specific information (as quantified using representational similarity analysis [RSA] on fMRI data) on a trial-by-trial level. As stimulus-specific information increased, alpha/beta power decreased, regardless of whether the information was externally presented or internally generated, or whether the information was visual or auditory in nature. Further analysis revealed that this effect is not driven by the fact that alpha/beta power decreases represent information, suggesting instead that these decreases provide conditions which are beneficial for information representation.

Our central finding demonstrates that as alpha/beta power decreases, the fidelity of stimulus-specific information within the cortex increases. Task-related decreases in alpha/beta power are observable across tasks (Crone et al., 1998; Griffiths et al., 2016; Hanslmayr et al., 2009; Krause et al.,

1994; Obleser & Weisz, 2012; Pfurtscheller et al., 1994; Waldhauser et al., 2016), sensory modalities (Crone et al., 1998; Krause et al., 1994; Pfurtscheller et al., 1994), and species (Chatila et al., 1992; Haegens et al., 2011; Pfurtscheller et al., 1994; Wiest & Nicolelis, 2003). Given their ubiquity, it stands to reason that they reflect a highly general cognitive process. Our results suggest that these alpha/beta power decreases are a proxy for information representation. Mechanistically speaking, these decreases may mark information representation as they allow for a reduction of neuronal noise correlations (which map onto local field potential; LFP; Cui et al., 2016). Numerous studies have demonstrated that task-irrelevant correlated activity between pairs of neurons is detrimental to stimulus processing (Harris & Thiele, 2011; Zohary, Shadlen, & Newsome, 1994), particularly for large networks of correlated neurons (Averbeck et al., 2006) that, incidentally, are more likely to be detected in the LFP. Following the hypothesis that alpha/beta power decreases are a proxy for reductions in noise correlations (as opposed to a proxy for increased signal representation), one would predict that alpha/beta power decreases do not carry representational information about a stimulus. Rather, they provide favourable conditions (i.e. reduced noise) in which another mechanism can allow the internal representation of said stimulus to come forth. In line with this hypothesis, we found moderate evidence to suggest that alpha/beta power decreases do not carry any stimulus-specific information during the perception or retrieval of the visual stimuli. Notably, this does not contradict previous findings showing that stimulus specific information is coded in the phase of alpha oscillations (Michelmann et al., 2016). As the power and phase of an oscillation are mathematically independent, it is entirely plausible to suggest that one carries stimulus-specific information while the other does not. As such, one could view alpha/beta power decreases as a marker for the potential for information representation, rather than actually representing information.

Alpha/beta activity has also been linked to information representation based on the ideas of information theory (Hanslmayr et al., 2012; Shannon & Weaver, 1949). Information theory proposes that little information can be gathered from a highly predictable input (e.g. a network of highly correlated, spiking neurons) – if you can predict an upcoming event, you must already know details

about the event. In contrast, a lot of information can be gathered from unpredictable inputs (e.g. uncorrelated spiking neurons) – you learn a lot from a completely novel experience. It has been theorised that desynchronisation within the alpha and beta bands reduces the predictability of neuronal firing and hence boosts information processing abilities (Hanslmayr et al., 2012). For example, earlier work has demonstrated that tasks which involve greater semantic elaboration (i.e. greater information representation) produce greater alpha/beta power decreases (Hanslmayr et al., 2009). Our central result fits neatly within this framework as we find that alpha/beta power parametrically decreases with an increase in stimulus-specific information. Moreover, our finding that alpha/beta power does not directly represent stimulus-specific information fits with this idea, as these power decreases are theorised to allow complex neuronal patterns to emerge rather than generate the complex patterns themselves. Taken together, one could speculate that alpha/beta power decreases allow for the rich representation of stimulus-specific information by reducing the predictability of neural firing patterns. Notably, the information theoretic interpretation (i.e. predictable firing is bad for information representation) is highly similar to the idea that correlated firing (i.e. noise correlations) is bad for information representation because correlations are inherently predictable. This opens an exciting new line of investigation which would aim to tease apart these two hypotheses. One could directly compare whether the indiscriminate attenuation of all synchronised neuronal firing (i.e. the reduction of any form of neural synchrony) better benefits information representation than the selective attenuation of neurons that contribute to noise correlations (i.e. the sole reduction of task-irrelevant neural synchrony). Evidence supporting the former would suggest that information theory would be a better framework for understanding cortical information representation, while evidence supporting the latter would suggest that noise correlations better describe cortical information representation.

Several established accounts have interpreted high-amplitude alpha oscillations as a marker for inhibition (Jensen & Mazaheri, 2010; Klimesch et al., 2007; Pfurtscheller et al., 1996). One may wonder, then, how the current results can be reconciled with these established accounts. Quite simply, we view the information representation account and the existing inhibition accounts as two sides of the

same coin. Earlier accounts focus upon how alpha power increases reflect inhibition, our framework focuses on the complementary idea that alpha power decreases boost information representation through disinhibited networks. Importantly, we expand on these earlier accounts by demonstrating that alpha/beta power does not simply reflect a binary division between inhibition and disinhibition. Rather, alpha/beta power can parametrically track the degree to which a network can represent information. In other words, as alpha/beta power gets progressively weaker, the network becomes progressively disinhibited and, therefore, more capable of establishing detailed neural representations.

It is worth noting that we did not observe a correlation between stimulus-specific information and pre-stimulus alpha/beta power. This presents an apparent contradiction to earlier work which has shown that a decrease in pre-stimulus alpha power correlates with an increase in perceptual performance (Hanslmayr et al., 2007; van Dijk et al., 2008). A potential resolution to this peculiarity lies in a number of recent studies (Benwell et al., 2017; Iemi et al., 2017; Lange, Oostenveld, & Fries, 2013; Limbach & Corballis, 2016; Samaha, Iemi, & Postle, 2017; Whitmarsh, Oostenveld, Almeida, & Lundqvist, 2017; Wöstmann et al., 2019) which have used signal detection theory (Green & Swets, 1966) to disentangle objective and subjective measures of perceptual performance (termed 'sensitivity' and 'decision criterion' respectively). These studies demonstrate that the link between pre-stimulus alpha power and perceptual performance can be better explained by decision criterion (e.g. increases in responses rates; confidence; awareness) rather than by sensitivity (e.g. increased task accuracy). We view our measure of stimulus-specific information as one of sensitivity, as it reflects the veridical representation of information within the brain rather than the subjective experience of this information. As these previous studies have demonstrated consistently that pre-stimulus power does not correlate with measures of sensitivity, it is perhaps no surprise that we found no correlation between stimulus-specific information and pre-stimulus power.

Recent work has begun to emphasise the importance of distinguishing periodic neural activity (which can approximate oscillatory activity) from aperiodic activity (which reflects the 1/f power law; Haller et al., 2018; Miller et al., 2009). We attempted to address this question in our EEG and

combined EEG-fMRI analyses with partial success. In our EEG analyses, we demonstrated that stimulus-induced reductions in alpha/beta power are a summation of decreases in alpha/beta oscillatory activity, a flattening of the 1/f curve, and an overall increase in power. These results suggest that stimulus-induced decreases in alpha/beta power are more complicated than a simple reduction in oscillatory power. Intriguingly, memory-related change in alpha/beta activity could only be explained by a decrease in alpha/beta oscillatory power (confirming earlier findings which suggest that the 1/f curve cannot explain memory-related changes in power; Fellner et al., 2019). The contrast between these two tasks sheds light on what periodic and aperiodic measures of power may be reflecting on a cognitive level. Throughout this paper, we have emphasised how information representation is a task-general phenomenon; the fact that changes in slope only appear in post-stimulus vs. pre-stimulus perceptual contrasts and not in remembered vs. forgotten memory contrasts suggests that a change in slope does not meet the task-general requirement of an information representation hypothesis. However, the presence of alpha/beta oscillatory power decreases in both analyses means that changes in oscillatory activity may still relate to information representation. Unfortunately, we were unable to confirm this idea in the combined EEG-fMRI analyses. We would have expected stimulus-specific information to correlate with oscillatory power decreases but not changes in the slope. Our analyses, however, returned inconclusive evidence where no EEG measure appeared to correlate with stimulus-specific information. It is unclear why this occurred, but one plausible explanation is that the 1/f curve cannot be properly estimated for single-trial, event-related analyses. As the 1/f slope is a product of many seconds of recorded signal, it cannot be estimated 'instanteously' (Miller et al., 2009). Supplementary simulations (see Appendix A, figure 7.8) demonstrate this. Short epochs (<5 seconds) give unreliable estimates of the 1/f curve, but these estimates stabilise as epoch length increases (>20 seconds) or when epochs are averaged together. As our trial epochs are 1 second long, it seems implausible to suggest that any reliable separation of the 1/f curve and oscillatory power can be computed. Therefore, any result from this analysis should be treated with caution, with inferences best left to the condition-based analyses of oscillatory alpha/beta

power, which show that their decreases transcend both stimulus modality and task – fitting a domain-general information representation mechanism.

Intriguingly, our analysis revealed that the correlation between alpha/beta power decreases and stimulus-specific information was weakest during visual perception. Given that stimuli in the auditory perception task had to compete with the MRI scanner noise (potentially resulting in degraded neural representations) and the stimuli in the visual retrieval task may have been subject to retroactive interference, one would have anticipated that the measures of stimulus-specific information would have been most consistent in the visual perception task. In fact, this may be the very reason why the correlation was weakest in the visual perception task. Working on the assumption that alpha/beta power does correlate with stimulus-specific information, then in a task where neural representations of stimuli are near-perfect on every trial, alpha/beta power should not be expected to fluctuate greatly across trials either. If a small amount of noise is injected into either measure, then the correlation will be greatly reduced. If, however, neural representations of stimulus are highly variable across trials and alpha/beta power co-varies with these fluctuations, then a small amount of noise would have a less substantial impact on the correlation between stimulus-specific information and alpha/beta power. Simulations in Appendix A, figure 7.9, demonstrate this principle. In short, the comparatively small effect in the visual perception task relative to the auditory perception and memory retrieval tasks may be explained by a limited variation in stimulus representation across visual perceptual trials.

Both the causality and directionality of the central result remains open to debate. Perhaps the most critical question is whether alpha/beta power decreases are a prerequisite for information representation. We speculate that this is not the case. Our theoretical interpretation of the results views these power decreases as a means to boost a stimulus's signal-to-noise ratio by reducing noise correlations. Arguably however, the stimulus's signal-to-noise ratio can also be boosted by increasing the stimulus's signal intensity (Fries, 2015). This would lead us to hypothesise that alpha/beta power decreases are sufficient, though not necessary, for information representation. This hypothesis would explain the size of the per-subject correlation values observed here and in previous studies that linked

noise correlations and information representation (M. R. Cohen & Kohn, 2011; Zohary et al., 1994) – if other processes contribute to information representation, the correlation will not be perfect. Indeed, this hypothesis is supported by a study where task-related alpha/beta power decreases were disrupted by transcranial magnetic stimulation (TMS; Waldhauser et al., 2016). In this study, TMS reduced behavioural performance (suggesting that task-related alpha/beta power decreases facilitate information representation), but did not render participants completely incapable of recalling information (suggesting other processes also contribute to information representation). This reasoning generates an interesting question: does brain stimulation impair measures of stimulus-specific information in the BOLD signal by entraining alpha/beta activity? Addressing this question would help to clarify the extent to which alpha/beta activity influences the representation of stimulus-specific information within the cortex.

In this experiment, we focused on the alpha/beta frequencies (8-30Hz) for both theoretical (Hanslmayr et al., 2012) and pragmatic reasons (Fellner et al., 2016). This focus does ask, therefore, whether the theta and gamma frequencies (3-7Hz; 40-100Hz) relate to information in a similar manner. Both the perception and retrieval of stimuli typically induce power increases in the theta and gamma bands (Jutras et al., 2009). These power increases are not overtly congruent with the theories of information representation via neuronal decoupling (Averbeck et al., 2006; Harris & Thiele, 2011; Zohary et al., 1994) or neuronal unpredictability (Hanslmayr et al., 2012). As alpha/beta power decreases are proposed to facilitate information representation by reducing noise, however, these theta or gamma power increases could theoretically facilitate information representation through the complementary means of increasing signal strength. For example, the "communication through coherence" hypothesis proposes that neuronal representations of a stimulus are enhanced by an increase in gamma synchronicity (Fries, 2015). Given that alpha/beta power decreases frequently co-occur with gamma power increases (Burke et al., 2014), one could speculate that these two mechanisms interact such that the former reduces noise while the latter boosts signal to further optimise the efficiency of information representation.

In conclusion, we find evidence to suggest that alpha/beta power decreases track the fidelity of stimulus-specific information represented within the cortex. Given that these alpha/beta power decreases are observed across tasks (Crone et al., 1998; Griffiths et al., 2016; Hanslmayr et al., 2009; Krause et al., 1994; Obleser & Weisz, 2012; Pfurtscheller et al., 1994; Waldhauser et al., 2016), sensory modalities (Crone et al., 1998; Krause et al., 1994; Pfurtscheller et al., 1994), and species (Chatila et al., 1992; Haegens et al., 2011; Pfurtscheller et al., 1994; Wiest & Nicolelis, 2003), it stands to reason that they reflect a highly general cognitive process. Our findings suggest these power decreases reflect enhanced information representation. These power decreases may act as a proxy for information representation either through their link to reduced neuronal noise correlations (Averbeck et al., 2006; Cui et al., 2016; Harris & Thiele, 2011) or by reducing the predictability of neuronal activity (Hanslmayr et al., 2012). These results open numerous avenues for future research, such as how these decreases interact with other neural processes to facilitate the representation of stimulus-specific information, and whether brain stimulation can be used to manipulate the fidelity of information represented within the cortex. Ultimately, these results further illuminate how the ubiquitous phenomenon of task-related alpha/beta power decreases relate to the representation and comprehension of our physical and mental worlds.

2.4 Methods

2.4.1. Participants

Thirty-three participants were recruited. All participants were native English speakers with normal or corrected-to-normal vision. In return for their participation, they received course credit or financial reimbursement. Twelve of these participants were excluded from analysis: one participant was excluded due to recording issues relating to the MRI scanner, three participants were excluded due to recording issues relating to the EEG system, five participants had insufficient recalled pairs ($n<10$) following EEG artifact rejection, and three participants had insufficient forgotten pairs ($n<10$) following EEG artifact rejection. This left twenty-one participants for statistical analysis. Ethical approval was granted by the Research Ethics Committee at the University of Birmingham, complying with the Declaration of Helsinki.

2.4.2. Behavioural paradigm

Each participant completed a paired associates task (see figure 2.1b). During encoding, participants were presented with a 3 second video or sound, followed by a noun. There were a total of four videos and four sounds repeated throughout each block. All four videos had a focus on scenery that had a temporal dynamic, while the four sounds were melodies performed on 4 distinct musical instruments. Participants were asked to "vividly associate" a link between every dynamic and verbal stimulus pairing. For each pairing, participants were asked to rate how plausible (1 for very implausible and 4 for very plausible) the association they created was between the two stimuli (the plausibility judgement was used to keep participants on task rather than to yield a meaningful metric, and to ensure that motion in perceptual and retrieval blocks was consistent between tasks). The following trial began immediately after participants provided a judgement. If a judgement was not recorded within 4 seconds, the next trial began. This stopped participants from elaborating further on imagined association they had just created. After encoding, participants completed a 2-minute distractor task which involved making odd/even judgements for random integers ranging from 1 to 99. Feedback was given after every trial. During retrieval, participants were presented with every word that was presented in the earlier encoding stage and, 3 seconds later, asked to identify the associated video/sound from a list of all four videos/sounds shown during the previous encoding block. The order in which the four videos/sounds were presented was randomised across trials to avoid any stimulus-specific preparatory motor signals contaminating the epoch. Following selection, participants were asked to rate how confident they felt about their choice (1 for guess and 4 for certain). Each block consisted solely of video-word pairs or solely of sound-word pairs – there were no multimodal blocks. Each block consisted of 48 pairs, with each dynamic stimulus being presented an equal number of times (i.e. 12 repetitions of each dynamic stimulus). There were 4 blocks in total. After the second block, the structural T1-weighted image was acquired, giving participants a chance to rest. Any participant that had fewer than 10 "remembered" or 10 "forgotten" trials after EEG pre-processing were excluded from further analysis. All participants completed the task in the MRI scanner, with fMRI and EEG data acquisition occurring at both encoding and retrieval. Responses were logged using NATA response boxes.

2.4.3. Behavioural analysis

Trials were characterised as 'remembered' or 'forgotten'. Remembered trials corresponded to those in which the participant could link the verbal cue to the correct video/melody, and indicated that their decision was not a guess (i.e. confidence rating > 1). Forgotten trials corresponded to those in which the participant could not link the verbal cue to the correct video, or indicated that their decision was a guess (i.e. confidence rating = 1).

While earlier studies using this paradigm (Griffiths et al., 2019; Michelmann et al., 2016) have only considered 'highly confident' memories (i.e. max confidence rating), we chose a more lax confidence threshold to ensure that sufficient trials of each dynamic stimulus available for the fMRI representational similarity analysis. Under these criteria, participants (on average) correctly recalled 63.4% of the video-word pairs (s.d. 7.5%; range: 47.6-74.5%).

2.4.4. fMRI acquisition

The magnetic resonance imaging data was acquired using a 3T Philips scanner with a 32-channel SENSE receiver coil at the Birmingham University Imaging Centre (BUIC). Participants were instructed to avoid moving as much as they could, and motion was further restricted by placing foam pads inside the radiofrequency (RF) coil. Functional volumes consisted of 32 axial slices (4mm thickness) with 3x3mm voxels, providing full head coverage (field of view: 192x192x128mm), acquired through an echo-planar imaging (EPI) pulse sequence (TR=2s, TE=40ms, flip angle of 80°). Four dummy scans were acquired immediately prior to the beginning of each run to allow for magnetic field stabilisation. Eight runs were obtained (4 encoding runs and 4 retrieval runs), each of which acquired 255 volumes plus four dummy scans. A T1-weighted structural image (1x1x1mm voxels; TR = 7.4ms; TE = 3.5ms; flip angle = 7°, field of view = 256 x 256 x 176mm) was acquired after the second block.

2.4.5. fMRI pre-processing

Pre-processing of the fMRI data was conducted in SPM 12. The functional images first underwent slice time correction, followed by spatial realignment to the first volume of each run. The structural T1-weighted image was then co-registered to the mean image of the functional MRI data. The co-registered T1-weighted image was then segmented. For the univariate analysis, the functional and structural images were normalised to MNI space, and then smoothed using a 8x8x8mm full-width at half-maximum (FWHM) Gaussian kernel. For the RSA analyses, the data was kept in native space and not smoothed as this approach is optimal for searchlight analysis (Haynes, 2015).

2.4.6. fMRI representational similarity analysis

Searchlight-based representational similarity analysis (RSA) was conducted using a combination of the MRC CBU RSA toolbox (http://www.mrc-cbu.cam.ac.uk/methods-and-resources/toolboxes/) and custom scripts (https://github.com/benjaminGriffiths/reinstatement_fidelity). Representational distance was quantified as the

cross-validated Mahalanobis (CVM) distance (Nili et al., 2014; Walther et al., 2015), which provides an unbiased measure of pattern dissimilarity (Walther et al., 2015). The CVM approach takes a training dataset and finds weights that maximises the Euclidean distance between two stimuli. These weights are then applied to a testing dataset, and the weighted Euclidean (i.e. cross-validated Mahalanobis) distance is calculated between stimuli. For analysis of all tasks, the covariance was estimated on the training data across all four categories (that is, it is an estimate of the noise covariance). As this covariance may be rank deficient (Walther et al., 2015), the matrix underwent shrinking towards the diagonal matrix using the optimal shrinkage factor as described by Ledoit & Wolf (2004). For the analysis of the perceptual task, the time-corrected and spatially-realigned fMRI data was demeaned and then split into two partitions, with the first partition containing data from the first block and the second partition containing data from the second block. A general linear model (GLM) was then used to estimate the BOLD response for each category, separately for the two partitions (Nili et al., 2014; Walther et al., 2015). Four regressors of interest were included (that is, one regressor for each video). For each of these regressors, each video onset was modelled as a stick function spanning the duration of the video, which was then convolved with a canonical hemodynamic response function (HRF). The first partition served as training data for calculating CVM distance on the second partition, and the second partition served as training data for calculating distance on the first partition. CVM distance was computed between every stimulus pattern at encoding. The derived CVM distance was then correlated with a hypothesised model, which stated that (i) there would be a perfect correlation ($r = 1$) between the representation of each repetition of the same video, and (ii) there would be no correlation ($r = 0$) between the representation of differing videos. Spearman's correlation was used based on the ordinal nature of the hypothesised model. The resulting correlation co-efficient was then corrected using the Fisher z-transform to approximate a normal distribution. This analysis was conducted across the whole brain using searchlights with a radius of 10mm (i.e. 121 voxels). Searchlights that contained less than 60% of these 121 voxels (e.g. searchlights in the most lateral areas of the neocortex) were discarded from analysis. The Fisher z-value of each searchlight was placed in a brain map, at the centre voxel of the searchlight. For statistical inference, the resulting brain maps of each subject were analysed in a second-level one-sample t-test. The resulting group-level whole-brain map was thresholded in SPM using $p_{uncorr.} < 0.001$ and a cluster extent of $k = 10$. Clusters that were formed using this threshold were then considered "significant" if the cluster-level p_{FWE} value was less than 0.05. Notably, such cluster-forming thresholding may inflate from family-wise error rate from the expected 5% to 7-10% (Eklund, Nichols, & Knutsson, 2016) and hence classify marginal effects as

erroneously significant. As such, we cross-checked our results with a more conservative cluster-forming threshold of $p_{uncorr} < 0.0001$ and a cluster extent of k = 50 (see Appendix A, table 1). This stricter threshold did not influence the central results.

For the retrieval task, this analysis was adapted slightly. The cross-validation method used above assumes that each representation of the same video is identical, and while this is true for perception (participants always viewed one of the four identical video clips), the same is not true for retrieval (each memory consists of a unique word-video pair). To address this concern, trials that contained the same video were averaged together to maximise the video-stimulus "signal" and minimise the word-stimulus "noise". These mean patterns were then subjected to the same analysis as above. Weights maximising the Euclidean distance between each mean pattern were calculated on a training dataset, and applied to the testing dataset to allow the calculation of the CVM distance. This was conducted between every pattern at both perception and retrieval. The observed distances were then correlated with a hypothesised model, which stated that (i) there would be a perfect correlation (r = 1) between the mean representation of a video at retrieval and the mean representation of the same video at perception, and (ii) there would be no correlation (r = 0) between the mean representation of a video at retrieval and the mean representations of differing videos at perception. Any cases of perception-perception or retrieval-retrieval similarity were excluded from this model, meaning this model isolates the effects of memory reinstatement. As with the perceptual RSA analysis, the retrieval RSA analysis was conducted across the entire brain, and comparisons were corrected for accordingly. The approaches to searchlight analysis and statistical inference were identical to those described in the previous paragraph.

2.4.7. EEG acquisition

The EEG was recorded using a fMRI-compatible Brain Products system (Brain Products, Munich, Germany) and a 64-electrode cap with a custom layout (including an EOG and ECG channel). As movement within the scanner has been shown to profoundly impair EEG data quality (Fellner et al., 2016), motion sensors were attached to the EEG cap to assist in the attenuation of movement-related EEG artifacts (Jorge, Grouiller, Gruetter, van der Zwaag, & Figueiredo, 2015). Briefly, this method involves placing plastic tape under four electrodes (10-10 positions F5, F6, T7 and T8) to isolate these electrodes from the scalp, then adding an external wire to complete the circuit between the channel and the reference. Consequently, the activity recorded on these channels is the product of changes in magnetic flux. The EEG sampling rate was set to 5 kHz. Impedances were kept below 20 kΩ. All electrode positions, together with the nasion and left and right pre-auricular areas were

digitised using a Polhemus Fasttrack system (Polhemus, Colchester, VT) for use in the creation of headmodels for source localisation.

2.4.8. EEG preprocessing

All EEG analysis was carried out using MATLAB (MathWorks, Natwick, MA), the Fieldtrip (Oostenveld, Fries, Maris, & Schoffelen, 2011) and *fmrib* (Iannetti et al., 2005; Niazy, Beckmann, Iannetti, Brady, & Smith, 2005) toolboxes, and custom scripts. The raw data was first high-pass filtered (1Hz; FIR). Following this, the gradient artifact was corrected using the FASTR algorithm implemented in the *fmrib* toolbox (Iannetti et al., 2005; Niazy et al., 2005). The gradient template for each TR was modelled on the average gradient artifact of the 60 nearest TRs. Residual artifacts from the acquisition of each slice (32 slices in 2 seconds/16Hz) were filtered out using a bandstop (15.5-16.5Hz) Butterworth filter. The data was then down-sampled to 500Hz and the ballistocardiogram (BCG) artifact was corrected using optimal basis set, again implemented in the *fmrib* toolbox. Heartbeat onsets were taken from the MR scanner's physiological recordings. The continuous data was then inspected for large periods of movement which were marked and the associated MR scanner triggers deleted. Subsequently, the gradient and BCG corrections were repeated on the continuous data with the periods of movement excluded. This helped improve the accuracy of the gradient and BCG templates that were subtracted from the data. After gradient and pulse artefact correction, the data from the motion sensors were used in a multi-channel recursive least squares algorithm to regress out the remaining movement-related artifacts (Bouchard & Quednau, 2000; Masterton, Abbott, Fleming, & Jackson, 2007) [while retaining brain signal; Daniel et al., 2019)] using custom scripts previously implemented by Jorge and colleagues (2015).

All subsequent EEG pre-processing was conducted using the Fieldtrip toolbox (Oostenveld et al., 2011). First, the data was epoched into trials beginning 2 seconds before the onset of the video at perception/cue at retrieval and ending 4 seconds after the onset of the cue. Second, independent component analysis was used to remove blinks, saccades and any residual spatially-stationary noise that appeared to be linked to the cardiac artifact. Third, the data was demeaned, low-pass filtered (100Hz; Butterworth IIR) and re-referenced to the average of all channels. Fourth, the data was visually inspected to identify and reject any trials and/or channels containing residual artifacts (mean percentage of trials rejected: 23.1%; range: 10.4% to 39.1%). Fifth, the data was demeaned and re-referenced again to the average of all good channels (note that as any noise introduced by noisy channels in the earlier step will be shared by all good channels and therefore subtracted out during this re-

referencing). Lastly, the scalp level data was reconstructed in source space to attenuate residual muscle artifacts (for details, see below).

2.4.9. EEG source analysis

The preprocessed data was reconstructed in source space using individual head models, structural (T1-weighted) MRI scans and 4-layer boundary element models (BEM; using the dipoli method implemented in Fieldtrip). Electrode positions (as digitised via the Polhemus Fasttrack system) were mapped onto the surface of the scalp using fiducial points for reference. The timelocked EEG data was reconstructed using a Linearly Constrained Minimum Variance (LCMV) beamformer (van Veen, van Drongelen, Yuchtman, & Suzuki, 1997). The lambda regularisation parameter was set to 5%.

2.4.10. EEG time-frequency analysis

First, the source-reconstructed EEG data was convolved with a 6-cycle wavelet (-1 to 3 seconds, in steps of 25ms; 8 to 30Hz; in steps of 0.5Hz). Second, the resulting data was z-transformed using the mean and standard deviation of power across time and trials (Griffiths et al., 2016). Third, the data was restricted to two time/frequency windows of interest (-1000 to -375ms and 500 to 1500ms post-stimulus; both 8-30Hz; Michelmann et al., 2016) and then averaged across these windows, resulting in two alpha/beta power values per trial for each virtual electrode. To probe whether alpha/beta power decreased following stimulus onset these two values were contrasted in a one-tailed, non-parametric, cluster-based permutation-based t-test (Maris & Oostenveld, 2007) with 2000 randomisations. To investigate whether alpha/beta power decreased for remembered relative to forgotten trials, the data for the post-stimulus window was split by condition and contrasted using the same statistical approach.

2.4.11. Combined EEG-fMRI analysis

An adjusted CVM approach outlined in *fMRI representational similarity analysis* was used to quantify information for this analysis. Rather than use a searchlight, CVM distance was computed in a region of interest (ROI) defined by the searchlight analysis. Specifically, this ROI consisted of all voxels included in any significant cluster revealed in the earlier analysis plus all neighbouring voxels that would have been included in the searchlight that contributed to the cluster. This approach maximised signal-to-noise for the measure of stimulus-specific information by only focusing on voxels where stimulus-specific information could be detected (see below for a note on circularity). As before, a training dataset was used to find weights that maximally

discriminates two stimuli (per trial for encoding; averaged across repetitions for retrieval). In the case of retrieval data however, rather than project these weights onto stimulus-averaged testing dataset, these weights were projected onto the trial-level dataset. These trial-level BOLD responses were estimated using a GLM where each trial was considered as a separate regressor (using a stick function convolved with a canonical HRF as in the earlier analyses). This change in approach provides a measure of stimulus-specific information for every trial within the specified ROI.

Similarly, an adjusted approach was used to quantify EEG power per trial. Whereas the prior section measured EEG power across all virtual electrodes, this analysis was restricted to virtual electrodes included in regions that coded for stimulus-specific information (as determined by the fMRI searchlight analysis). This approach ensured that the analysed EEG signal originated from the same region as the fMRI similarity index.

These approaches yield a single measure of fMRI-derived stimulus-specific information and EEG-derived alpha/beta power for every trial. A multiple regression was then conducted for each participant, with stimulus-specific information used as the outcome variable, and post-stimulus alpha/beta power (500-1500ms) being used as the predictor. Three additional regressors were included to address potential confounds: confidence rating, BOLD amplitude within the ROI, and pre-stimulus alpha/beta power. This returned an t-value for every regressor of every participant. Group-level statistical analysis saw these t-values being contrasted against the null hypothesis ($t = 0$; there is no correlation) in a one-tailed, non-parametric, permutation-based t-test (Maris & Oostenveld, 2007) with 2000 randomisations where the observed data and null hypothesis were permuted.

We also addressed the spectral specificity of the effect. However, one should note that these results are difficult to interpret as both theta (3-7Hz) and gamma (>40Hz) bands are much more susceptible to distortion by the MRI scanner than the alpha/beta band (Fellner et al., 2016). Aside from changes to the frequencies of interest, the analysis matched that which is described above. We considered both tails of the t-test, testing two differing hypotheses: 1) a reduction in power reflects an increase in information (mirroring the central hypothesis of the paper), and 2) as theta/gamma power typically increases during cognitive engagement (Fries, 2015), an increase in power reflects an increase in information. This effect did not generalise to the theta (visual perception $p = 0.347$, visual memory retrieval $p = 0.486$, auditory perception $p = 0.163$) or gamma bands (perception $p > 0.5$, visual memory retrieval $p = 0.153$, auditory perception $p > 0.5$).

2.4.12. EEG-confidence correlation

It is plausible to suggest that the more information one recalls about an associated pair, the more confident they are in selecting the correct video. Therefore, it could be argued that alpha/beta power decreases are a confidence signal. To address this potential confound, we took our measure of EEG alpha/beta power and correlated this with the confidence rating provided on each trial. The derived r-value underwent Fisher z-transformation to approximate a normal distribution. These Fisher z-values were contrasted against the null hypothesis (there is no correlation; z = 0) across participants in a one-sample t-test. We found a significant negative correlation ($p = 0.033$, Cohen's $d = 0.48$), where a reduction in alpha/beta power was accompanied by an increase in confidence rating. While these results indicate a link between alpha/beta power and confidence, this link does not explain the link between alpha/beta power and stimulus-specific information (as evidenced by the regression analysis reported in the results section).

2.4.13. EEG Irregular-Resampling Auto-Spectral Analysis (IRASA)

IRASA analyses was conducted using the Matlab toolbox created by Wen and Liu (2016) (available at: https://purr.purdue.edu/publications/1987/1). The power spectral density (PSD) was estimated for each trial and then averaged across trials from the same condition (either post-stimulus power or pre-stimulus power for perceptual analyses; either remembered or forgotten power for the memory retrieval analysis) to get a robust estimate of the 1/f curve. The averaged PSD were then subjected to the IRASA algorithm, which splits the PSD into two power spectra – the fractal component (approximating the 1/f curve) and the oscillatory component (approximating underlying oscillatory activity). To get the slope and intercept of the 1/f curve, the fractal power spectrum (A) and its associated frequencies (B) were put into log-space (to provide a linear line), and then the linear equation $A = Bx+y$ was solved using least-squares regression, where x is the slope of the 1/f curve and y is the intercept. Oscillatory power was the calculated as the mean power between 8 and 25Hz (as the maximum frequency to be derived is one quarter of the sampling rate [100Hz]), matching the approach used for the wavelet analysis to facilitate cross-analysis comparison.

For the combined EEG-fMRI analysis, IRASA was computed on the single-trial level and then all three resulting estimates (slope, intercept, oscillatory power) were entered into a multiple regression in the same manner reported for the wavelet-based EEG-fMRI analyses. No effect was found for any element, perhaps because the 1/f cannot be robustly estimated over short time windows (Miller et al., 2009) (see Appendix A, figure 7.8).

2.4.14. A note on circularity

The use of data-driven regions of interest (ROIs) can, in some cases, introduce circularity into the analysis (Kriegeskorte, Simmons, Bellgowan, & Baker, 2009). As a result, this can overestimate the size of an effect. However, we contend that our use of data-driven ROIs does not fall foul to this analytical flaw. Explicitly stated, the concern here is that by selecting the ROI that carries stimulus-specific information in the BOLD signal, we inflate the chance of finding a correlation between BOLD-derived stimulus-specific information and alpha/beta power in the same ROI. This concern is only valid when alpha/beta power also carries stimulus-specific information. In such an instance, we would essentially be limiting our correlation between two metrics of stimulus-specific information to a ROI where we know that (in this dataset) stimulus-specific information is represented. However, a Bayesian inference of RSA conducted on alpha/beta power (see results and section below) demonstrated that there is moderate evidence in favour of the null hypothesis that alpha/beta power does not carry stimulus-specific information. In light of this, we can infer that the use of data-driven ROIs in this instance does not introduce circularity into our analysis.

2.4.15. EEG representational similarity analysis

To identify whether alpha/beta power carried stimulus-specific information, representational similarity analysis was conducted on the EEG time-frequency data (for perception and successful retrieval separately). The time-frequency data was derived in the same manner as described in the earlier section, but rather than average over time/frequency (as described in the third step), the individual time and frequency bins were retained. Representational similarity was quantified using Spearman's correlation across all features (i.e. time, frequency and location) of every pair of trials. The resulting value underwent Fisher-z transformation to approximate a normal distribution. The observed similarity was then contrasted against the same models used in the earlier RSA approaches. This resulted in a single value describing stimulus-specific information for each subject, which was tested against the null hypothesis (there is no stimulus-specific information in alpha/beta power) in a one-tailed, non-parametric, permutation-based t-test (Maris & Oostenveld, 2007).

As we found insignificant evidence to support the alternative hypothesis, we then took a Bayesian approach to the statistical analysis. The same values used in above were analysed in a Bayesian one-sample t-test (as implemented in JASP, version 0.9 (JASP-Team, 2018)). We interpreted the resulting Bayes factor in line with the rule of thumb (Lee & Wagenmakers, 2013).

CHAPTER 3: HIPPOCAMPAL "FAST" AND "SLOW" GAMMA OSCILLATIONS PLAY UNIQUE ROLES IN EPISODIC MEMORY FORMATION AND RETRIEVAL.

Hippocampal gamma oscillations (30-100Hz) are thought to support both episodic memory formation and retrieval. While these oscillations have traditionally been viewed as a singular band, recent evidence suggests that they can be divided into "fast" (~60Hz) and "slow" (~40Hz) gamma bands, with the former supporting encoding and the latter supporting retrieval. Here, we test this hypothesis by analysing human intracranial EEG data recorded during two associative memory tasks. We find that hippocampal "fast" gamma activity is more prominent during memory encoding while hippocampal "slow" gamma activity is more pronounced during retrieval. Moreover, we demonstrate that this is functionally relevant to memory success – enhanced "fast" gamma activity reflects successful memory formation while "slow" gamma activity reflects successful memory retrieval. These findings provide the first empirical evidence to suggest that two dissociable gamma bands exist in the human hippocampus that have functionally distinct roles in episodic memory formation and retrieval.

Published in:

Griffiths, B. J., Parish, G., Roux, F., Michelmann, S., van der Plas, M., Kolibius, L. D., Chelvarajah, R., Rollings, D. T., Sawlani, V., Hamer, H., Gollwitzer, S., Kreiselmeyer, G., Staresina, B., Wimber, M., & Hanslmayr, S. (2019). Directional coupling of slow and fast hippocampal gamma with neocortical alpha/beta oscillations in human episodic memory. Proceedings of the National Academy of Sciences of the United States of America. doi: 10.1073/pnas.1914180116

3.1. Introduction

An episodic memory is a high-detailed memory of a personally-experienced event (Tulving, 2002; Tulving & Thomson, 1973). The formation of such memories hinge upon: i) the representation of information relevant to the event, and ii) the binding of this information into a coherent episode. The latter of these processes is thought to be facilitated by the synchronisation of hippocampal gamma oscillations (~60Hz; Axmacher, Mormann, Fernández, Elger, & Fell, 2006; Nyhus & Curran, 2010). These gamma oscillations match the rhythm required for spike-timing dependent plasticity (STDP; a form of long-term potentiation; LTP) to occur (Bi & Poo, 1998). Therefore, an increase in the amplitude of hippocampal gamma oscillations may reflect an increase in STDP (Nyhus & Curran, 2010). Such a hypothesis would provide a mechanistic interpretation of how increases in hippocampal gamma power relate to episodic memory formation.

Intriguingly, increases in hippocampal gamma power have also been linked to episodic memory retrieval (e.g. Montgomery & Buzsáki, 2007; Staresina et al., 2016). These findings are harder to reconcile with the idea that hippocampal gamma power increases reflect STDP, as STDP during retrieval has the potential to damage a memory trace by unintentionally binding the reinstated memory with current sensory experience. A resolution to this apparent contradiction, however, has emerged in several animal models. Colgin and Moser (2010) have proposed that two gamma oscillations co-exist in the hippocampal circuit: a "fast" gamma oscillation (~60Hz) generated in the medial entorhinal cortex (MEC), and a "slow" gamma oscillation (~40Hz) generated in the hippocampal subfield CA3. The fast gamma oscillation is purported to facilitate encoding by routing information into the hippocampus via the MEC, while the slow gamma oscillation facilitates retrieval by routing reinstated memory traces out of CA3 to CA1, and then to the neocortex. Providing empirical support for this idea, Bragin and colleagues (1995) demonstrated that lesions to the MEC impaired both the generation of the "fast" gamma rhythm and the animal's ability to learn new associations, without impairing the "slow" gamma rhythm or the animal's ability to retrieve old associations. While several studies have

found support for the "fast" vs. "slow" gamma distinction in animals (e.g. Bragin et al., 1995; Colgin et al., 2009), evidence for this in humans is absent. Here, we address this gap in knowledge.

In this experiment, we asked whether the spectral profile of hippocampal gamma power varies as a function of encoding and retrieval. Specifically, we hypothesised that "fast" gamma oscillations (~60Hz) would support encoding while "slow" gamma oscillations (~40Hz) would support memory retrieval (Colgin, 2015b; Colgin et al., 2009). To test this, twelve patients implanted with stereotactic EEG electrodes for the treatment of medication-resistant epilepsy completed one of two associative memory tasks (see figure 3.1a-b; n=7 in task 1; n=5 in task 2). In task 1, they related life-like videos/sounds to words that followed. Following a short distractor task, participants attempted to recall the previously presented videos/sounds using the words as cues. In task 2, they related an object to pairs of visual stimuli that followed (face-place, face-face or place-place). Following a short distractor task, participants attempted to recall both stimuli, using the object as a cue. Foreshadowing the results below, we show that increases in hippocampal "fast" gamma power selectively support successful memory formation, while increases in hippocampal "slow" gamma power selectively support successful memory retrieval.

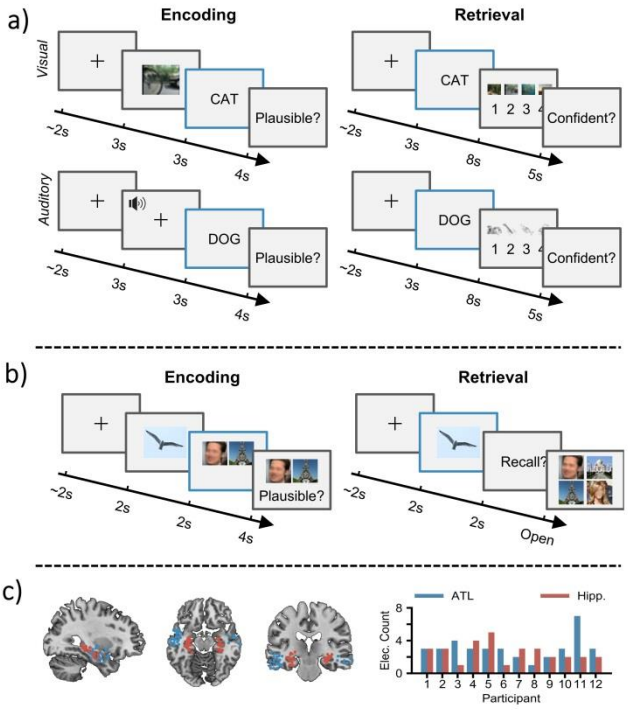

Figure 3.1. Experiment setup. (a) During encoding, participants are tasked with forming an associative link between a life-like dynamic stimulus (either a video or sound) and a subsequent verbal stimulus. During retrieval, participants are presented with verbal stimuli from the previous encoding block and asked to retrieve the associated dynamic stimulus. Electrophysiological analysis was conducted during the presentation of the verbal stimulus at encoding and retrieval (blue outline). **(b)** During encoding, participants are tasked with forming an associative link between an object, a face and a scene. During retrieval, participants are presented with the object and asked to retrieve the associated face and scene. Electrophysiological analysis was conducted during the presentation of the verbal stimulus at encoding and retrieval (blue outline). **(c)** Plot of each electrode location (left; red represents hippocampal electrode; blue represents ATL. Bar plot (right) depicts number of electrodes for each participant.

3.2. Results

3.2.1. Behavioural results

Participants, on average, recalled 47.9% of all pairs in the first task, a percentage much greater than what would be expected by chance (25%). When breaking trials down by modality, participants recalled 52.7% of video-word pairs and 45.9% of sound-word pairs. An independent samples t-test (only a subset of participants completed both variants of the task) revealed no significant difference in memory performance for video-word and sound-word pairs ($p > 0.5$, $d = 0.275$). As there was no apparent difference in memory performance between the two trials types, and electrode contacts were not located in anatomical regions that should respond uniquely to one of these sensory modalities, trials involving video-word and sound-word pairs were combined for all further analyses. In the second task, participants recalled both associated items on 66.2% of trials - a percentage much greater than what would be expected by chance (16.7%; where the probability of selecting the first item correctly is 50% and the probability of selecting the second item correctly is 33%, making the joint probability 50% x 33% ~ 16.7%).

3.2.2. A shift in "fast" and "slow" gamma between the formation and retrieval of episodic memories

We first investigated whether distinct gamma frequency bands can be identified during encoding and retrieval processes (Colgin, 2015b; Colgin et al., 2009). To test this, the 1/f-corrected broadband hippocampal gamma power (30-100Hz) for successfully remembered pairs at encoding and retrieval was calculated and contrasted in a group level, non-parametric permutation test. "Fast" hippocampal gamma frequencies (60-80Hz) exhibited significantly greater power during encoding trials, relative to retrieval trials (60-70Hz, $p_{fdr} = 0.001$, $d = 1.308$; 70-80Hz, $p_{fdr} = 0.020$, $d = 0.947$; see figure 3.2b-e). In contrast, "slow" hippocampal gamma frequencies (40-50Hz) exhibited greater power during retrieval trials, relative to encoding trials ($p_{fdr} = 0.023$, $d = 0.754$). No significant difference between encoding and retrieval could be observed during the epochs of forgotten stimuli (see Appendix B,

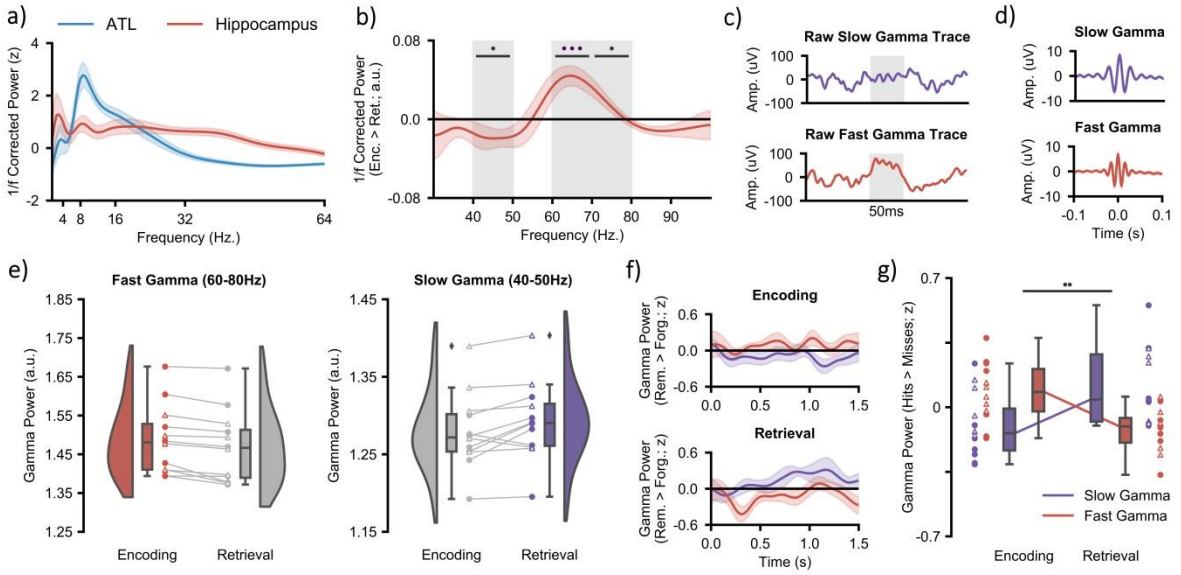

Figure 3.2. Hippocampal gamma power during encoding and retrieval. **(a)** the mean 1/f corrected power spectrum (with shaded standard error of the mean) across all encoding and retrieval trials reveals theta and gamma peaks in the hippocampus and an alpha/beta peak peak in the ATL. **(b)** the mean difference in gamma power (with shaded standard error of the mean) between encoding and retrieval reveals a peak in encoding-related, "fast" gamma at 60-80Hz and a peak in retrieval-related, "slow" gamma at 40-50Hz (*pfdr < 0.05, ***pfdr < 0.001. **(c)** raw slow gamma signal during retrieval (top) and fast gamma signal during encoding (bottom) from a hippocampal contact of participant 1. The shaded grey region indicates a period of 50 milliseconds. **(d)** mean peak-locked averaged signal across participants for slow (top) and fast (bottom) gamma (with shaded standard error of the mean). **(e)** raincloud plots depicting the difference in fast (left) and slow (right) gamma power between encoding and retrieval. Coloured circles represent participants who took part in experiment 1. Uncoloured triangles represent participants who took part in experiment 2. **(f)** time-series of slow (in purple) and fast (in red) memory-related gamma power for encoding and retrieval. **(g)** interaction between fast and slow gamma activity during encoding and retrieval. Encoding sees a relative increase of memory-related fast gamma power, while retrieval sees a relative increase of memory-related slow gamma power.

figure 8.2). Peak "fast" and "slow" gamma frequencies for each participant were derived from the "encoding vs. retrieval" contrast and used in all subsequent analyses (see methods for details; see Appendix B, table 8.1, for individual peak frequencies). These findings suggest that two dissociable gamma band oscillations relate to episodic memory formation and retrieval in humans.

To rule out the possibility that the difference in "fast"/"slow" gamma was driven by the 1/f slope and/or its removal, the beta weights describing the 1/f slope at encoding and retrieval were extracted and averaged across time, electrodes and trials. These weights were then contrasted between encoding and retrieval in a group level, non-parametric permutation test. This test revealed no significant difference in the beta weights for remembered items ($p = 0.198$) or for forgotten items ($p = 0.246$),

suggesting the distinction in gamma rhythms between encoding and retrieval was not driven by differences in the 1/f slope.

3.2.3. Hippocampal gamma power increases track the successful formation and retrieval of episodic memories

To examine how memory-related fluctuations in "fast" and "slow" gamma power differentially contribute to successful episodic memory encoding and retrieval, we conducted a group level, non-parametric, permutation-based, 2x2 repeated measures ANOVA that investigated the influence of factors 'gamma frequency' ("fast" vs. "slow") and 'memory operation' (encoding vs. retrieval) on memory-related power (remembered > forgotten) collapsed across time. We anticipated an interaction whereby "fast" gamma selectively supports successful memory formation and "slow" gamma selectively supports successful memory retrieval. Indeed, group analysis revealed a significant interaction ($p = 0.003$, partial $\eta^2 = 0.294$; see figure 3.2g), indicating that "fast" and "slow" gamma exhibited dissimilar memory-related power fluctuations during encoding and retrieval. In other words, "fast" and "slow" gamma band oscillations differentially contributed to the successful formation and retrieval of episodic memories in humans.

Analysis of the power time series showed that the opposing effect of "fast" and "slow" gamma was particularly prominent during retrieval. When successfully recalling a stimulus, a rapid decrease in "fast" gamma power was observed (200-400ms, $p_{fdr} = 0.025$, $d = 0.862$, see figure 3.2f), followed by an increase in "slow" gamma power (800-1000ms, $p_{fdr} = 0.007$, $d = 1.177$, see figure 3.2f), relative to stimuli that were not recalled. Perplexingly, a similar effect was not observed during encoding even though the time series of the two gamma bands trend in the correct directions (i.e. an increase in "fast" gamma and a decrease in "slow" gamma; see figure 3.2f). As will be revealed in the next chapter, this absence may be driven by the fact that gamma power changes are not time-locked to stimulus onset during encoding, but are rather time-locked to the neocortical power decreases that precede hippocampal "fast" gamma activity.

3.3. Discussion

To successfully encode and recall episodic memories, we must be capable of 1) representing detailed multisensory information, and 2) binding this information into a coherent episode. The latter of these tasks is thought to relate to on hippocampal gamma synchronisation (as measured by increases oscillatory gamma power; Colgin, 2015b; Hanslmayr et al., 2016, 2012; Lisman & Jensen, 2013). Here, we demonstrate that two functionally distinct gamma oscillations exist within the hippocampus. Specifically, we uncover evidence to suggest that increases in "fast" hippocampal gamma power (60-80Hz) facilitate episodic memory formation while increases in "slow" hippocampal gamma power (40-50Hz) facilitate episodic memory retrieval.

Numerous studies have linked increases in hippocampal gamma power to the formation of episodic memories (for reviews, see Colgin & Moser, 2010; Hanslmayr et al., 2016; Nyhus & Curran, 2010). Given the hippocampal gamma oscillations resonating at around 60Hz are optimal for inducing STDP (Bi & Poo, 1998), these gamma power increases have been interpreted as a proxy for increases in STDP (Nyhus & Curran, 2010). However, such a hypothesis fails to explain why similar increases in hippocampal gamma power facilitate episodic memory retrieval. STDP is not required, and indeed may be detrimental, to memory retrieval. An alternative view proposes that there are, in fact, two distinct gamma oscillations in the hippocampus: a "fast" gamma oscillation (~60Hz) generated in MEC and a "slow" gamma oscillation (~40Hz) generated in CA3 (Colgin & Moser, 2010). The former is thought to facilitate encoding while the latter is thought to facilitate retrieval. While several animal studies have drawn empirical support for this idea (Bragin et al., 1995; Colgin et al., 2009), evidence in humans has remained elusive. The results reported above address this gap in knowledge. We demonstrate that "fast" gamma power increases (60-80Hz) uniquely reflect successful episodic memory formation while "slow" gamma power increases (40-50Hz) uniquely reflect successful memory retrieval.

As our observed "fast" gamma power increases map neatly onto the optimal STDP timing (Bi & Poo, 1998), they support earlier interpretations of memory-boosting gamma power increases during

encoding. Moreover, as our observed "slow" gamma power increases are notably slower than the optimal STDP timing, our results explain how gamma power increases can arise during retrieval without representational binding occurring between the retrieved memory trace and current sensory experience. Moreover, this view integrates neatly with information routing within the hippocampus (Colgin et al., 2009). In combination, one could speculate that the "fast" gamma oscillations facilitate coupling between the MEC and CA1, allowing information represented within the neocortex to flow into the hippocampus at a frequency optimal for STDP. The "slow" gamma oscillations, in contrast, facilitate coupling between CA3 and CA1, allowing memory traces reinstated in CA3 to be passed into CA1, and then passed onwards to the neocortex, at a frequency too slow for STDP to arise.

One question does remain however: are the observed "fast"/"slow" gamma bands truly reflective of two true narrowband oscillations? While we have uncovered a distinction between "fast" and "slow" gamma frequencies during encoding and retrieval, we cannot say with certainty whether these differences are driven by two distinct oscillators, as proposed by others (Bragin et al., 1995; Colgin, 2016; Colgin et al., 2009). Indeed, one could argue that the observed differences are driven by fluctuations in the frequency of a single oscillator. While we are unaware of such a phenomenon in hippocampal gamma, such an effect has been reported in neocortical alpha (Benwell et al., 2018). Notably however, the reported alpha-band fluctuations were very subtle (<0.5Hz), so it'd be highly questionable to interpret the much larger 25Hz shift between "fast" and "slow" hippocampal power as originating from this alpha-band 'fluctuation' mechanism. One could alternatively argue that the bandwidth of a single oscillator frequency may fluctuate as a function of memory operation, giving an apparent shift in the ratio between "fast" and "slow" gamma. However, such an effect should introduce a symmetrical change around the peak. This is not present in our data, which suggests that such an effect is ill-suited to explain the observed difference in "fast" and "slow" gamma. In short, while any electrophysiological effect can be interpreted in many ways, it seems the most parsimonious explanation is that distinct "fast" and "slow" gamma bands differentially influence memory operations, as proposed by Colgin (2015b).

In summary, we uncover evidence to suggest that distinct hippocampal gamma oscillations service human episodic memory formation and retrieval, with faster (~60-80Hz) oscillations supporting encoding and slower (~40-50Hz) oscillations supporting retrieval. The former may facilitate STDP, strengthening associative connections between stimuli being passed to the hippocampus from the neocortex, via the MEC. In contrast, the latter may reflect the transference of memory traces within CA3 to CA1, before reinstatement in the neocortex.

3.4. Methods

3.4.1. Participants

Twelve patients (n = 8 from Queen Elizabeth Hospital Birmingham, UK; n = 4 from University Hospital Erlangen, Germany; 41.7% female; mean age = 35.5 years, range = 24 to 53 years) undergoing treatment for medication-resistant epilepsy took part in the experiment. These participants had intracranial depth electrodes implanted for diagnostic purposes. Ethical approval was granted by the NHS Health Research Authority (15/WM/0219) and the Ethik-Kommission der Friedrich-Alexander Universität Erlangen-Nürnberg (142_12 B). Informed consent was obtained in accordance with the Declaration of Helsinki.

3.4.2. Behavioural paradigm: word-dynamic associative task

Seven of the twelve participants completed this paired associates task (see figure 3.1c). During encoding, participants were presented with a 3 second video or sound, followed by a word in the participant's native language (English, n = 6; German; n = 1; presented for 3 seconds). There were a total of four videos and four sounds, repeated throughout each block. All four videos had a focus on scenery that had a temporal dynamic, while the four sounds were melodies performed on 4 distinct musical instruments. Due to time restraints, some participants only completed the experiment using one modality of dynamic stimulus (sound, n=1; video, n=5; both, n=2). Participants were asked to "vividly associate" these two stimuli. For each pairing, participants were asked to rate how plausible (1 for very implausible and 4 for very plausible) the association they created was between the two stimuli (the plausibility judgement was used to keep participants on task rather than to yield a meaningful metric). The following trial began immediately after participants provided a judgement. If a judgement was not recorded within 4 seconds, the next trial began. This stopped participants from elaborating further on imagined association they had just created. After encoding, participants completed a 2-minute

distractor task which involved making odd/even judgements for random integers ranging from 1 to 99. Feedback was given after every trial. During retrieval, participants were presented with every word that was presented in the earlier encoding stage and, 3 seconds later, asked to identify the associated video/sound from a list of all four videos/sounds show during the previous encoding block. The order in which the four videos/sounds were presented was randomised across trials to avoid any stimulus-specific preparatory motor signals contaminating the epoch. Following selection, participants were asked to rate how confident they felt about their choice (1 for guess and 4 for certain). Each block consisted solely of video-word pairs or solely of sound-word pairs – there were no multimodal blocks. Each block initially consisted of 8 pairs, with each dynamic stimulus being present in two trials. However, the number of pairs increased by steps of 8 if the number of correctly recalled pairs was greater than 60% - this ensured a relatively even number of hits and misses for later analysis. Participants completed as many blocks/trials as they wished. Any participant that had fewer than 10 "remembered" or 10 "forgotten" trials after iEEG pre-processing were excluded from further analysis.

All participants completed the task on a laptop brought to their bedside. Responses were logged using the 'f', 'g', 'h' and 'j' keys, which corresponded to values '1', '2', '3', and '4'. To aid comprehension, snippets of paper were placed on top of each relevant keyboard keys with the associated numerical value written upon them. The auditory stimuli were presented via the laptop's speakers due to concerns that earphones could prove painful to the participants following electrode implantation just above the ear.

3.4.3. Behavioural paradigm: animal-face-place associative task

Five of the twelve participants completed this paired associates task (see figure 3.1d). During encoding, participants were first presented with an image cue of an animal for 2 seconds, followed by a pair of 2 images made up of any combination of a famous face or a famous place (i.e. face-place, face-face or place-place pairs; presented for 2 seconds). There were initially a total of 20 image pairs, repeated throughout each block. This number was reduced if the hit-rate fell below 66.25%, or increased if the hit-rate surpassed 73.75%. Participants were asked to "vividly associate" these two stimuli. For each pairing, participants were asked whether the association was plausible or implausible (the plausibility judgement was used to keep participants on task rather than to yield a meaningful metric). Participants were self-paced in providing a judgement, and the following trial began immediately afterwards. After encoding, participants completed a distractor task which involved making odd/even judgements for 15 sequentially presented random integers, ranging from 1 to 99. Feedback was given after every trial. During retrieval, participants were presented with every animal image cue that was presented in

the earlier encoding stage and, 2 seconds later, asked how many of the associated face or place pairs they could remember (participants had the option of responding with 0, 1 or 2). If the participant remembered at least one image, they were then asked to select the pair of images from a panel of four images shown during the previous encoding block (2 targets & 2 distractors). Participants were self-paced during the retrieval stage, though the experiment ended after a runtime of 40 minutes in total. All participants completed the task on a laptop brought to their bedside. Any participant that had fewer than 10 "remembered" or 10 "forgotten" trials after iEEG pre-processing were excluded from further analysis.

3.4.4. Behavioural coding

For the first associative task, trials were classified as "remembered" if the participant selected the correct dynamic stimulus and stated that they were highly confident about their choice (i.e. scored 4 on the 4-point confidence scale). Trials were classified as "forgotten" if the participant selected the incorrect dynamic stimulus, did not respond, or stated that they guessed their choice (i.e. scored 1 on the 4-point confidence scale). For the second associative task, trials were classified as "remembered" only if the participant indicated that they remembered both images and subsequently selected both correctly from the panel. Trials were classified as "forgotten" in all other cases, where the participant indicated that they did not remember at least one image and/or subsequently selected one of the images incorrectly from the panel.

3.4.5. Statistical analysis

While the two tasks differed in external stimulation, the underlying cognitive and neural phenomena relating to hypotheses is expected to be consistent across tasks. Therefore, the data for the two tasks were pooled. Unless explicitly stated otherwise in the results section, all statistics were conducted on the group level (i.e. random effects) using non-parametric, permutation based statistical tests. In analyses where multiple comparisons were made (e.g. time-series differences), the false-discovery rate correction (Benjamini & Hochberg, 1995) was applied (denoted as p_{fdr}). Effect sizes accompany each reported p-value; Cohen's d was used for all t-tests (denoted as d). For reference, Cohen (J. Cohen, 1988) suggested that d=0.8 indicates a large effect, d=0.5 indicates a medium effect, and d=0.2 indicates a small effect. Partial eta squared was used as a measure of effect size for all ANOVAs (denoted as partial η^2). For reference, partial $\eta^2 = 0.25$ indicates a large effect, partial $\eta^2 = 0.09$ indicates a medium effect, and partial $\eta^2 = 0.01$ indicates a small effect.

3.4.6. iEEG acquisition and preprocessing

First, the raw data was epoched; for encoding trials, epochs began 2 seconds before the onset of the visual/auditory stimulus and ended 4 seconds after verbal stimulus onset (9 seconds in total); for retrieval trials, epochs began 2 seconds before, and ended 4 seconds after, the onset of the verbal cue (6 seconds in total). Second, the data was filtered using a 0.2Hz finite-impulse response high-pass filter and 3 finite-impulse response band-pass filters at 50±1Hz, 100±1Hz and 150±1Hz, attenuating slow-drifts and line noise respectively. Third, as the iEEG data was sampled at the physician's discretion (512Hz, n=1; 1024Hz, n=11), all data was down-sampled to 500Hz. Fourth, the data from each electrode was re-referenced to an electrode on the same shaft that was positioned in white matter (determined by visual inspection of the participant anatomy; see below). The use of a common reference electrode for both the hippocampus and neocortex ensured that any difference in electrophysiological signal from the two regions could not be explained by a difference in reference. Finally, the data was visually inspected and any trials exhibiting artefactual activity were excluded from further analysis. Any electrodes exhibiting persistent ictal and interictal activity (as identified through visual inspection) were discarded from analysis.

3.4.7. Electrode localisation

First, hippocampal and white matter contacts were defined based on anatomical location through visual inspection of the T1-weighted anatomical scan. For visualisation in figure 3.1d, every electrode from every participant was given a diameter of 1cm and then placed in a template brain registered in MNI space.

3.4.8. 1/f correction

Spectral power was computed using 199 linearly-spaced 5-cycle wavelets ranging from 1 to 100Hz. The time-frequency decomposition method was kept consistent across all frequency bands to ensure that only a single slope (characterising the full extent of the 1/f dynamic) needed to be calculated and subsequently subtracted from the signal (in line with previous experiments that have extracted the 1/f characteristic from the signal; e.g. Manning et al., 2009; Zhang & Jacobs, 2015). A vector containing values of each wavelet frequency (A) and another vector containing the power spectrum for each electrode-sample pair (B) were then log-transformed. The linear equation $Ax = B$ was solved using least squares regression, where x is an unknown constant describing the curvature of the 1/f characteristic. The 1/f fit (Ax) was then subtracted from the log-transformed power-spectrum (B).

3.4.9. Peak frequency analysis

Raw signal recorded at every contact for each epoch was convolved with a 5-cycle wavelet (0 to 1500ms post-stimulus [padded with real data for lower frequencies], in steps of 25ms; 30Hz to 100Hz, in steps of 0.5Hz). The 1/f noise was subtracted using the method described above to help pronounce the peaks in the power-spectrum. The data was then smoothed using a Gaussian kernel (full-width half-maximum 200ms; 5Hz) to attenuate inter- and intra-individual differences in spectral responses (Benwell et al., 2018) and to help approximate normally distributed data (an assumption frequently violated in small samples). The data was averaged across all time-points, trials and contacts. Peaks of 1/f corrected absolute power were then identified using the *findpeaks()* peak-detection algorithm implemented in Matlab. The power-spectra for encoding and retrieval were then collapsed in seven 10Hz bins and contrasted in a group level (i.e. random effects), non-parametric permutation test (Maris & Oostenveld, 2007) with 5000 randomisations. The multiple comparison issue was solved using the false-discovery rate correction (Benjamini & Hochberg, 1995). This analysis was repeated for the "forgotten" trials.

3.4.10. Selection of peak frequencies

The peak frequencies of each patient were determined using the MATLAB function *findpeaks()* on the averaged power spectrum around the approximate frequency bands ("slow" gamma: 30-60Hz; "fast" gamma: 50-100Hz). The bandwidths of these peaks were kept consistent across participants, set at ±10Hz (see Appendix B, table 8.1, for individual peak frequencies).

3.4.11. Spectral power analysis

For all spectral power analyses (i.e. encoding and retrieval epochs), the data underwent the same wavelet convolution, 1/f correction, and smoothing approaches described in the *peak frequency analysis* section. The data was then z-transformed using the means and standard deviations of each electrode-frequency pair (Griffiths et al., 2016). The time-frequency resolved data was then averaged over electrodes within the hippocampus. For time-series statistical analysis, trials were split into two groups based on whether the stimuli were remembered or forgotten. Then, the time-series were collapsed into seven time bins of 200ms and the two conditions were contrasted using the same non-parametric statistical procedure described in the *peak frequency analysis* section. For statistical analyses of the interaction between memory task (encoding vs. retrieval) and gamma frequency ("fast" vs. "slow"), this memory-related difference in power (i.e. SME and RSE) was averaged over time and contrasted in a non-parametric, permutation based 2x2 repeated measures ANOVA.

CHAPTER 4: DIRECTIONAL COUPLING OF SLOW AND FAST HIPPOCAMPAL GAMMA WITH NEOCORTICAL ALPHA/BETA OSCILLATIONS IN HUMAN EPISODIC MEMORY

Episodic memories hinge upon our ability to process a wide range of multisensory information and bind this information into a coherent, memorable representation. On a neural level, these two processes are thought to be supported by neocortical alpha/beta desynchronisation and hippocampal theta/gamma synchronisation, respectively. Intuitively, these two processes should couple to successfully create and retrieve episodic memories, yet this hypothesis has not been tested empirically. We address this by analysing human intracranial EEG data recorded during two associative memory tasks. We find that neocortical alpha/beta (8-20Hz) power decreases reliably precede and predict hippocampal "fast" gamma (60-80Hz) power increases during episodic memory formation; during episodic memory retrieval however, hippocampal "slow" gamma (40-50Hz) power increases reliably precede and predict later neocortical alpha/beta power decreases. We speculate that this coupling reflects the flow of information from neocortex to hippocampus during memory formation, and hippocampal pattern completion inducing information reinstatement in the neocortex during memory retrieval.

Published in:

Griffiths, B. J., Parish, G., Roux, F., Michelmann, S., van der Plas, M., Kolibius, L. D., Chelvarajah, R., Rollings, D. T., Sawlani, V., Hamer, H., Gollwitzer, S., Kreiselmeyer, G., Staresina, B., Wimber, M., & Hanslmayr, S. (2019). Directional coupling of slow and fast hippocampal gamma with neocortical alpha/beta oscillations in human episodic memory. Proceedings of the National Academy of Sciences of the United States of America. doi: 10.1073/pnas.1914180116

4.1. Introduction

An episodic memory is a high-detailed memory of a personally-experienced event (Tulving, 2002; Tulving & Thomson, 1973). The formation and retrieval of such memories hinge upon: i) the representation of information relevant to the event, and ii) the binding of this information into a coherent episode. A recent framework (Hanslmayr et al., 2016) and computational model (Parish et al., 2018) suggest that the former of these processes is facilitated by the desynchronisation of neocortical alpha/beta oscillatory networks (8-20Hz; reflected in decreases in oscillatory power; Hanslmayr, Staudigl, & Fellner, 2012), while the latter is facilitated by the synchronisation of hippocampal theta and gamma oscillations (3-7Hz; 40-100Hz; reflected in increases in oscillatory power; Colgin, 2015b; Nyhus & Curran, 2010) [see figure 4.1a]. Critically, the framework posits that these two mechanisms need to cooperate, as an isolated failure of either of these mechanisms would produce the same undesirable outcome: an incomplete memory trace. Here, we test this framework and uncover evidence of an interaction between neocortical desynchronisation and hippocampal synchronisation during the formation and retrieval of human episodic memories.

Within the neocortex, desynchronised alpha/beta activity is thought to facilitate information representation (Hanslmayr et al., 2012). This hypothesis is based on the principles of information theory (Shannon & Weaver, 1949), which proposes that a system of unpredictable states (e.g. desynchronised neural activity, where the firing of one neuron is not predictive of the firing of another; see Hanslmayr et al., 2012 for details) is optimal for information coding (see figure 4.1b). Neural desynchronisation in humans is most often measured by a decrease in oscillatory power, as a strong correlation exists between neural synchronisation and power (Buzsáki, Anastassiou, & Koch, 2012; though this link is strictly correlative). In support of the information-via-desynchronisation hypothesis, many studies have observed neocortical alpha/beta power decreases during successful episodic memory formation (Fellner, Bäuml, & Hanslmayr, 2013; Greenberg, Burke, Haque, Kahana, & Zaghloul, 2015; Griffiths et al., 2016; Guderian, Schott, Richardson-Klavehn, & Duzel, 2009; Hanslmayr et al., 2009, 2011; Lega, Germi, & Rugg, 2017; Noh, Herzmann, Curran, & De Sa, 2014;

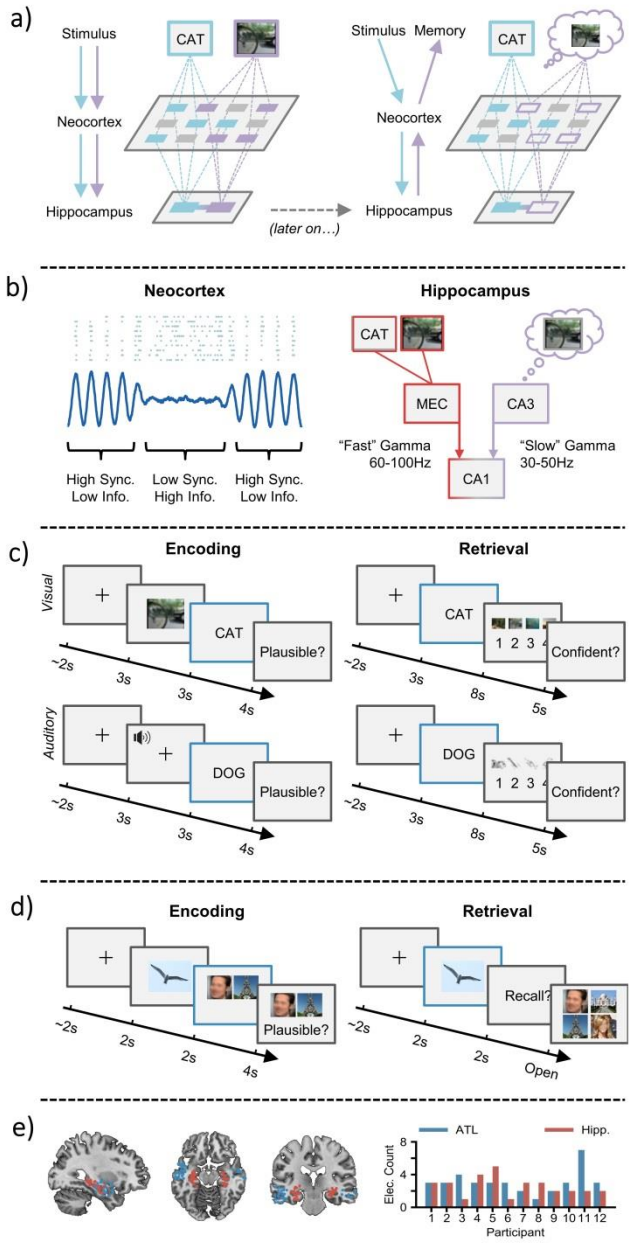

Figure 4.1. The sync-desync framework. (a) Incoming stimuli are independently processed by relevant sensory regions of the neocortex (left), and then passed onto the hippocampus where they are bound together. At a later stage (right), a partial cue reactivates the hippocampal associative link, which in turn reactivates neocortical patterns coding for the memory representation, giving rise to conscious recollection. **(b)** Reduced oscillatory synchronisation (blue line) within the neocortex allows individual neurons (blue dots) to fire more freely and create a more flexible neural code. "Fast" gamma activity allows from the transferal of neocortical information to the hippocampus by boosting connectivity between the entorhinal cortex (MEC) and CA1. "Slow" gamma enhances retrieval by boosting connectivity between CA3 and CA1, allowing reinstated memories to be passed to the neocortex. **(c)** During encoding, participants are tasked with forming an associative link between a life-like dynamic stimulus (either a video or sound) and a subsequent verbal stimulus. During retrieval, participants are presented with verbal stimuli from the previous encoding block and asked to retrieve the associated dynamic stimulus. Electrophysiological analysis was conducted during the presentation of the verbal stimulus at encoding and retrieval (blue outline). **(d)** During encoding, participants are tasked with forming an associative link between an object, a face and a scene. During retrieval, participants are presented with the object and asked to retrieve the associated face and scene. Electrophysiological analysis was conducted during the presentation of the verbal stimulus at encoding and retrieval (blue outline). **(e)** Plot of each electrode location (left; red represents hippocampal electrode; blue represents ATL. Bar plot (right) depicts number of electrodes for each participant.

Weiss & Rappelsberger, 2000) and retrieval (Burgess & Gruzelier, 2000; Dujardin, Bourriez, & Guieu, 1994; Khader & Rösler, 2011; Michelmann et al., 2016; Waldhauser et al., 2016; Zion-Golumbic, Kutas, & Bentin, 2010). For example, neocortical alpha/beta power decreases scale with the depth of semantic processing during episodic memory formation (Hanslmayr et al., 2009). Critically, synchronising alpha/beta rhythms via repetitive transcranial magnetic stimulation impairs both episodic memory formation and retrieval, suggesting that alpha/beta desynchronisation plays a causal role in these processes (Hanslmayr et al., 2014; Waldhauser et al., 2016). In conjunction, these

studies suggest that neocortical alpha/beta desynchronisation underpins the representation of event-related information, facilitating the formation and later recollection of highly detailed episodic memories.

Within the hippocampus, synchronised gamma activity (30-100Hz) is thought to be critical in the binding of event-related information, and the later retrieval of this information when prompted by a cue (Colgin, 2015b; Davachi, 2006; Lisman & Jensen, 2013; Nyhus & Curran, 2010). Entraining neurons to rhythms of approximately 60Hz (i.e. a "fast" gamma oscillation) allows for spike-timing dependent plasticity (STDP; a form of long-term potentiation) to occur (Bi & Poo, 1998), which strengthens synaptic connections between hippocampal neurons. As such, an increase in hippocampal "fast" gamma activity (60-100Hz) may be a proxy for STDP (Axmacher et al., 2006; Jutras et al., 2009) and, therefore, representational binding. In contrast, a slower hippocampal gamma rhythm (30-50Hz) has been proposed to facilitate memory retrieval (Colgin, 2015b; Colgin et al., 2009; Colgin & Moser, 2010). "Slow" gamma activity originates from the CA3 subfield of the hippocampus and may play a pivotal role in pattern completion (De Almeida, Idiart, & Lisman, 2007; Rolls, 2013). The trade-off between these two gamma oscillations is thought to dictate whether encoding or retrieval takes place (Colgin, 2015a). Evidence suggests that periods of increased "fast" gamma activity enhances connectivity between CA1 and the entorhinal cortex (Bragin et al., 1995; Colgin et al., 2009) (allowing information to flow into the hippocampus; see figure 4.1b) and aids representational binding through STDP (Axmacher et al., 2006; Bi & Poo, 1998). Meanwhile, periods of enhanced "slow" gamma activity sees an increase in connectivity between CA1 and CA3 (allowing for the transfer of completed memory pattern into the neocortex; see figure 4.1b; Bragin et al., 1995; Colgin et al., 2009). In conjunction, these findings and theories would suggest that "fast" and "slow" gamma rhythms differentially support the hippocampal ability to associate and reactivate discrete elements of an episodic memory.

Here, we investigated the co-ordination between alpha/beta power decreases in the anterior temporal lobe (ATL) and gamma power increases in the hippocampus during episodic memory

formation and retrieval. Specifically, we tested two hypotheses: 1) that neocortical power decreases will precede hippocampal power increases during memory formation (reflecting information representation preceding representational binding), and 2) hippocampal power increases will precede neocortical power decreases during retrieval (reflecting pattern completion preceding information reinstatement; Hanslmayr et al., 2016).

Twelve patients implanted with intracranial EEG electrodes for the treatment of medication-resistant epilepsy completed one of two associative memory tasks (see figure 4.1c-d; n=7 in task 1; n=5 in task 2). In task 1, they related life-like videos or sounds to words that followed. Following a short distractor task, participants attempted to recall the previously presented videos/sounds using the words as cues. In task 2, they related an object to pairs of visual stimuli that followed (face-place, face-face or place-place). Following a short distractor task, participants attempted to recall both stimuli, using the object as a cue. While external stimulation is different between the two tasks, the underlying cognitive and neural processes relating to our hypotheses are consistent: both tasks require sensory processing followed by representational binding during memory formation, and hippocampal pattern competition prior to neocortical reinstatement during memory retrieval. As such, the data from the two tasks were pooled together for analysis. We conducted these analyses in two ROIs (see figure 4.1e): the hippocampus (a hub for representation binding) and the anterior temporal lobe (ATL; a hub for semantic-based information representation; Visser, Jefferies, & Lambon Ralph, 2010). Foreshadowing the results below, we show that ATL alpha/beta power decreases precede hippocampal "fast" gamma power increases during successful memory formation, and that hippocampal "slow" gamma power increases precede ATL alpha/beta power decreases during successful memory retrieval.

4.2. Results

4.2.1. Neocortical alpha/beta power decreases precede hippocampal "fast" gamma power increases during episodic memory formation

During the formation of episodic memories, we hypothesised that neocortical power decreases can predict the degree to which hippocampal "fast" gamma power subsequently increases. On a cognitive level, this would signify information representation within the neocortex preceding representational binding in the hippocampus. To test this hypothesis, we used a cross-correlation where the time-series of neocortical alpha/beta power is offset relative to the time-series of hippocampal gamma power to identify at what time lag the two time-series most strongly correlate. A negative lag indicates that early neocortical signals correlate with late hippocampal signals, while a positive lag indicates that early hippocampal signals correlate with late neocortical signals. Like traditional correlations, a negative correlation (from here termed 'anticorrelation') indicates an increase in one metric is accompanied by a decrease in the other. The cross-correlation was computed for every trial, and the memory-related difference was calculated by subtracting the mean cross-correlation across forgotten items from the mean cross-correlation across remembered trials. By calculating the memory-related difference, any correlation between the two time-series that is driven by shared noise (i.e. originating from a shared reference) is removed, as this reference-related correlation is consistent across remembered and forgotten trials (see Appendix B for additional analysis which demonstrates that shared reference activity does not account the observed effects reported here). Furthermore, the memory-related difference highlights memory-specific dynamics in neocortical-hippocampal links, rather than general, memory-unspecific connectivity.

In line with our hypothesis, later remembered items showed a significant anticorrelation at a negative lag between ATL alpha/beta power and hippocampal "fast" gamma power relative to later forgotten items ($p_{fdr} = 0.006$, $d = 0.961$; see figure 4.2a for difference line plot). This cross-correlation suggests that alpha/beta power decreases precede "fast" gamma power increases by approximately 100-200ms. No correlation was observed between ATL alpha/beta power and hippocampal "slow"

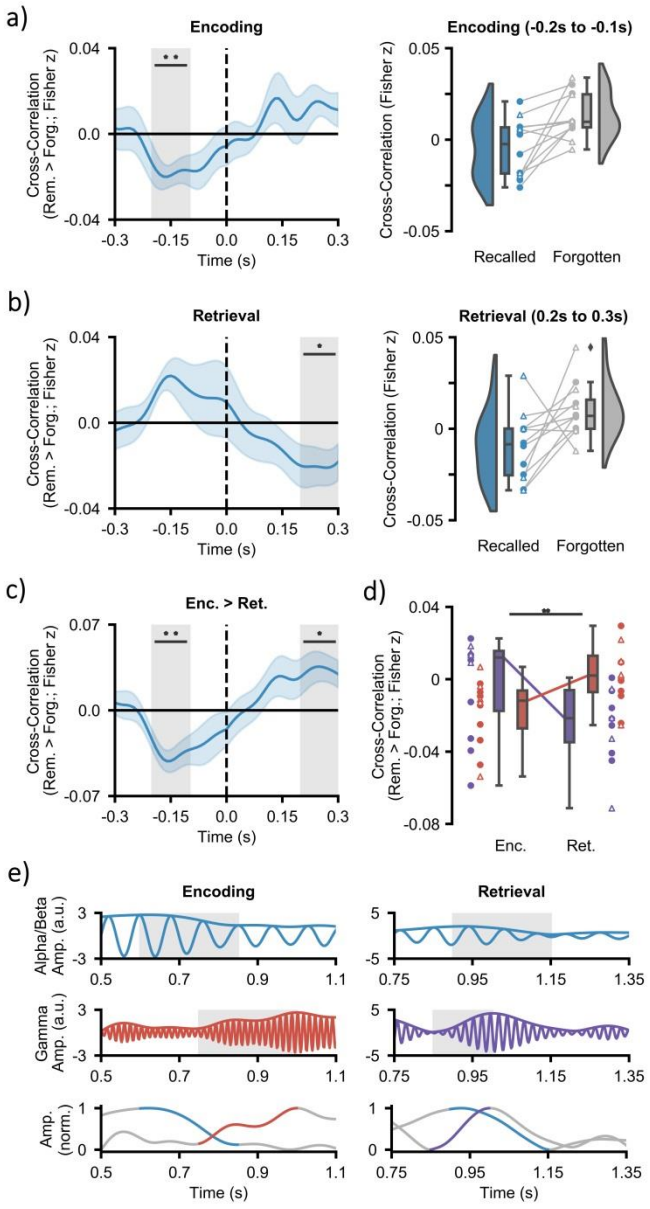

Figure 4.2. Hippocampal-neocortical time-series cross-correlations. (a) mean cross correlation (with shaded standard error of the mean; left) between the hippocampal "fast" gamma power and ATL alpha/beta power during encoding [$^{**}p_{fdr}<0.01$]. ATL power decreases precede hippocampal "fast" gamma power increases. Raincloud plot (right) depicts the difference in cross-correlation between remembered and forgotten items. Coloured circles represent participants who took part in experiment 1. Uncoloured triangles represent participants who took part in experiment 2. **(b)** mean cross correlation (with shaded standard error of the mean; left) between the hippocampal "slow" gamma power and ATL alpha/beta power during retrieval [$^{*}p_{fdr} < 0.05$]. Hippocampal "slow" gamma power increases precede ATL alpha/beta power decreases. Raincloud plot (right) depicts the difference in cross-correlation between remembered and forgotten items. Coloured circles represent participants who took part in experiment 1. Uncoloured triangles represent participants who took part in experiment 2. **(c)** the contrast of cross-correlation activity between encoding and retrieval [$^{*}p_{fdr} < 0.05$,$^{**}p_{fdr}<0.01$]. **(d)** Mean cross-correlation between neocortical alpha/beta power and hippocampal gamma power ("slow" in purple; "fast" in red; with standard error of the mean) as a function of memory operation (top: subject level; bottom: electrode-pair level). A repeated-measures ANOVA reveals an interaction between hippocampal gamma frequency and memory task when predicting memory-related hippocampal-neocortical cross-correlation ($^{**}p < 0.01$). **(e)** filtered single trial traces at encoding (left) and retrieval (right), in the ATL (top) and hippocampus (middle). The envelopes of these traces are plotted beneath. During encoding, a reduction in ATL alpha/beta activity precedes an increase in hippocampal "fast" gamma power. During retrieval, an increase in hippocampal "slow" gamma power precedes a decrease in ATL alpha/beta activity.

gamma power at any lag. These results indicate that a unique connection exists between the ATL and the hippocampus during episodic memory formation, where ATL power decreases precede hippocampal "fast" gamma power increases. It is worth noting that while the absolute magnitude of the Fisher z-transformed correlation coefficient is small, one should exercise caution in interpreting such a value. As we focus on the difference in the ATL-hippocampal cross-correlation for remembered and forgotten items, we only probe the fraction of the total cross-correlation that can be explained by cognition and not that which can be accounted for by numerous undefinable variables

(e.g. measurement noise, placing of electrodes, resting connectivity). As such, it is better to consider the variance in cross-correlation across participants. Here, the variance is minimal and hence returns a small p-value (p_{fdr} = 0.006) and a large effect size (d = 0.961), indicating that ATL alpha/beta power decreases precede hippocampal "fast" gamma power increases reliably across participants.

4.2.2. Hippocampal "slow" gamma power increases precede neocortical alpha/beta power decreases during episodic memory retrieval

We then investigated whether this relationship reverses during episodic memory retrieval (i.e. hippocampal power increases precede neocortical power decreases). On a cognitive level, this would represent pattern completion in the hippocampus preceding information reinstatement in the neocortex. To test this, we repeated the cross-correlation analysis in the same manner as above for epochs covering the presentation of the retrieval cue and then calculated the memory-related difference by subtracting the mean cross-correlation across forgotten items from the mean cross-correlation across remembered trials. Relative to forgotten items, remembered items showed a significant anticorrelation at a positive lag between ATL alpha/beta power and hippocampal "slow" gamma power (p_{fdr} = 0.037, d = 0.731; see figure 4.2b), where an increase in hippocampal gamma power preceded a decrease in ATL alpha/beta power by 200-300ms). No correlation was observed between ATL alpha/beta power and hippocampal "fast" gamma power at any lag. These results indicate that hippocampal "slow" gamma power increases precede ATL alpha/beta power decreases during the retrieval of episodic memories – a reversal of the dynamic observed during episodic memory formation.

We then examined how the neocortical-hippocampal dynamics differed between encoding and retrieval. To this end, the subsequent memory effect (SME; remembered minus forgotten cross-correlation at encoding) for ATL alpha/beta power and hippocampal "fast" gamma power was contrasted with the retrieval success effect (RSE; remembered minus forgotten cross-correlation at retrieval) for ATL alpha/beta power and hippocampal "slow" gamma power in a group level, non-parametric, permutation test. This revealed an interaction whereby ATL power decreases preceded

hippocampal power increases during encoding (p_{fdr} = 0.005, d = 1.181; 100-200ms) but hippocampal power increases preceded ATL power decreases during retrieval (p_{fdr} = 0.025, d = 0.855; 200-300ms) [see figure 4.2c]. These results support those reported in the previous two paragraphs; 1) ATL alpha/beta power decreases precede hippocampal "fast" gamma power increases during episodic memory formation and 2) hippocampal "slow" gamma power increases precedes ATL alpha/beta power decreases during episodic memory retrieval.

Lastly, we examined whether the "fast" gamma effect was specific to encoding and the "slow" gamma effect was specific to retrieval. To this end, we conducted a non-parametric, permutation-based, 2x2 repeated measures ANOVA (memory operation x gamma frequency), taking encoding-related activity from the -200 to -100ms time bin and retrieval-related activity from the 200 to 300ms time bin. Analysis revealed a significant interaction between the two factors (p = 0.001; partial η^2 = 0.172). The interaction (as pictured in figure 4.2d) suggests that the hippocampal "fast" gamma power negatively cross-correlated with ATL alpha/beta power to a greater degree than hippocampal "slow" gamma power during encoding, while the hippocampal "slow" gamma power negatively cross-correlated with ATL alpha/beta power to a greater degree than hippocampal "fast" gamma power during retrieval.

Notably, these effects cannot be explained by any epileptic activity such as IEDs (inter-epileptical discharges) travelling between the cortex and hippocampus. IEDs are broadband, so, one may expect that IEDs that are temporally-correlated across regions may give rise to spurious coupling between frequency bands. While certainly true, this cannot explain the effects observed here for two reasons. (1) Our findings are bidirectional – there would need to be pathological activity generated in both the ATL and the hippocampus to produce such bidirectional hippocampal-cortical interactions, where IEDs generated in the ATL travel to the hippocampus to produce the encoding effect, and IEDs generated in the hippocampus travel to the ATL produce the retrieval effect. None of the patients who took part in the experiment had pathological tissue in both the ATL and the hippocampus, so the IED confound explanation cannot explain the directionality of our effect. (2) IEDs are broadband, yet our

effects are narrowband. During encoding, we observe the cross-correlation between neocortical alpha/beta and hippocampal fast gamma, but importantly not neocortical alpha/beta and hippocampal slow gamma. Any IED-induced broadband artifact would inherently yield cross-correlations with alpha/beta power and both gamma bands, and not within one singular band. Complementary quantitative analysis to support this conclusion can be found in Appendix B.

4.3. Discussion

To successfully encode and recall episodic memories, we must be capable of i) representing detailed multisensory information, and ii) binding this information into a coherent episode. Numerous studies have suggested that these two processes are accomplished by neocortical desynchronisation (as measured by decreases in oscillatory power) and hippocampal synchronisation (as measured by increases in fast and slow oscillatory gamma power) respectively (Colgin, 2015b; Hanslmayr et al., 2016, 2012; Lisman & Jensen, 2013). Here, we show that these two processes co-exist and interact. During successful episodic memory formation, alpha/beta power decreases in the anterior temporal lobe (ATL) reliably precede "fast" hippocampal gamma power increases (60-80Hz) by 100-200ms. In contrast, "slow" hippocampal gamma power increases (40-50Hz) precede alpha/beta power decreases by 200-300ms during successful episodic memory retrieval. These findings demonstrate that the interaction between neocortical alpha/beta power decreases and hippocampal power increases in distinct, functionally-relevant gamma rhythms underpins the formation and retrieval of episodic memories.

Our central finding demonstrates that ATL alpha/beta power decreases and hippocampal fast and slow gamma power increases interact during the formation and retrieval of episodic memories, respectively. This result draws together a multitude of conflicting studies, some of which indicate that synchronisation benefits memory (e.g Heusser, Poeppel, Ezzyat, & Davachi, 2016; Staudigl & Hanslmayr, 2013; Tort, Komorowski, Manns, Kopell, & Eichenbaum, 2009) and others which indicate that desynchronisation benefits memory (e.g. Hanslmayr et al., 2011; Khader & Rösler, 2011; Spitzer, Hanslmayr, Opitz, Mecklinger, & Bäuml, 2009), and provides a possible empirical resolution to the

so-called "synchronisation-desynchronisation conundrum" (Hanslmayr et al., 2016). These findings are in line with previous observations demonstrating that hippocampal gamma power increases precede hippocampal alpha power decreases during associative memory retrieval (Staresina et al., 2016). However, we also show that this sequence reverses during encoding, and that these two mechanisms interact across brain regions (via simultaneous hippocampal-neocortical recordings unavailable to Staresina et al., 2016). We speculate that the delay in hippocampal response relative to ATL alpha/beta power decreases during encoding reflects the need for the ATL to process semantic details prior to the hippocampus binding this information into a coherent representation of the event (Davachi, 2006; Lisman & Jensen, 2013). In contrast, we posit that the ATL delay in response relative to hippocampal gamma power increases during retrieval reflects the need for the hippocampal representational code to be reactivated prior to reinstating highly-detailed stimulus-specific information about the event (Rugg, Johnson, Park, & Uncapher, 2008). Anatomically speaking, this reciprocal communication may be facilitated by the "direct intrahippocampal pathway" – a route with reciprocal connections between the ATL and hippocampus via the entorhinal cortex (Duvernoy, 2005; Poppenk & Moscovitch, 2011). These anatomical connections would allow the ATL and hippocampus to cooperate during episodic memory formation and retrieval, facilitating the flow of neocortical information into the hippocampus during encoding and the propagation of hippocampal retrieval signals into the neocortex during retrieval.

In combination with the gamma-band analyses presented in the previous chapter, the current results produce a detailed picture of information flow during episodic memory formation and retrieval. Based on earlier frameworks (Colgin, 2015b; Hanslmayr et al., 2016) and models (Parish et al., 2018), we postulate that the link between neocortical alpha/beta power decreases and hippocampal "fast" gamma power increases during memory formation reflects the flow of semantic information (processed in the ATL) to entorhinal cortex (Davachi, 2006) via the direct intrahippocampal pathway (Duvernoy, 2005; Poppenk & Moscovitch, 2011), where "fast" gamma synchronicity between the entorhinal cortex and CA1 passes this information onto the hippocampus (Colgin et al., 2009; Kemere,

Carr, Karlsson, & Frank, 2013). In contrast, the link between hippocampal "slow" gamma power increases and neocortical alpha/beta power decreases during memory retrieval reflects the flow of reactivated representational codes from CA3 to CA1 (via "slow" gamma synchronicity; Colgin et al., 2009; Kemere et al., 2013), which propagates out into the neocortex (Rugg et al., 2008) via reciprocal connections in the direct intrahippocampal pathway, reinstating semantic details in the desynchronised ATL. However, future research with direct recordings from these hippocampal sub-regions in humans is needed to empirically test this proposed flow of information during episodic memory formation and retrieval.

It remains an open question as to whether similar bi-directional streams of information flow exist between the hippocampus and other neocortical regions. As it was not medically necessary, electrode coverage did not expand to every neocortical region linked to episodic memory. Therefore, we could not test this theory. We speculate, however, that similar bi-directional links do exist. For example, hippocampal gamma power increases may interact with alpha/beta power decreases in the visual cortex to facilitate the encoding and retrieval of visual memories (Waldhauser et al., 2016). Speculating further, hippocampal gamma power increases may be the metaphorical spark that lights the fuse of memory replay, coded in desynchronised neocortical alpha phase patterns (Michelmann et al., 2016).

In summary, we demonstrate that neocortical power decreases and hippocampal power increases cooperate during the formation and retrieval of episodic memories, providing evidence that may help resolve the so-called "synchronisation-desynchronisation conundrum" (Hanslmayr et al., 2016). These results further illuminate our understanding of how interactions between the neocortex and hippocampus help build and retrieve memories of our past experiences.

4.4. Methods[†]

4.4.1. Electrode localisation

First, hippocampal and white matter contacts were defined based on anatomical location through visual inspection of the T1-weighted anatomical scan. Then, the native space co-ordinates of all remaining contacts were determined by visual inspection of each participant's post-implantation T1 scan. These contact co-ordinates were then transformed from native space to MNI space using a transform matrix obtained by normalising participant T1 scans in SPM 12. These contacts were then marked as within the anterior temporal lobe (ATL) or elsewhere (this latter group was excluded from further analysis).The ATL was defined as all parts of the temporal lobe (as defined by the *wfupickatlas* plugin (Maldjian, Laurienti, Kraft, & Burdette, 2003) for SPM 12) anterior to a plane perpendicular to the long axis of the temporal lobe (Rice et al., 2015). The plane was slightly shifted from that described in (Rice et al., 2015) to [y=-5, z=-30; y=15, z=-5] for the pragmatic reason of ensuring that all participants had electrode contacts in the ATL ROI. For visualisation in figure 4.1d, every electrode from every participant was given a diameter of 1cm and then placed in a template brain registered in MNI space.

4.4.2. 1/f correction

Spectral power was computed using 199 linearly-spaced 5-cycle wavelets ranging from 1 to 100Hz. The time-frequency decomposition method was kept consistent across all frequency bands to ensure that only a single slope (characterising the full extent of the 1/f dynamic) needed to be calculated and subsequently subtracted from the signal (in line with previous experiments that have extracted the 1/f characteristic from the signal; e.g. Manning et al., 2009; Zhang & Jacobs, 2015). A vector containing values of each wavelet frequency (*A*) and another vector containing the power spectrum for each electrode-sample pair (*B*) were then log-transformed. The linear equation $Ax = B$ was solved using least squares regression, where x is an unknown constant describing the curvature of the 1/f characteristic. The 1/f fit (Ax) was then subtracted from the log-transformed power-spectrum (B).

4.4.3. Peak frequency analysis

Raw signal recorded at every contact for each epoch was convolved with a 5-cycle wavelet (0 to 1500ms post-stimulus [padded with real data for lower frequencies], in steps of 25ms; 1Hz to 100Hz, in steps of 0.5Hz).

[†] As the details of the participants and tasks are identical to those presented in chapter 3, these details have been excluded here to avoid needless repetition.

The 1/f noise was subtracted using the method described above to help pronounce the peaks in the power-spectrum. The data was then smoothed using a Gaussian kernel (full-width half-maximum: 200ms, 1Hz) to attenuate inter- and intra-individual differences in spectral responses (Benwell et al., 2018) and to help approximate normally distributed data (an assumption frequently violated in small samples). The data was averaged across all time-points, trials and contacts (separately for the hippocampus and ATL). Peaks of 1/f corrected absolute power were then identified using the *findpeaks()* peak-detection algorithm implemented in Matlab. To identify the memory-related difference in the dominant gamma bands, the power spectra for "remembered" trials were calculated in an identical manner, except that the Gaussian kernel was expanded to account for the greater variability of high-frequency oscillatory responses (200ms, 5Hz). The power-spectra for encoding and retrieval were then collapsed in seven 10Hz bins ranging from 30Hz to 100Hz and contrasted.

4.4.4. Selection of peak frequencies

The peak frequencies of each patient were determined using the MATLAB function *findpeaks()* on the averaged power spectrum around the approximate frequency bands (theta: 1-7Hz; alpha/beta: 8-20Hz; "slow" gamma: 30-60Hz; "fast" gamma: 50-100Hz). The bandwidths of these peaks were kept consistent across participants, and were determined through inspection of the group-averaged bandwidth of the peaks (theta: ±0.5Hz; alpha/beta: -1Hz/+5Hz [capturing the observed asymmetry in the peak]; "slow"/"fast" gamma: ±10Hz). Individual peak frequencies are reported in Appendix B, Table 8.1.

4.4.5. Spectral power analysis

For all spectral power analyses (i.e. encoding and retrieval epochs), the data underwent the same wavelet convolution, 1/f correction, and smoothing approaches described in the *peak frequency analysis* section. The data was then z-transformed using the means and standard deviations of each electrode-frequency pair (Griffiths et al., 2016). The time-frequency resolved data was then averaged over electrodes of each ROI. For time-series statistical analysis, trials were split into two groups based on whether the stimuli were remembered or forgotten. Then, the time-series were collapsed into seven time bins of 200ms and the two conditions were contrasted using the same non-parametric statistical procedure described in the *peak frequency analysis* section. For statistical analyses of the interaction between memory task (encoding vs. retrieval) and gamma frequency ("fast" vs. "slow"), this memory-related difference in power (i.e. SME and RSE) was averaged over time and contrasted in a non-parametric, permutation based 2x2 repeated measures ANOVA.

4.4.6. Cross-correlation analysis

For all cross-correlation analyses (i.e. encoding and retrieval epochs), the data underwent the same wavelet convolution, 1/f correction, and smoothing approaches described in the *spectral power analysis* section, with two exceptions: 1) wavelet convolution occurred in steps of 10ms rather than 50ms (enhancing temporal resolution), and 2) the temporal aspect of the smoothing kernel was reduced to 50ms to avoid excessive smoothing obscuring the temporal dynamics of the neocortical-hippocampal cross-correlation. For each "trial x electrode combination" pair, the cross-correlation between the hippocampus and the ATL, was computed using the Matlab function *crosscorr()* with a lag of 300ms (meaning the correlation between hippocampus and ATL was considered for every offset from where the ATL preceded the hippocampus by 300ms to where the ATL lagged behind the hippocampus by 300ms). This returned a time-series of Pearson correlation values describing the relationship between hippocampus and ATL at all considered lags. These correlation values were then averaged over electrodes and split into two groups: remembered and forgotten. These two groups were individually averaged over trials for each participant, collapsed into bins of 100ms, and then contrasted using the same non-parametric statistical procedure described in the *peak frequency analysis* section. We term the "remembered > forgotten" difference in cross-correlation for encoding data "the subsequent memory cross-correlation" and the difference for retrieval data "the retrieval success cross-correlation".

To test the "encoding-retrieval" x "lag-lead" difference, we contrasted the subsequent memory cross-correlation with the retrieval success cross-correlation using the same non-parametric statistical procedure described in the *peak frequency analysis* section. Lastly, to test the influence of the "memory task" x "gamma frequency" interaction on the memory-related cross-correlation differences, we conducted a non-parametric, permutation-based 2x2 repeated measures ANOVA in the same manner as described in the *spectral power analysis* section.

CHAPTER 5: DISENTANGLING THE ROLES OF NEOCORTICAL ALPHA/BETA AND HIPPOCAMPAL THETA/GAMMA ACTIVITY IN HUMAN EPISODIC MEMORY

Episodic memories rely on two processes: 1) our ability to process a vast amount of sensory information, and 2) our ability to bind these sensory representations together to form a coherent memory. The first process is thought to rely on neocortical alpha/beta desynchronisation while the second is thought to be supported by hippocampal theta and gamma synchronisation. Given that many episodic memory tasks involve a temporal overlap of stimulus processing and representational binding, however, it remains unclear whether alpha/beta desynchronisation and theta/gamma synchronisation are truly dissociable. We addressed this question by using a paradigm that temporally separated these two cognitive processes. In this task, we found that memory-related decreases in neocortical alpha/beta power only arose during the perception and retrieval of task-relevant information, conforming to the idea that neocortical desynchronisation reflects information representation. In contrast, memory-related increases in hippocampal theta/gamma phase-amplitude coupling only arose during representational binding, conforming to the idea that such coupling reflects the binding of a memory. These results suggest that alpha/beta desynchronisation and hippocampal theta/gamma synchronisation are dissociable phenomena that contribute to distinct processes in episodic memory formation and retrieval.

In preparation for:

Griffiths, B. J., Martin-Buro, M. C., Staresina, B., & Hanslmayr, S. (2019). Disentangling the roles of neocortical alpha/beta and hippocampal theta/gamma activity in human episodic memory.

5.1. Introduction

An episodic memory is a detail-rich, long-term memory that is anchored to a unique point in time and space (Tulving, 2002). The formation and retrieval of these memories are thought to rely on neocortical alpha/beta desynchronisation and hippocampal theta/gamma synchronisation (Hanslmayr et al., 2016), both of which are prevalent in a wide range of episodic memory tasks (for reviews, see Hanslmayr & Staudigl, 2014; Nyhus & Curran, 2010). While there is substantial evidence to suggest that they reflect distinct cognitive processes (information representation and representational binding respectively; Hanslmayr et al., 2016), the findings presented in chapter 4 suggest that the amount of hippocampal synchrony during episodic memory formation can be predicted by preceding neocortical desynchrony, and vice versa during episodic memory retrieval. Given this correlation, it becomes reasonable to question whether that these neural phenomena reflect two distinct processes, or two neural responses to the same process. Here, we provide empirical evidence in favour of the former. Memory-related decreases in neocortical alpha/beta alpha/beta power uniquely arise during periods of stimulus processing, while memory-related increases in hippocampal theta/gamma coupling peaked during periods of representational binding.

Decreases in alpha/beta power (an index of neural desynchronisation; Buzsáki, Anastassiou, & Koch, 2012) are prevalent during the formation and retrieval of episodic memories (e.g. Griffiths, Mazaheri, Debener, & Hanslmayr, 2016; Hanslmayr, Spitzer, & Bauml, 2009; Long & Kahana, 2015; Martín-Buro, Wimber, Henson, & Staresina, 2019; Sederberg et al., 2007; Staresina et al., 2016). One mechanistic framework proposes that alpha/beta desynchrony is beneficial for information representation (Hanslmayr et al., 2012). This idea is derived from the tenets of information theory, which propose that unpredictable states (e.g. a desynchronised network, where the firing of one neuron cannot predict the firing of another) can convey substantially more information than predictable states. In chapter 2, we demonstrated that the amount of stimulus information present in fMRI BOLD signal can be predicted by neocortical alpha/beta power, suggesting that alpha/beta power directly correlates with information representation within the brain. Moreover, memory-related alpha/beta power

decreases only occur for meaningful material, further supporting the idea that there is a link between the depth of information representation and alpha/beta power decreases (Fellner et al., 2019). Critically, interfering with alpha/beta power decreases via transcranial brain stimulation impairs both episodic memory formation and retrieval (Hanslmayr et al., 2014; Waldhauser et al., 2016), suggesting that these power decreases play a causal role in memory. Based on these findings (and others; e.g. Fellner, Bäuml, & Hanslmayr, 2013; Long & Kahana, 2015; Sederberg et al., 2007), one can hypothesise that alpha/beta power decreases reflect the representation of information during episodic memory formation and retrieval.

Increases in the synchronisation of hippocampal theta and gamma oscillations also correlate with the formation and retrieval of episodic memories. An increase in synchronisation can take the form of an increase in theta or gamma power (e.g. Burke et al., 2013; Griffiths, Parish, et al., 2019; Long & Kahana, 2015; Montgomery & Buzsáki, 2007; Osipova et al., 2006; Sederberg et al., 2007; Staresina et al., 2016), or an increase in the coupling of these two oscillations (e.g. Bahramisharif, Jensen, Jacobs, & Lisman, 2018; Heusser, Poeppel, Ezzyat, & Davachi, 2016; Staudigl & Hanslmayr, 2013; Tort, Komorowski, Manns, Kopell, & Eichenbaum, 2009). Mechanistically speaking, an increase in hippocampal synchronisation is thought to facilitate the binding of information into a coherent memory trace (Hanslmayr et al., 2016; Nyhus & Curran, 2010). This is, in part, dictated by the phase of theta, which determines whether long-term potentiation (LTP) or long-term depression (LTD) occurs (Hasselmo, Bodelón, & Wyble, 2002). Synchronisation of gamma activity compliments this process by driving neurons to fire at the frequency optimal for spike-timing dependent plasticity (STDP, a form of LTP; Bi & Poo, 1998; Jutras, Fries, & Buffalo, 2009; Nyhus & Curran, 2010). By coupling gamma power to the phase of theta that is optimal for LTP, the propensity for representational binding is further enhanced.

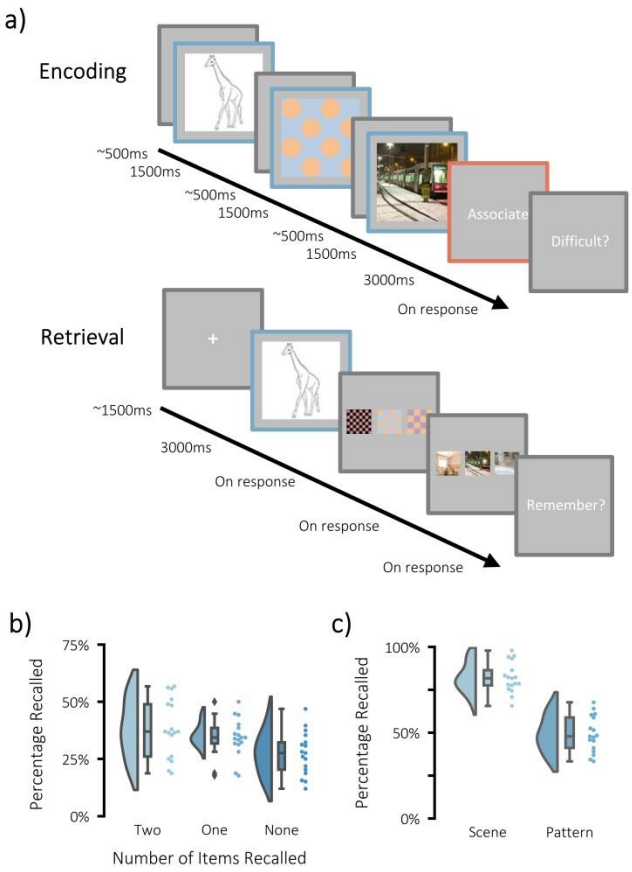

Figure 5.1. Overview of behavioural task. (a) Paradigm schematic. Participants were presented with a sequence of three visual stimuli. The sequence always began with a line drawing of an object, and was then followed by a pattern and a scene (each with a brief fixation cross shown between). Participants were then given a short interval to create a mental image incorporating the three stimuli. They were then asked to rate how difficult they found it to create the mental image. After a distractor task, participants were presented with the object as a cue and asked to recall both the pattern and the scene, each from a choice of three stimuli. After selection, participants had to rate how confident they felt about their response. Windows of information representation are outlined in blue, and windows of representational binding are outlined in red. **(b)** Raincloud plot depicting memory performance as a function of number of items recalled for each participant. **(c)** Raincloud plot depicting memory performance for each stimulus type. Scene stimuli were better recalled than pattern stimuli.

Critically however, the amount of hippocampal synchronisation is contingent on the amount of neocortical desynchronisation during episodic memory formation, and vice versa during episodic memory retrieval (see chapter 4). While we interpreted this as two cognitive processes interacting, one could argue that this instead reflects two neural responses to a singular cognitive process. Here, we contrasted these ideas using a paradigm that temporally separates information representation and representational binding. Seventeen participants underwent MEG recordings and were presented with sequences of stimuli before being asked to create a unique mental image incorporating all the stimuli. Their memory for these sequences was later tested in a cued recall task (see figure 5.1). In this paradigm, information representation should predominately arise during sequence presentation and sequence recall (outlined in blue), while representational binding should predominately arise during mental association (outlined in red). If neocortical desynchronisation and hippocampal synchronisation reflect distinct processes, we would therefore expect that (1) neocortical alpha/beta power decreases should be most prevalent during sequence perception and retrieval, and (2) hippocampal theta/gamma power increases and phase-amplitude coupling should be most prevalent

during association (see pre-registration: https://osf.io/4nt23/; see supplementary materials). Foreshadowing the results below, we find evidence to suggest that memory-related occipital alpha/beta power decreases accompany sequence perception and retrieval, but not association, while memory-related increases in hippocampal theta-gamma coupling arise during association, but not perception or retrieval. These results indicate that the roles of neocortical alpha/beta desynchrony and hippocampal theta/gamma synchrony in episodic memory are temporally dissociable, lending further support to the idea that they reflect distinct cognitive processes.

5.2. Results

5.2.1. Behavioural results

Participants, on average, correctly recalled both the associated pattern and associated scene on 38.3% of trials, recalled only one associated stimulus on 34.4% of trials, and failed to recall either associated stimulus on 27.3% of trials (see figure 5.1b). Participants correctly recalled the associated pattern on 49.2% of trials, and correctly recalled the associated scene on 82.1% of trials (both of which are well above chance performance [33.3%]; see figure 5.1c). A paired-samples t-test revealed that memory for scenes was substantially greater than memory for patterns ($p < 0.001$, Cohen's $d = 4.57$).

5.2.2. Neocortical alpha/beta power decreases predict successful memory formation

We first investigated the extent to which spectral power fluctuates as a function of memory performance during visual perception. We hypothesised that, as information surrounding the three stimuli need to be processed in order to form a complete memory, alpha/beta power should decrease as a function of the number of items recalled. To test this, the time-series of sensor-level MEG gradiometer data was decomposed into spectral power using 6-cycle Morlet wavelets (for low frequencies; 2-40Hz) and Slepian multitapers (for high frequencies; 40-100Hz), and then baseline-corrected using z-transformation. Spectral power was averaged over the three stimulus presentation windows to get a measure of mean spectral power during perception. The resulting trials were split into three memory conditions: complete memories (where both the pattern and the scene were

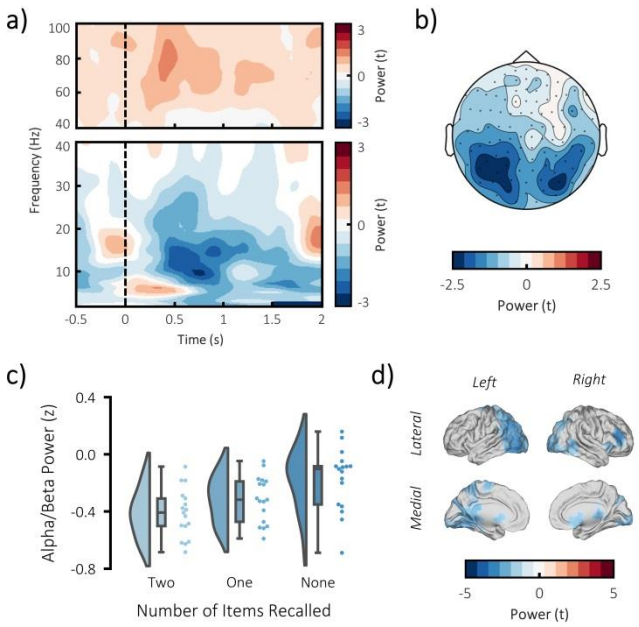

Figure 5.2. Alpha/beta power decreases during perception correlate with increased memory performance. (a) Time-frequency representation over occipital and parietal sensors shows that a decrease in low-frequency power (8-20Hz) correlates with later memory success. **(b)** A topographic plot of post-stimulus alpha/beta power suggests that memory-related power decreases were most prominent over the occipital lobe. **(c)** Raincloud plot depicting alpha/beta power as a function of items recalled. Power appeared to linearly decrease with greater memory performance. **(d)** Source reconstruction of this effect implicated the occipital lobe and parts of the parietal lobe and ventral medial prefrontal cortex.

recalled), partial memories (where only one of the associated stimuli was recalled), and forgotten items (where neither associated stimulus was recalled). The three conditions were then contrasted in a linear regression where spectral power was fitted to a model describing the number of stimuli recalled (i.e. 0, 1, or 2). Here, a positive t-value (i.e. beta weight divided by standard error of fit) would indicate that spectral power increases with the number of items recalled and a negative t-value would indicate that spectral power decreases with the number of items recalled. To address the issue of multiple comparisons, these t-values were entered into a cluster-based, permutation test (Maris & Oostenveld, 2007). This analytical approach revealed a significant effect where power decreases correlated with an increase in memory performance (p_{corr} = 0.013, cluster r^2 = 0.80). Visual inspection of the cluster suggests that the effect was greatest over the occipital lobe, bilaterally, between 8 and 20Hz (see figure 5.2). The reconstruction of this effect on source level suggests that this effect arose in the occipital lobe. A second topographic cluster was observed within the gamma band, but this did not survive multiple comparison correction (p_{corr} = 0.117, cluster r^2 = 0.08).

It is important to note that three types of statistical pattern can produce the linear trend we uncovered: (1) a linear trend where power steadily decreases with increasing memory performance (the “linear model”), (2) a binary division where any successful encoding produces a power decrease

relative to the forgotten triads, but no distinction exists between triads that were completely recalled and triads that were only partially recalled (the "hit vs. miss model"), and (3) a binary division where successful encoding of the entire triad produces a power decrease relative to the partial and forgotten triads, but no distinction exists between triads that were partially recalled and triads that were forgotten (the "all-or-nothing model"). To examine which model best fit the data, the power in the cluster was fitted to each model, and the variance explained by each model was descriptively compared. Indeed, it seemed the linear model best described the observed data, explaining 80.3% of the variance. The other models explained a highly similar degree of variance (perhaps owning to the fact that they are very similar models) but, critically, explained less than the linear model (hit vs. miss: 76.5%; all-or-nothing: 72.4%). This suggests that power linearly decreases with the amount of information encoded.

Notably, the observed effect was spectrally broad, ranging from around 8 to 20Hz. As such, it is reasonable to suggest that this effect may not reflect a change in oscillatory activity, but rather a change in the underlying 1/f characteristic (Haller et al., 2018; Miller et al., 2009). To address this, the 1/f characteristic of this cluster was isolated from the oscillatory signal by subtracting a linear fit of the 1/f characteristic in log-log space (see methods for details). This approach provides a power spectrum that describes memory-related changes in oscillatory power, and a beta weight that describes the 1/f characteristic. Both of these measures were subjected to the same statistical analysis as above. This revealed a significant effect for oscillatory power ($p_{corr} = 0.024$), where a decrease in alpha power (8-11Hz) correlated with an increase in memory performance. No significant cluster was observed for the beta weight describing the 1/f characteristic. These results suggest that a decrease in oscillatory alpha power, rather than a shift in 1/f, correlates with greater memory performance.

5.2.3. Neocortical alpha/beta power increases predict successful binding

We then asked how spectral power fluctuates as a function of memory performance during the binding window. We hypothesised that theta and gamma power should linearly increase as a function

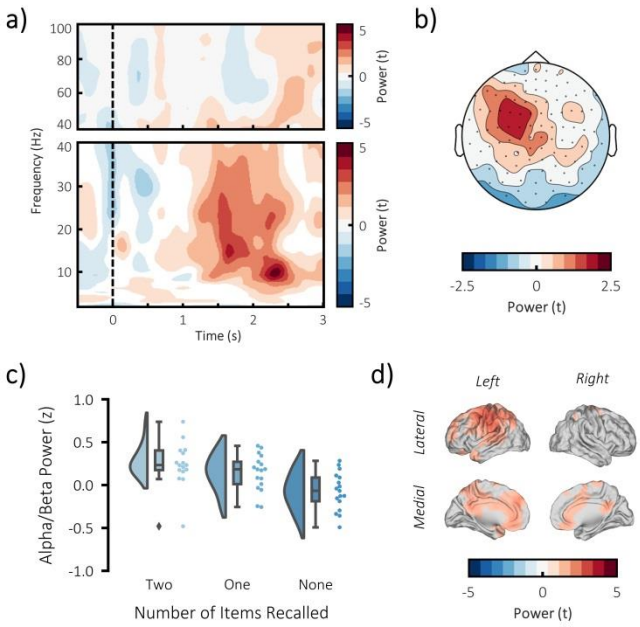

Figure 5.3. Alpha/beta power increases during representational binding correlate with increased memory performance. (a) Time-frequency representation over left frontal sensors shows that an increase in low-frequency power (7-35Hz) correlates with later memory success. **(b)** A topographic plot of post-stimulus alpha/beta power suggests the memory-related power decreases were most prominent over the left frontal regions. **(c)** Raincloud plot depicting power as a function of items recalled. Power appeared to linearly increase with greater memory performance. **(d)** Source reconstruction of this effect suggested that this was a result of parietal and frontal contributions.

of memory performance, reflecting an increase in hippocampal binding. The analytical approach matched that reported above. Intriguingly however, our analysis did not reveal any memory-related changes in theta or gamma power (theta: $p > 0.5$; cluster $r^2 = 0.34$; gamma: $p > 0.5$; cluster $r^2 = 0.14$). As we had hypothesised that such effects would originate from the hippocampus, and deep sources can obscured by more superficial sources (Ruzich et al., 2019), we re-ran our analysis using a hippocampal region of interest, but still found no memory-related change in theta or gamma power.

Instead, a significant effect was observed in which low frequency power increases correlated with an increase in memory performance ($p_{corr} < 0.001$, cluster $r^2 = 0.80$; see figure 5.3). Visual inspection of the cluster suggests that the effect was greatest over left frontal regions, between 7 and 35Hz. The reconstruction of this effect on source level further clarified this effect, implicating a wide range of regions including the parietal cortex, left dorsolateral prefrontal cortex and bilateral ventromedial prefrontal cortex. When examining which model best fit the power in the observed cluster, it appeared that the linear model again best described the observed data, explaining 79.7% of the variance (hit vs. miss: 75.4%; all-or-nothing: 70.6%). This suggest that alpha/beta power linearly increases with the amount of information later recalled.

Again, the observed effect was spectrally broad, ranging from around 7 to 35Hz. As such, it is again reasonable to suggest that this effect may not reflect a change in oscillatory activity, but rather a

change in the underlying 1/f characteristic (Haller et al., 2018; Miller et al., 2009). Control analyses (conducted in the same manner as above) revealed a significant effect for oscillatory power (p_{corr} = 0.005), where an increase in beta power (20-25Hz) correlated with an increase in memory performance. Again, no significant cluster was observed for the beta weight describing the 1/f characteristic. These results suggest that an increase in oscillatory beta power, rather than a shift in 1/f, correlates with greater memory performance during representational binding.

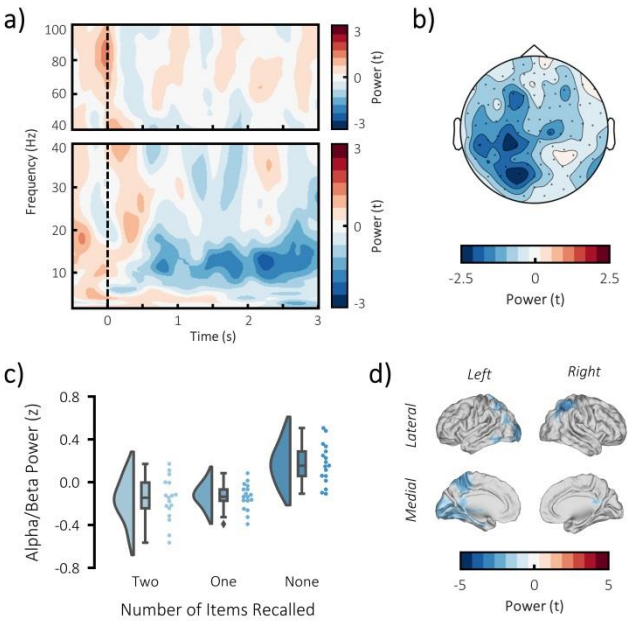

Figure 5.4. Alpha/beta power decreases during memory retrieval correlate with increased memory performance. (a) Time-frequency representation over left parietal sensors (top left) shows that a decrease in low-frequency power (8-20Hz) correlates with later memory success. **(b)** A topographic plot of post-stimulus alpha/beta power suggests the memory-related power decreases were most prominent over the left parietal and occipital regions. **(c)** Raincloud plot depicting power as a function of items recalled. Power appeared to decrease when successfully recalling a stimulus, but power did not vary as a function of the number of items recalled. **(d)** Source reconstruction of this effect identified parietal and occipital regions.

5.2.4. Neocortical alpha/beta power decreases predict successful memory retrieval

We then asked how spectral power fluctuates as a function of memory performance during memory retrieval. We hypothesised that alpha/beta power should parametrically decrease as a function of memory performance, reflecting an increase in the representation of reinstated information. The analytical approach matched that reported above. In line with our hypothesis, we found a significant effect where post-stimulus alpha/beta power decreases correlated with an increase in memory performance (p_{corr} = 0.025, cluster r^2 = 0.77; see figure 5.4). Visual inspection of the cluster suggests that the effect was greatest over the left parietal and occipital lobes, between 6-20Hz. Source reconstruction localised this effect to the parietal and occipital lobes. When examining which model best fit the power in the observed cluster, it appeared that the hit vs. miss model explained an

equivalent amount of variance (76.7%) as the linear model (76.9%) described the observed data (all-or-nothing: 46.0%). Indeed, visual inspection of the raincloud plot in figure 5.4 supports the idea that power decreases for complete and partial memories are similar.

While this effect appeared to be more oscillatory in appearance than those in the previous sections, we nevertheless ran further analysis to confirm this. Indeed, control analyses (conducted in the same manner as above) revealed a significant effect for oscillatory power (p_{corr} = 0.013), where a decrease in alpha/beta power (10-15Hz) correlated with an increase in memory performance. Again, no significant cluster was observed for the beta weight describing the 1/f characteristic. These results suggest that a decrease in oscillatory alpha/beta power, rather than a shift in 1/f, correlates with greater memory performance during successful memory retrieval.

5.2.5. Hippocampal theta/gamma phase-amplitude coupling predicts successful memory formation

Lastly, we probed how theta/gamma phase-amplitude coupling relates to episodic memory formation and retrieval. To address this, we went straight to the source level as we had strong *a priori* hypotheses about the hippocampal source of this effect (see https://osf.io/4nt23/; see supplementary materials), and such a deep source can often be masked by more superficial sources (Ruzich et al., 2019). We first extracted the theta and gamma peaks in the hippocampal power spectrum for each participant individually. This ensured that we were looking at the coupling between two oscillatory signals (Aru et al., 2014). The source-reconstructed hippocampal time-series were then filtered to extract the ongoing phase of hippocampal theta activity and the power of hippocampal gamma activity. Every sample of hippocampal gamma power was then binned according to hippocampal theta phase, and the modulation index (Tort, Komorowski, Eichenbaum, & Kopell, 2010) was computed for each memory condition (against the null hypothesis that the distribution of gamma power is uniform across the theta phase). The resulting modulation index was averaged across all hippocampal virtual sensors to provide a single measure of theta/gamma phase-amplitude coupling for each memory condition, and for every participant. These values were then entered into a linear regression for statistical analysis in the same manner as above. During representational binding, a significant

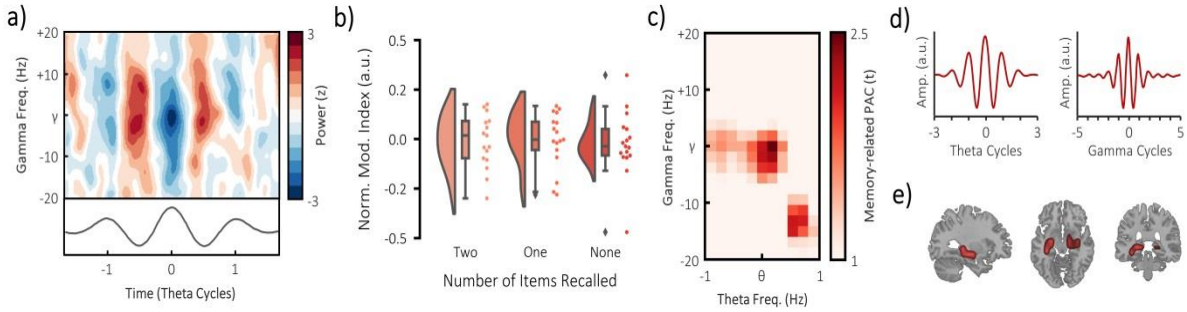

Figure 5.5. Increases in hippocampal theta/gamma coupling during representational binding correlate with increased memory performance. (a) the modulation of peak gamma power as a function of peak theta phase across all trials. Peak gamma appears to decrease during the peaks of the theta phase, and increase during troughs of the theta phase. **(b)** raincloud plot depicting the fit between memory performance and hippocampal theta-gamma coupling (each dot represents a participant). **(c)** the specificity of memory-related hippocampal theta-gamma phase-amplitude coupling. Only peak gamma power appears to lock to peak theta phase, suggesting a coupling of two oscillations rather than the coupling of broadband power to theta phase. **(d)** peak-locked average of peak theta (left) and gamma (right) frequencies, averaged across all participants. For both, theta and gamma the waveforms appear symmetric thus excluding a distortion of the cross-frequency coupling measure due to waveshape. **(e)** source plot of theta-gamma phase-amplitude coupling within the hippocampal ROI.

increase in theta/gamma phase-amplitude coupling correlated with greater memory performance observed ($p = 0.028$, $r^2 = 0.07$; see figure 5.5). When examining which model best fit hippocampal phase-amplitude coupling, it appeared that the linear model of memory performance explained the most variance (7.0%; relative to hit vs. miss [6.8%] and all-or-nothing [0.1%] models). Notably, the variance explained the phase-amplitude coupling data is substanially less than the variance explained by the spectral power data presented above. This can be explained by the fact that the spectral power data has one source of analytical noise: spectral power within the band of interest. In contrast, the phase-amplitude coupling data has three sources of analytical noise: spectral power in the gamma band, phase estimates in the theta band, and the interaction between these two noise sources. As such, one can anticipate that the phase-amplitude coupling measures suffer three times the amount of noise relative to the spectral power measures. If one also accounts for the depth of the sources (that is, a shallow source for power and a deep source for phase-amplitude coupling), it becomes entirely reasonable to expect that hippocampal phase-amplitude coupling measures explain less variance than neocortical power measures.

No significant coupling was observed during perception ($p > 0.5$, $r^2 = 0.02$) or retrieval ($p = 0.148$, $r^2 = 0.03$). These results suggest that memory-related theta/gamma phase-amplitude coupling is most prominent during periods of representation binding.

To confirm the spatial specificity of the effect observed during representational binding, we re-ran this analysis using four additional regions of interest: the frontal lobe, parietal lobe, temporal lobe (excluding the hippocampus), and the occipital lobe. Only the parietal lobe showed a trending effect of theta-gamma phase-amplitude coupling (frontal: $p = 0.496$, $r^2 = 0.01$; parietal: $p = 0.091$, $r^2 = 0.06$; temporal: $p = 0.265$, $r^2 = 0.02$; occipital: $p = 0.344$, $r^2 = 0.02$). These results suggest the memory-related enhancement in theta/gamma phase-amplitude coupling predominately arises in the hippocampus.

5.3. Discussion

During episodic memory formation, the amount of hippocampal synchrony can be predicted by the amount of preceding neocortical desynchrony (see chapter 4). Similarly, the amount of neocortical desynchrony during episodic memory retrieval can be predicted by the preceding hippocampal synchrony. While this has been interpreted as the interaction between information representation within the neocortex and representational binding in the hippocampus (Hanslmayr et al., 2016), such a correlation between two neural phenomena could also be ascribed to a singular cognitive process. Here, we disentangle these two ideas by using a paradigm that temporally separated information representation and representational binding. In this task, we found that memory-related decreases in neocortical alpha/beta power only arose during the perception and retrieval of the sequence, fitting with the idea that these decreases reflect information representation. In contrast, memory-related increases in hippocampal theta/gamma phase-amplitude coupling only arose during the association window, fitting with the idea that such coupling reflects the representational binding of a memory. These results suggest that alpha/beta desynchronisation and hippocampal theta/gamma synchronisation reflect two distinct cognitive processes in episodic memory formation and retrieval.

The representation of information relating to an ongoing event or retrieved memory is thought to be supported by the desynchronisation of neocortical alpha/beta oscillations (Hanslmayr et al., 2012). Information theory proposes that unpredictable states carry more information than predictable states (Shannon & Weaver, 1949). As spiking in desynchronised neural networks is less predictable than spiking in synchronised networks, the former is thought to benefit information representation. Our findings add to the ever-increasing number of studies implicating neocortical alpha/beta power decreases in the successful formation and retrieval of episodic memories (e.g. Fell, Ludowig, Rosburg, Axmacher, & Elger, 2008; Fellner, Bäuml, & Hanslmayr, 2013; Griffiths et al., 2016; Hanslmayr et al., 2009, 2011; Long & Kahana, 2015; Sederberg et al., 2007; Waldhauser et al., 2016). Notably, our paradigm was sensitive to the amount of information encoded/retrieved. Therefore, it allowed us to ask if neocortical alpha/beta power decreases not only correlate with *whether* a memory is encoded/recalled or not (as investigated in the studies above), but *how much* of the memory is encoded/recalled. During perception, our analysis suggests that alpha/beta power decreases directly correspond to the amount of information encoded about a memory. This result neatly ties in with earlier findings which suggest that neocortical alpha/beta power decreases track the quantity of information reinstated within the brain (see chapter 2; Martín-Buro et al., 2019). Seemingly, the results presented here, in conjunction with those that from previous studies, suggest that alpha/beta power decreases track the quantity of information being encoded and retrieved as an episodic memory.

However, our analysis of alpha/beta power during retrieval presented a somewhat contradictory picture. Here, it seemed that a linear model of alpha/beta power explained approximately the same amount of variance as a hit vs. miss model. We speculate that this is driven by the complexity of the reinstated traces of scenes relative to patterns. While both are processed to the same extent during encoding (i.e. explored for the same amount of time), which induces a similar reduction in alpha/beta power for the two stimulus types, the same cannot be said for retrieval. Here, only a small amount of information need be reinstated about the pattern (i.e. the shape of the pattern [polkadot or check] and the two colours) to identify the correct pattern, whereas large amounts of detail about the scene (e.g.

objects in the foreground, semantic context, spatial position of elements) are needed to be reinstated to identify the associated scene. As such, one can speculate that alpha/beta power decreases during retrieval are likely to be substantially greater for scenes relative to patterns. Given that scene memory was substantially higher than pattern memory (82% vs. 49%), one can also speculate that partial memories are more likely to reflect the recall of the scene rather the pattern. Therefore, the recall of a complete memory (i.e. scene and pattern) is likely to induce an alpha/beta power decrease that is only marginally greater than that for a partial memory (predominately scenes). Such an idea would explain why a linear decrease in alpha/beta power was not apparent during retrieval.

We had hypothesised that alpha/beta power decreases should not arise during the binding window, as information representation should have predominantly arisen during the presentation of the sequence. Strictly speaking, we were correct in our hypothesis – alpha/beta power did not decrease during binding. Instead, we observed a substantial increase in alpha/beta power correlating with memory performance. Such increases are not unprecedented (Meeuwissen, Takashima, Fernandez, & Jensen, 2011; Tuladhar et al., 2007; Wianda & Ross, 2019). For example, Meeuwissen and colleagues (2011) reported that beta power increases during working memory maintenance predicted enhanced long-term memory performance. Based on this, one could speculate that the power increases we observe could also reflect maintenance of the sequence. Indeed, the maintenance of the sequence after presentation is perhaps essential for representational binding – without a maintained representation of the sequence, nothing is available to be bound together. An alternative explanation of the alpha/beta power increases mirrors our interpretation of the alpha/beta power decreases. Namely, these power increases reflect a reduction in information representation. During the binding of a sequence, it would be beneficial to attenuate the processing of any incoming information that may interfere with the sequence representation. Both theories provide plausible yet distinct explanations as to why alpha/beta power increases correlate with enhanced memory during the binding window.

We also investigated the role of hippocampal theta and gamma oscillations, with the hypothesis that their synchronisation (both independently as power increases, and their conjunction in phase-

amplitude coupling) would scale with memory performance during the binding window. Again, we were partially correct. We found that hippocampal theta-gamma phase-amplitude coupling scaled with memory performance – theta-gamma coupling increased with memory performance. Mechanistically speaking, these increases may reflect a heightened degree of long-term potentiation (LTP) within the hippocampus. By coupling gamma oscillations resonating at a frequency optimal for spike-timing dependent plasticity (STDP; Bi & Poo, 1998; Nyhus & Curran, 2010) to the phase of theta optimal for LTP (Hasselmo et al., 2002), the potential for building synaptic connections between hippocampal neurons is increased greatly. One could therefore speculate that the increase in theta-gamma coupling reflects an increase in underlying plasticity within the hippocampus. Alternatively, these increases in coupling may reflect enhanced representation of the sequence structure within the hippocampus. Numerous studies have suggested that theta-gamma phase-amplitude coupling provides an intricate mechanism well-suited for the representation and maintenance of sequences (Bahramisharif et al., 2018; Heusser et al., 2016; Lisman & Jensen, 2013) as well as complex event memories (Griffiths & Fuentemilla, 2019). Under these ideas, the observed increase in theta-gamma phase-amplitude coupling would be interpreted as reflecting a more robust representation of the sequence within the hippocampus, and perhaps this enhanced representation facilitates the encoding and retrieval of this sequence. Unfortunately, we cannot untangle these two ideas based on the data from the current paradigm. However, these two ideas needn't be adversarial. Indeed, sequence representation may be a convenient by-product of enhanced LTP via theta-gamma coupling, or vice versa. Regardless, it would appear that hippocampal theta-gamma phase-amplitude coupling scales with the number of items recalled about a memory.

Intriguingly, we did not observe any memory-related fluctuations in theta or gamma power during the binding window. We had been exploring theories that hippocampal theta/gamma synchronisation is beneficial for long-term potentiation (Bi & Poo, 1998; Hanslmayr et al., 2016; Nyhus & Curran, 2010), which emphasise the importance of theta phase for LTP, rather than power. Such theories would not anticipate that theta power would increase with enhanced representational

binding, perhaps explaining the absence of theta power fluctuations here. The absence of gamma power increases is more perplexing. Indeed, as increases in gamma power have been hypothesised to reflect increases in STDP, it is odd to not observe a strong increase in gamma power correlating with successful memory formation. However, our observed theta-gamma coupling effect may explain this. If memory-related increases in gamma power are restricted to particular phases of theta and theta is not stimulus-locked across trials, then across-trial averages of gamma power are unlikely to reveal any memory-related change as the temporal onset of these gamma power increases are not consistent across trials.

It is worth noting that we have, throughout this paper, considered information representation to arise solely during sequence perception and sequence retrieval, and representational binding to arise solely during the binding window. However, it seems plausible to suggest these cognitive processes are not completely restricted to their respective windows. Indeed, one may anticipate that representation of the stimulus also arises during mental association of the stimuli (Dijkstra, Bosch, & van Gerven, 2019), and that some representational binding arises during sequence perception (Griffiths & Fuentemilla, 2019; Heusser et al., 2016). We do not dispute these ideas, but do suggest that any information representation that does arise during the binding window will be substantially smaller than during stimulus presentation, as we anticipate that the vast majority of stimulus representation to occur when participants are first shown the stimulus. Similarly, while some binding may arise during sequence perception, this will be substantially less than the binding that occurs at the end of the sequence, simply because any binding that arises before the end of the sequence has fewer stimuli to bind together. In short, while the two cognitive processes are unlikely to be completely segregated in this paradigm, there still is a substantial degree of segregation that allows us to investigate the distinct neural correlates of these processes.

In sum, we demonstrate that decreases in neocortical alpha/beta power and increases in hippocampal theta/gamma phase-amplitude coupling are functionally dissociable in episodic memory. These results add further support to the idea that neocortical desynchrony supports memory-related

information representation while hippocampal synchrony supports representational binding (Hanslmayr et al., 2016).

5.4. Methods

5.4.1. Participants

Twenty-eight participants were recruited (mean age = 25.4; age range = 20-33; 68% female; 82% right-handed). In return for their participation, they received course credit or financial reimbursement. One participant was excluded for excessive head movement (greater than 2 standard deviations above group mean). Four participants were excluded for poor quality data (more than 50% of trials rejected for artifacts). Six participants were excluded for extreme memory performance (fewer than 15 trials in one of the three memory conditions). All exclusion criteria were pre-registered (see https://osf.io/4nt23/; see supplementary materials). This left seventeen participants for further analysis. Ethical approval was granted by the Research Ethics Committee at the University of Birmingham, complying with the Declaration of Helsinki.

5.4.2. Behavioural paradigm

Each participant completed a visual associative memory task (see figure 5.1). During encoding, participants were presented with a line drawing of an object, a pattern, and a scene (each for 1500ms, with a 500ms fixation cross shown between each stimulus). The order in which the pattern and scene were presented was swapped between each block. A prompt then appeared on screen instructing the participants to vividly associate these three items for a later memory test. Participants were then asked how difficult they found associating the triad. This question was used to keep participants attending to the task, rather than provide a meaningful metric for analysis. The next trial began after the participant had responded to the difficulty question. After associating 48 triads, participants started the distractor task. In the distractor task, participants attended to a fixation cross in the centre of a black screen. The fixation cross would flash from light grey to either white or dark grey momentarily (~100ms) approximately every 20 seconds. The participants were instructed to count the number of times the fixation cross changed to white (ignoring the times it turned dark grey) and report this value at the end of the task (approximately 2.5mins later). The retrieval task followed the distractor. Here, participants were presented with the line drawing and asked to recall the association they made earlier. After 3000ms, participants were presented with three patterns (one correct and two lures) to select from. After responding, participants were presented with three scenes (one correct and two lures). On blocks where scenes preceded

patterns during perception, the presentation order at retrieval was also reversed. After responding, participants were then asked to indicate how confident they were about their choices. They could select 'guess' (i.e. they guessed their choice), 'unsure' (i.e. they could not remember the item, but had a feeling it was the correct choice), or 'certain' (i.e. they could vividly remember the item). Participants were asked to recall all 48 triads learnt in the earlier encoding phase. Participants completed 4 blocks of this task (192 trials in total).

5.4.3. Behavioural analysis

For each trial, memory performance was coded as either 'complete' (i.e. they remembered both the scene and the pattern), 'partial' (i.e. they remembered only one of the associates), or 'forgotten' (i.e. they remembered neither the scene nor the pattern). Any trial where the participant indicated that they guessed was marked as a 'miss'.

5.4.4. MEG acquisition

MEG data was recorded using a 306-channel (204 gradiometers, 102 magnetometers) whole brain Elekta Neuromag TRIUX system (Elekta, Stockholm, Sweden) in a magnetically shielded room. Participants were placed in the supine position for the duration of the experiment. Data was continuously recorded at a sampling rate of 1000Hz. The headshape of each participant (including nasion and left/right ear canal) was digitised prior to commencing the experiment. Continuous head position indicators (cHPI) were recorded throughout. The frequencies emitted by the cHPI coils were 293Hz, 307Hz, 314Hz and 321Hz. Magnetometer data was excluded from the main analysis as they contained substantial noise that could not be effectively removed or attenuated.

5.4.5. MEG preprocessing

All data analysis was conducted in Matlab using Fieldtrip (Oostenveld et al., 2011) in conjunction with custom scripts. First, the data was low-pass filtered at 165Hz to remove the signal generated by the HPI coils. Second, the data was epoched around each event of interest. At encoding, the epochs reflected the time windows when each stimulus was presented (from here termed 'perception') and when the 'associate' prompt was presented (termed 'association'). At retrieval, the epochs reflected the time window when the object cue was presented (termed 'retrieval'). Perception epochs began 2000ms before stimulus onset and ended 3500ms after onset (that is, 2000ms after stimulus offset). Association and retrieval epochs began 2000ms before stimulus onset and ended 4500ms after onset (that is, 2000ms after stimulus offset). Third, independent components

analysis was conducted, and any identifiable eye-blink or cardiac components were removed. Fourth, the data was visually inspected and any artefactual epochs or sensors were removed from the dataset.

5.4.6. Movement correction

To identify participants were extreme head motion during MEG recordings, the recorded data was first high-pass filtered to 250Hz to isolate the cHPI signal. Second, the variance of the signal for each sensor was computed across every time point of the continuous recording. Third, the variance was mean averaged across sensors to provide a singular estimate of change in cHPI signal across the duration of the experiment. Fourth, the mean variance and its standard deviation was calculated across participants. Lastly, participants with extreme head motion were identified as those with variance greater than two standard deviations above the group mean. These participants were excluded from further analysis.

To help attenuate motion-related confounds in the spectral power analyses, a trial-by-trial estimate of motion was calculated. First, the data was high-pass filtered at 250Hz. Second, the data was epoched into trials matching those outlined in the section above. Third, the envelope of the signal in each epoch was then calculated (to avoid issues of mean phase angle difference in cHPI signal across trials). Fourth, the envelope was averaged over time to provide a single value for each epoch and channel. Fifth, the dot product across sensors was computed between the first epoch and every other epoch. This provided a single value for each trial that described how similar the topography of that trial was to the first trial (with the assumption that the more dissimilar a cHPI topography is to the starting topography, the more the head has deviated from its starting position). These values were entered into a linear regression which described the observed data as a sum of motion (i.e. cHPI topographic dissimilarity) and residuals ($y = ax + b$; where y is the signal, x is motion, b is the residuals and a is an unknown constant). This equation was solved and the residuals were extracted to provide an estimate of the data that cannot be explained by head motion.

5.4.7. Time-frequency analysis

Sensor-level time-frequency decomposition was conducted on the three epochs (perception, association, and retrieval). For low frequencies, the preprocessed data was first convolved with a 6-cycle wavelet (-0.5 to 3 seconds, in steps of 50ms; 2 to 40Hz; in steps of 1Hz). For high frequencies, Slepian multitapers were used to estimate power (-0.5 to 3 seconds, in steps of 50ms; 40 to 100Hz, in steps of 4Hz). For this latter analysis, frequency smoothing was set to one quarter of the frequency of interest and temporal smoothing was set to 200ms. Second, planar gradiometers were combined by summing the power of the vertical and horizontal

components. Third, movement-related changes in power were regressed out as described in the above section. Fourth, for perceptual trials only, power was then averaged over the three stimulus presentation windows of each triad to provide mean power during perception of the triad. Any triads where one or more epochs had been rejected during preprocessing were excluded at this stage. Fifth, the data was baseline correlated by z-transformation (Griffiths et al., 2016). To this end, power was first averaged over time for each trial, channel and frequency band. The mean and standard deviation of this time-averaged power was then computed across trials. This mean was then subtracted from power for each trial, and the resulting value was divided by the standard deviation.

For statistical analysis, the data for each participant was split based on memory performance (complete, partial, and forgotten), and averaged over trial repetitions. Every channel-frequency-time bin was then subjected to a linear regression across participants where observed power was fitted to a model of memory performance, where forgotten memories were given a value of 0, partial memories a value of 1, and complete memories a value of 2. As such, a positive t-value (i.e. beta weight divided by standard error of fit) would indicate that spectral power increases with better memory and a negative t-value would indicate that spectral power decreases with better memory. To address the issue of multiple comparisons, the resulting t-values were subject to a one-tailed cluster-based permutation test (2000 permutations; Maris & Oostenveld, 2007). Clusters that produced a p-value less than 0.05 were considered significant.

5.4.8. Model comparison

To examine the statistical pattern that produced the result observed in our regression analyses, we generated three models that could, theoretically, produce such a trend:

> *Linear model:* A linear trend where power decreases with increasing memory performance. Here, complete memories were coded with the value 2, partial memories with the value 1, and forgotten triads were coded with the value 0.
>
> *Hit vs. miss model:* A binary division where any successful encoding produces a power decrease relative to the forgotten triads, but no distinction exists between triads that were completely recalled and triads that were only partially recalled. Here, complete and partial memories were coded with the value 1, and forgotten triads were coded with the value 0.

All-or-nothing model: A binary division where successful encoding of the entire triad produces a power decrease relative to the partial and forgotten triads, but no distinction exists between triads that were partially recalled and triads that were forgotten (the "all-or-nothing model"). Here, complete memories were coded with the value 1, and partial and forgotten triads were coded with the value 0.

These predictors were entered into a linear regression (using the Matlab function *fitlm*) with additional participant-specific binary regressors aimed at capturing participant-unique changes in power. These predictors were fitted to observed power within the cluster returned by the cluster-based regression analysis. The r^2 of each model was then calculated and compared to evaluate which model best fit the data.

5.4.9. Source analysis

The preprocessed data was reconstructed in source space using individual head models and structural (T1-weighted) MRI scans. The headshape (together with the HPI coil positions) of each participant was digitised using a Polhemus Fasttrack system. The timelocked EEG data was reconstructed using a Linearly Constrained Minimum Variance (LCMV; van Veen, van Drongelen, Yuchtman, & Suzuki, 1997) beamformer. The lambda regularisation parameter was set to 1%.

5.4.10. 1/f correction

To isolate oscillatory contributions, 1/f activity was attenuated in the time-frequency data by subtracting the linear fit of 1/f characteristic (Griffiths et al., 2019; Manning et al., 2009; Zhang & Jacobs, 2015). To this end, a vector containing values of each derived frequency (A) and another vector containing the power spectrum, averaged over all time-points and trials of the relevant memory condition, (B) were log-transformed at approximate a linear function. The linear equation $Ax = B$ was solved using least-squares regression, where x is an unknown constant describing the curvature of the 1/f characteristic. The 1/f fit (Ax) was then subtracted from the log-transformed power spectrum (B). As this fit can be biased by outlying peaks (Haller et al., 2018), an iterative algorithm was used that removed probable peaks and then refitted the 1/f. Outlying peaks in this 1/f-subtracted power spectrum were identified using a threshold determined by the mean value of all frequencies that sat below the linear fit. The MEG power spectrum is the summation of the 1/f characteristic and oscillatory activity (i.e. at no point does oscillatory activity subtract from the 1/f), therefore all values that sit below the linear fit can be seen an error of the fit driven by oscillatory peaks. Any peaks that exceed the threshold were

removed from the general linear model, and the fitting was repeated. Notably, as power for the low frequencies (2-40Hz) and high frequencies (40-100Hz) was calculated using different methods (wavelets and Slepian multitapers, respectively), the two bands have disparate levels of temporal and spectral smoothing. To avoid a spurious fitting due of the 1/f across these bands because of these differences, the 1/f correction was conducted separately for these two bands. When investigating whether the 1/f slope could explain memory-related differences in power, the low-frequency beta weight was used as this mapped onto the frequency bands that exhibited the memory-related difference.

5.4.11. MEG phase-amplitude coupling analysis

To calculate the extent to which hippocampal gamma activity coupled to hippocampal theta phase, the modulation index (MI) was calculated (Tort et al., 2010). First, the peak theta and gamma frequencies were calculated by estimating power across all hippocampal virtual sensors using the Fourier Fast Transform (FFT) and then subtracting the 1/f characteristic. The Matlab function *findpeaks()* was then used to extract the most prominent peak within the theta (2-7Hz) and gamma (40-100Hz) bands for each participant. Across participants, the mean theta peak was at 5.4Hz, and the mean gamma peak was at 75.5Hz. Second, the time-series of the hippocampal virtual sensors were duplicated, with the first being filtered (FIR) around the theta peak (±0.5Hz) and the second being filtered around the gamma peak (±5Hz). Third, the Hilbert transform was applied to the theta- and gamma-filtered time-series, with the phase of the former and power of the latter being extracted. Fourth, the time-series data was re-epoched, beginning 500ms after the onset of the stimulus/fixation cross and ending 500ms before the onset of the next screen. This attenuated the possibility that an event-related potential and/or edge artifacts from the filtering/Hilbert transform could influence the phase-amplitude coupling measure (Aru et al., 2014). Fifth, gamma power was binned into 12 equidistant bins of 30Hz, according to the concurrent theta phase. This binning was conducted across trials of the same memory condition, but for each sensor separately as theta phase differences across sensors may mask any coupling (Lubenov & Siapas, 2009). Notably, as differences in trial number can bias the phase-amplitude coupling estimate, trial numbers for each memory condition were balanced. This was achieved by identifying the condition with the smallest number of trials and then taking a matching number of trials from the other conditions (evenly distributed across the duration of the experiment). Sixth, the MI was computed by comparing each memory condition to a uniform distribution, and these MI values were averaged over virtual sensors to provide a single value of phase-amplitude coupling for each participant and each memory condition. Seventh, these results were subjected to the same statistical

procedure as outlined above; namely, a linear regression that compared changes in phase-amplitude coupling to changes in memory performance.

As the modulation index is computed across trials, single trial motion correction could not be applied. To rule out the possibility that motion drives the observed effect during the binding window, the coupling of flanking gamma frequencies were considered. As head movement within the dewar induces spectrally broad effects (that is, motion effects are not restricted to a single frequency band), any effect driven by motion should be observable in theta-gamma coupling across a range of gamma frequencies. This was tested by computed the modulation index for a frequencies ranging from peak gamma minus 20Hz to peak gamma plus 20Hz. As can be seen in figure 5.5c, the theta-gamma coupling effect is primarily restricted to the exact peak gamma frequency, and cannot be considered spectrally-broad. As such, it seems more plausible to view the current result as one driven by brain-related differences between conditions rather than motion-related differences between conditions.

CHAPTER 6: SUMMARY OF RESULTS AND FUTURE QUESTIONS

Throughout this thesis, I have asked how neocortical desynchronisation, hippocampal synchronisation, and the interactions between them underpin both the successful formation and successful retrieval of episodic memories. In this final chapter, I integrate the findings of each empirical chapter, highlighting what has been learnt and what is still to be figured out. Additionally, I discuss how these findings may be applied in population at large.

6.1. Alpha/beta power decreases as a marker for information representation

The desynchronisation of alpha/beta oscillatory activity during cognitive engagement is one of the most ubiquitous electrophysiological phenomena to be observed in humans (Berger & Gloor, 1969; Buzsaki & Draguhn, 2004). These task-related decreases in alpha/beta synchrony can be observed across sensory modalities (Crone et al., 1998; Krause et al., 1994; Pfurtscheller et al., 1994) and a wide-range of cognitive tasks (Hanslmayr et al., 2011; Obleser & Weisz, 2012; Pfurtscheller et al., 1994). Indeed, alpha/beta desynchrony seems to have been preserved across our evolutionary history, as witnessed by their presence in monkeys, cats and even honeybees (Chatila et al., 1992; Haegens et al., 2011; Pfurtscheller et al., 1994; Popov & Szyszka, 2019). Given the ubiquity of alpha/beta desynchronisation, it stands to reason that they reflect a highly general neural mechanism. This has generated the hypothesis that alpha/beta desynchrony reflects information representation (Hanslmayr et al., 2012). One mechanistic explanation suggests that desynchronisation would attenuate the task-irrelevant noise correlations within the neocortex, allowing weak signals to be more clearly communicated (e.g. Averbeck, Latham, & Pouget, 2006). An alternative account, derived from information theory, proposes that desynchronised networks carry substantial more entropy than synchronised networks and hence can represent more information (Hanslmayr et al., 2012; Shannon & Weaver, 1949). Empirical research in humans has provided numerous indirect links between alpha/beta desynchrony and the representation of information within the neocortex. For example, task instructions which ask participants to deeply process a stimulus produce greater decreases in alpha/beta power than task instructions which only required superficial stimulus processing (Hanslmayr et al., 2009). However, a direct link between alpha/beta activity and an objective measure of information representation has been missing, making it difficult to conclude that alpha/beta power decreases are directly correlated with information representation within the neocortex.

In chapter 2, we addressed this by presenting evidence to suggest that alpha/beta power decreases track the fidelity of information representation. Utilising simultaneous EEG-fMRI recordings, we were able to track the co-fluctuation of information representation and alpha/beta power on a trial-by-trial

level. When participants watched brief video clips, we could predict how much information about the clip was represented within the neocortex based on concurrent alpha/beta power. In other words, as alpha/beta power decreased, information representation increased. We went on to demonstrate that this phenomenon transcends both stimulus modality and task demands by replicating the effect in an auditory perception task and a visual memory retrieval task. This thrice-demonstrated phenomenon provides strong evidence to suggest that alpha/beta power decreases are linked to an objective measure of information representation within the neocortex. Moreover, these results were, in part, corroborated in chapter 5. In this experiment, we found that the more associates a participant could later remember on a given trial, the greater the alpha/beta power decrease was during perception. Together these results indicate that alpha/beta power decreases parametrically track the amount of information represented within the neocortex.

While these findings implicate alpha/beta power decreases in information representation, they are not able to elucidate the underlying mechanistic process. Indeed, the two theories linking alpha/beta desynchrony and information representation are only distinguishable on the neuronal level. The information-via-desynchronisation account proposes that total desynchrony of neurons within a network is optimal for information representation. In contrast, the noise correlation account proposes that only the desynchronisation of neurons that are irrelevant to the task at hand is required. To distinguish these two theories, therefore, one would need to record the activity of single units and examine whether total desynchrony (as predicted by the information-via-desynchronisation account) or selective desynchrony (as predicted by the noise correlation account) better explains information representation. Such a test would help elucidate the underlying process by which alpha/beta desynchronisation aids information representation.

It is also worth noting that the correlative nature of these studies means that it cannot be concluded that alpha/beta power decreases *cause* the representation of information. To answer such a question, direct influence over neural activity is required. Intriguingly, several studies have demonstrated that disrupting alpha/beta activity via non-invasive brain stimulation (NIBS) impairs

indirect measures of information representation (e.g. performance on a variety of tasks, across a variety of sensory modalities; Hanslmayr, Matuschek, & Fellner, 2014; Waldhauser, Braun, & Hanslmayr, 2016). By combining these techniques with the methodology used in chapter 2, future studies can ask whether the exogenously disrupting of alpha/beta activity impairs the representation of stimulus information (as measured by fMRI). Speculatively, such work would elucidate a causal link between alpha/beta activity and information representation.

Advances in NIBS also provide an interesting insight into how our findings may be applied to help clinical populations overcome cognitive impairments. Several NIBS techniques have become common in scientific research over the last few decades, including transcranial magnetic stimulation (TMS; which can directly induce neuronal firing; Barker, Jalinous, & Freeston, 1985; Walsh & Cowey, 2000) and transcranial alternating stimulation (tACS; which can influence the membrane potential of a neuron and induce an oscillation; Herrmann, Rach, Neuling, & Strüber, 2013; but also see Lafon et al., 2017). In cases of high amplitude alpha/beta oscillations, arrhythmic TMS may help neurons fire across the oscillatory phase and, in essence, artificially desynchronise the network (Tamura et al., 2005). Therefore, exogenously-induced desynchrony may help perception and memory by desynchronising alpha/beta oscillations and hence boosting information representation in those who have difficulty with such tasks (and, indeed, the population at large; e.g. Gagnon, Schneider, Grondin, & Blanchet, 2011). In contrast, tACS could be used to entrain alpha/beta oscillatory rhythms within a cortical network and hence boost alpha/beta synchrony. Intuitively, this may appear to be only detrimental to cognitive function as it would impair information representation. However, given that many cognitive disorders involve the intrusion of unwanted memories (e.g. in post-traumatic stress disorder; PTSD) or thoughts (e.g. in anxiety/depressive disorders), impairing information representation may help those suffering these maladies escape from these unwanted cognitions (Jianjun Chen et al., 2013; Karsen, Watts, & Holtzheimer, 2014). While the implementation of NIBS still requires refinement (Braun, Sokoliuk, & Hanslmayr, 2017; Hanslmayr, Axmacher, & Inman,

2019; Santarnecchi et al., 2015), it seems plausible to suggest that integrating our findings with these techniques may help alleviate a number of cognitive maladies.

Conclusion

The desynchronisation of alpha/beta oscillations during cognitive engagement is one of the most well-documented phenomena in human electrophysiological research. Here, we demonstrate that these decreases parametrically scale with the fidelity of information represented within the neocortex, supporting ideas that alpha/beta desynchrony reflects information representation. While the causal nature and exact mechanistic underpinnings of these phenomena remain murky, these results nonetheless provide an exciting step forward in our understanding of how information can be represented in the brain.

6.2. Distinct gamma oscillations mark the formation and retrieval of episodic memories

During both the formation and retrieval of episodic memories, hippocampal gamma activity sees a sharp increase in power (Colgin, 2016; Hanslmayr & Staudigl, 2014; Nyhus & Curran, 2010). Mechanistically speaking, increases in hippocampal gamma activity may reflect an increase in spike-timing dependent plasticity (STDP; a form of long-term potentiation; Bi & Poo, 1998). STDP is optimal when neurons fire at approximately ~60Hz, so an oscillation resonating at this frequency (i.e. hippocampal gamma) could help drive the neuronal firing that induces STDP. However, such an explanation does not elucidate why similar increases are observed during successful memory retrieval (e.g. Montgomery & Buzsáki, 2007; Staresina et al., 2016). STDP has no functional relevance during retrieval (or, at least in many of the paradigms where retrieval-related gamma power increases are observed; Nyhus & Curran, 2010). These retrieval-related gamma power increases may be better explained as a change in information routing within the hippocampus. Numerous studies in rodents have shown that “fast” gamma (~60Hz) generated in the medial entorhinal cortex (MEC) can entrain neurons in the hippocampal subfield CA1 to help neocortical information flow into the hippocampus, while “slow” gamma (~40Hz) generated in CA3 can entrain neurons in CA1 to facilitate reinstated

memory traces flow out of the hippocampus (Colgin et al., 2009). Evidence for such a phenomenon in humans, however, has been lacking.

In chapter 3, we addressed this by contrasting hippocampal gamma activity during episodic memory formation and retrieval. In line with data from rodents, we found that "fast" gamma (60-80Hz) power was greater during memory encoding, while "slow" gamma (40-50Hz) power during memory retrieval. We went on to demonstrate an interaction between these gamma bands and memory performance – memory-related increases in "fast" gamma power benefitted encoding, while memory-related increases in "slow" gamma power benefitted retrieval. This provides the first empirical evidence in humans to suggest that two separable hippocampal gamma oscillations differentially contribute to episodic memory formation and retrieval.

In chapter 4, we took this finding further by demonstrating that "fast" and "slow" hippocampal gamma oscillations interact with neocortical alpha/beta activity in distinct ways. Increases in "fast" gamma power followed neocortical alpha/beta power decreases during successful memory formation. In contrast, "slow" gamma power increases preceded neocortical alpha/beta power decreases during successful memory retrieval. These findings are particularly relevant to the information routing hypothesis. As the information routing hypothesis predicts that "fast" gamma helps transfer information from the neocortex into the hippocampus, "fast" gamma increases must follow from markers of neocortical information representation (i.e. alpha/beta power decreases). We observed just that. Moreover, as the information routing hypothesis predicts that "slow" gamma helps transfer reinstated memory traces to the neocortex, "slow" gamma power fluctuations must precede neocortical power decreases during memory retrieval. Indeed, our results support this hypothesis.

Notably, our uncovering of this dissociation does not discredit the STDP hypothesis of hippocampal gamma. As mentioned above, a key incongruency with the STDP hypothesis is that gamma power increases not only occur during encoding (where STDP is highly beneficial), but also during retrieval (where STDP is irrelevant to the task at hand). If STDP arises during retrieval, it could damage the retrieved memory trace by associating it with irrelevant elements from current sensory

experience. Our results, however, present a nuanced picture where "fast" gamma resonating at a frequency optimal for STDP supports episodic memory formation, and "slow" gamma resonating at a frequency that is too slow to effectively support STDP supports episodic memory retrieval. By taking care to appreciate the differences in the resonating frequency of hippocampal gamma, one can see how these oscillations can support encoding via STDP (when the rhythm is "fast") and also support retrieval without catastrophic association arising between the retrieved memory trace and current sensory experience.

However, open questions remain about how these dissociable gamma bands operate and interact. One central issue revolves around how "fast" and "slow" gamma oscillations coexist without interfering with one another. The information routing hypothesis proposes that CA1 neurons can be entrained by both the "fast" gamma oscillator in the MEC and the "slow" gamma oscillator in CA3. In instances when information is simultaneously being encoded and retrieved (such as memory integration; Griffiths & Fuentemilla, 2019; Koster et al., 2018), this would seemingly introduce competition between the two oscillators and result in catastrophic interference for both the to-be-encoded information and to-be-retrieved memory traces. One resolution to this idea is that coherence between CA1 neurons and the competing MEC/CA3 oscillators fluctuates as a function of theta phase (Colgin, 2015b). At the peak of the theta cycle, CA1 couples to the MEC, allowing information to flow into the hippocampus for encoding. At the trough of the theta cycle, CA1 couples to CA3 allowing reinstated memory traces to flow into the neocortex. This idea neatly couples with the theoretical, computational and empirical bodies of work which suggest that hippocampal theta oscillations switch the hippocampus between an encoding state and a retrieval state (Clouter et al., 2017; Hasselmo, 2005; Kerrén et al., 2018; Schapiro et al., 2017). Numerous studies have demonstrated that the coupling of gamma oscillations to theta phase underpins the formation of episodic memories (Bahramisharif et al., 2018; Heusser et al., 2016; Staudigl & Hanslmayr, 2013), which could be interpreted as evidence to support the idea that information influx into the hippocampus varies as a function of theta phase (Colgin, 2015b). Indeed, our findings in chapter 5

bring further support to this idea: the coupling of "fast" hippocampal gamma activity (~70Hz in this study) to hippocampal theta phase underpins the successful binding of an episodic memory. However, we did not observe such a phenomenon during retrieval. Elsewhere, there is little empirical work in humans linking theta-gamma coupling to successful retrieval, leading some to conclude that gamma does not couple to theta during memory retrieval (Nyhus & Curran, 2010). As such, it remains open to debate whether theta-gamma coupling is a viable mechanism to prevent interference between the "fast" and "slow" gamma rhythms.

As brain stimulation is difficult to apply to subcortical structures such as the hippocampus (though not theoretically impossible; Grossman et al., 2017), other techniques are necessary to apply our findings in clinical settings. One potentially fruitful avenue is through sensory entrainment. In brief, sensory entrainment involves "flickering" a stimulus (that is, rapidly turning the stimulus off and then on again) at the frequency you wish to entrain. Research suggests that sensory entrainment at the hippocampal theta frequency can boost memory performance (Clouter et al., 2017); however, similar approaches have not been undertaken at the gamma frequency. Our results suggest that flickering at a "fast" gamma rhythm would facilitate episodic memory formation, while flickering at a "slow" gamma rhythm would facilitate retrieval. Not only would such an effect demonstrate a causal link between these gamma bands and episodic memory, but they would also provide a simple, unobtrusive method to enhance memory function in both clinical and healthy populations.

Conclusion

Gamma oscillations have long been linked to episodic memory formation and retrieval across species (Colgin & Moser, 2010; Hanslmayr & Staudigl, 2014; Nyhus & Curran, 2010). Traditionally, they have been viewed as a marker for enhanced STDP, however such a theory does not explain why increases in gamma activity are also observed during memory retrieval. Here, we find evidence to suggest that two distinct gamma oscillations operate within the hippocampus: a "fast" gamma rhythm resonating between 60 and 80Hz, and a "slow" gamma rhythm resonating between 40 and 50Hz. Speculatively, "fast" gamma facilities information flow into the hippocampus (via MEC) at a

frequency optimised for STDP, while the "slow" gamma oscillation helps memory traces (reinstated in CA3) to be transferred to the neocortex for a vivid recollection of the experience.

6.3. Interactions between neocortical alpha/beta activity and hippocampal gamma activity underpin the formation and retrieval of episodic memories

Electrophysiological research into human episodic memory formation and retrieval has repeatedly uncovered the paradoxical finding that both oscillatory synchronisation and oscillatory desynchronisation appear to predict memory performance. The sync/desync framework (SDF; Hanslmayr, Staresina, & Bowman, 2016) addressed this conundrum by proposing that an oscillatory division of labour exists between neocortical desynchronisation and hippocampal synchronisation. Specifically, only when these processes interact can an episodic memory be successfully formed or retrieved.

In chapter 4, we uncovered direct evidence to support of this idea. During memory formation, neocortical alpha/beta power decreases preceded hippocampal "fast" gamma power increases. Conceptually speaking, this may reflect information being processed in the neocortex and then being passed onto the hippocampus for binding. During retrieval, hippocampal "slow" gamma power increases preceded neocortical alpha/beta power decreases. This may reflect the reactivation of this hippocampal trace being transferred back to the neocortex to induce vivid recollection. These results provide the first empirical support for an interaction between oscillatory synchronisation and oscillatory desynchronisation in service of episodic memory.

The results of chapter 4, however, did introduce a statistical problem in need of resolution. If neocortical desynchrony and hippocampal synchrony correlate, it becomes difficult to determine whether they reflect two distinct cognitive processes that interact, or whether they reflect two neural responses to a singular cognitive process. In chapter 5, we resolved this issue. Using MEG, we demonstrated that neocortical alpha/beta power decreases are restricted to time windows where information representation can unfold (i.e. during perception and memory retrieval), while increases in

hippocampal theta/gamma coupling are restricted to time periods where binding can unfold. These results suggest that, while the two neural correlates can overlap and correlate, they reflect distinct cognitive processes.

While these results provide a strong base of support for the SDF, it is worth considering two aspects in which the empirical data did not align with the hypotheses of the framework. Specifically: the distinction between "fast" and "slow" hippocampal gamma oscillations, and the role of hippocampal theta oscillations.

In chapter 3 and 4, we uncovered evidence to suggest that hippocampal gamma oscillations can be divided into functionally-distinct "slow" and "fast" rhythms (matching studies in rodents; e.g. Bragin et al., 1995; Colgin et al., 2009), and this distinction is critical to the interaction between the neocortex and hippocampus. However, the SDF only considered a singular hippocampal gamma oscillation. As such, the framework overlooks the nuanced nature of hippocampal gamma activity. This can be resolved by updating the SDF to incorporate the "fast"/"slow" gamma distinction, and the hippocampal subfields that are supposedly responsible for this distinction. Here, decreases in neocortical alpha/beta power reflect an increase in information representation, with said information being passed to the MEC. Increases in "fast" gamma activity enhances coherence between the MEC and CA1 (Colgin et al., 2009), allowing neocortical information to be passed into the hippocampus. When a cue is later encountered, pattern competition occurs within CA3. Increases in "slow" gamma activity then enhance coherence between CA3 and CA1 allowing the reinstated memory trace to returned to the neocortex via the subiculum (Rolls, 2007). Neocortical alpha/beta power decreases then allow information about the reinstated trace to be vividly processed and re-experienced. While this derivation of the SDF is more complex than the original, it perhaps provides a more accurate representation of how neocortical synchrony and hippocampal synchrony interact.

The SDF, its derived computational model (Parish et al., 2018), and a plethora of empirical studies (for review, see Nyhus & Curran, 2010) have placed hippocampal theta oscillations at the heart of how episodic memories are formed and retrieved. Intriguingly, we did not uncover a correlative link

between neocortical alpha/beta power decreases and hippocampal theta power increases. This may be explained by the idea that hippocampal theta phase, rather than hippocampal theta power, predicts memory performance. Computational models have proposed that the hippocampus switches between encoding and retrieval states as function of theta phase (e.g. Hasselmo, 2005), and empirical studies in humans have supported this claim (Clouter et al., 2017; Kerrén et al., 2018). The importance of theta to episodic memory was further discussed in the previous section, where theta phase may play an essential role in avoiding interference between to-be-encoded and to-be-retrieved traces within CA1 by dictating whether coupling arises between MEC and CA1, or CA3 and CA1 (Colgin, 2015b). These ideas suggest that theta phase plays a critical role in episodic memory. While theta phase has been acknowledged in the SDF, this has been restricted to encoding. However, it can be generalised to both encoding and retrieval. Here, information would arrive at the MEC from a desynchronised neocortex, and at the peak of theta, be transferred to CA1 via "fast" gamma activity. Meanwhile, reinstated information is transferred from CA3 to CA1, and then back to the neocortex, at the trough of theta via "slow" gamma activity. By restricting the encoding and retrieval processes to particular phases of theta, interference between to-be-encoded and to-be-retrieved information is avoided. By cementing focus on the phase of theta, such a theory would reconcile the SDF principle that hippocampal theta is important to episodic memory formation and retrieval, without contradicting the empirical evidence presented here that suggests there is no link between hippocampal theta power and neocortical alpha/beta power.

Conclusion

Empirical research into human episodic memory has consistently demonstrated that both successful memory formation and successful memory retrieval can be predicted by the presence of oscillatory synchrony and, paradoxically, oscillatory desynchrony. Following a recent framework, we demonstrate that these two processes interact. Specifically, neocortical power decreases precede hippocampal power increases during encoding while hippocampal power increases precede neocortical

power decreases during retrieval. These findings provide an empirical resolution to the so-called synchronisation-desynchronisation conundrum.

6.4. A final summary

In conclusion, the work presented in this thesis suggests that interactions between neocortical alpha/beta desynchrony and hippocampal gamma synchrony underpin the formation and retrieval of episodic memories. In this division of labour, neocortical alpha/beta desynchrony appears to facilitate the representation of highly-detailed information while hippocampal gamma synchrony may help route information through the hippocampal subfields and bind this together into a coherent representation. The work presented here provides a consistent series of results that support SDF (Hanslmayr et al., 2016).

APPENDIX A: SUPPLEMENTARY MATERIALS FOR THE EEG-FMRI DATASET

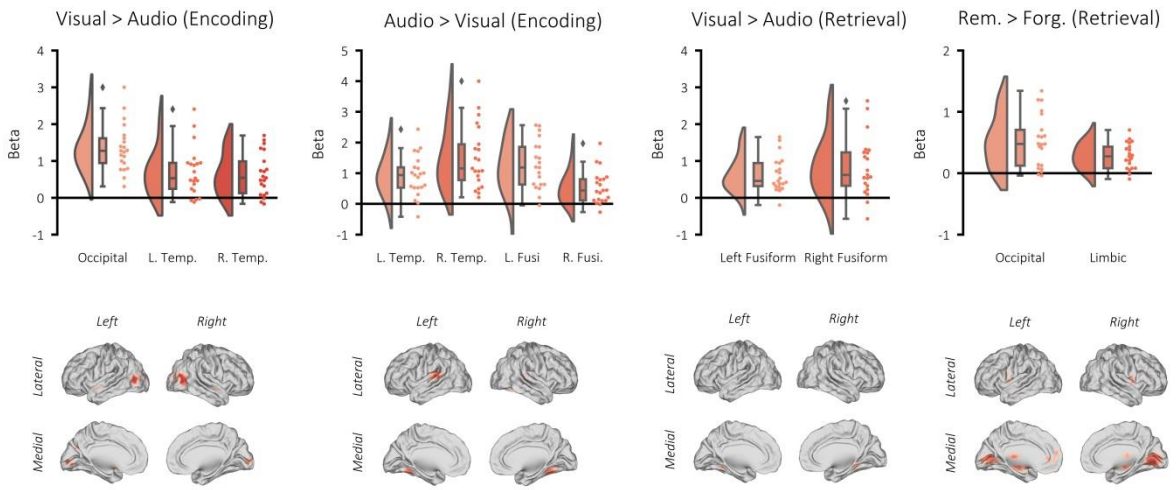

Figure 7.1. Univariate BOLD contrasts. Top: raincloud plots depicting the contrasted beta weights for each participant. Bottom: brain maps depicting the clusters revealed from the contrasts (non-significant voxels masked). A GLM was created per participant where these events were modelled as stick functions that had been convolved with a canonical hemodynamic response function (HRF). In addition, a regressor modelling button presses, six movement regressors and eight regressors modelling each run were added to the GLM. The derived beta weights for visual perception and auditory perception were then contrasted. The resulting contrast image of each participant was statistically appraised in a one-sample t-test across participants. Using a cluster-forming threshold of puncorr < 0.001 and k = 10, three significant clusters showed greater activation during visual perception relative to auditory perception: one in the occipital lobe (pFWE < 0.001, k = 975, MNI [x = 42, y = -70, z = 10], Cohen's d = 2.09), one in the left temporal pole (pFWE = 0.008, k = 67, MNI [x = -48, y = 2, z = -10], Cohen's d = 1.06), and one in the right temporal pole (pFWE = 0.005, k = 72, MNI [x = 48, y = 5, z = -14], Cohen's d = 1.11). Four significant clusters showed greater activation during auditory perception relative to visual perception: two bilaterally in the auditory cortex (left: pFWE < 0.001, k = 324, MNI [x = -63, y = -31, z = 14], Cohen's d = 1.35; right: pFWE < 0.001, k = 217, MNI [x = 60, y = -31, z = 14], Cohen's d = 1.47), and two bilaterally in the fusiform gyrus (left: pFWE < 0.001, k = 112, MNI [x = -24, y = -49, z = 14], Cohen's d = 1.18; right: pFWE < 0.001, k = 203, MNI [x = 27, y = -49, z = -18], Cohen's d = 1.00). Two significant clusters showed greater activation during visual retrieval relative to auditory retrieval: one in the left fusiform gyrus (pFWE = 0.001, k = 89, MNI [x = 21, y = -37, z = -14], Cohen's d = 1.05), and one in the right temporal pole (pFWE = 0.001, k = 99, MNI [x = -30, y = -46, z = -6], Cohen's d = 1.33). No clusters showed greater activation during auditory retrieval relative to visual retrieval. Two significant clusters showed greater activation during successful visual memory retrieval relative to unsuccessful visual memory retrieval: one in the occipital lobe (pFWE < 0.001, k = 1178, MNI [x = 12, y = -52, z = -14], Cohen's d = 1.21), and one spanning the limbic system, including the hippocampus (pFWE < 0.001, k = 1447, MNI [x = -21, y = -16, z = 2], Cohen's d = 1.33). No clusters showed greater activation during successful auditory memory retrieval relative to unsuccessful auditory memory retrieval.

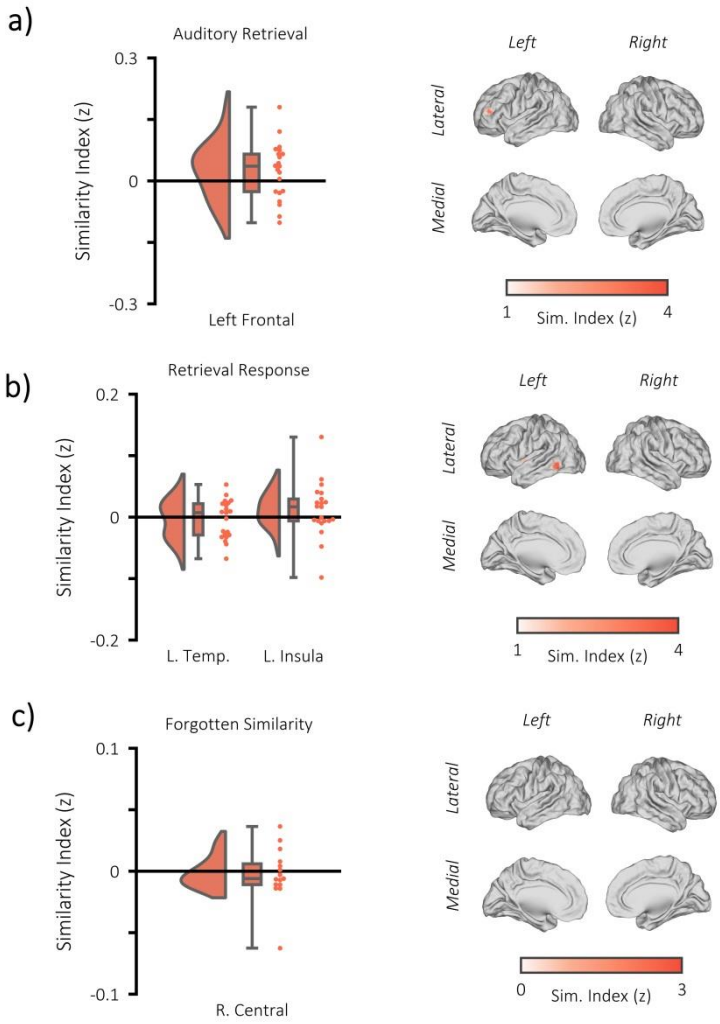

Figure 7.2. Additional fMRI RSA searchlight analysis. (a) raincloud plot (left) depicting the degree to which matching and differing stimuli could be distinguished from one another during auditory memory retrieval, per participant (single dots), within the significant cluster, and brain map (right) depicting the cluster where matching and differing stimuli could be distinguished from one another. The left frontal cluster did not pass threshold to be deemed statistical significant ($p = 0.153$, $k = 28$, MNI = [x = -39, y = 44, z = 14]). (b) raincloud plot (left) and brain map (right) for stimulus discriminability during the response period of the memory retrieval task (when still images of the stimuli were presented on screen [approximately 3 seconds after the retrieval cue]). Two significant clusters were identified (left temporal: $p = 0.002$, $k = 70$, MNI = [x = -39, y = 44, z = 14], Cohen's $dz = 0.12$; left insula: [= 0.013, k = 49, MNI = [x = -36, y = -4, y = -2], Cohen's $dz = 0.27$). However, neither overlapped with the fusiform clusters identified during the moment of visual memory retrieval, suggesting the still images did not drive the reported encoding-retrieval pattern similarity effect. (c) raincloud plot (left) and brain map (right) for encoding-retrieval similarity of forgotten stimuli. One cluster was formed, but did not pass threshold for significance (right central: $p = 0.681$, $k = 13$, MNI = [x = 39, y = -7, z = 66], Cohen's $dz = 0.13$).

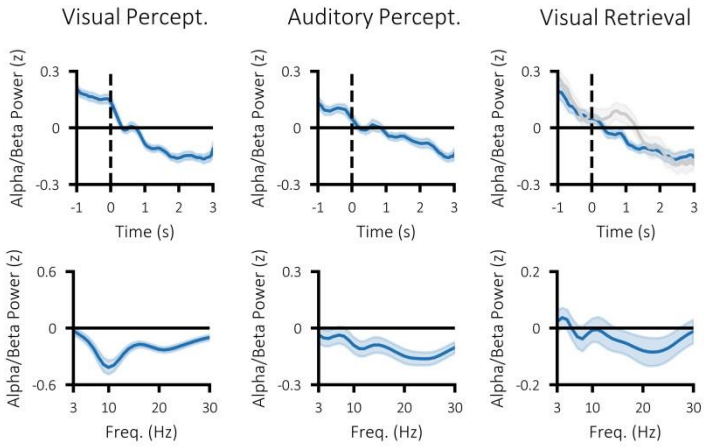

Figure 7.3. Alpha/beta power for each task. Time-series (top) and difference in spectral power (bottom) for visual perception (left; post-stimulus > pre-stimulus), auditory perception (middle; post-stimulus > pre-stimulus) and visual memory retrieval (right; hits > misses). Dark blue line indicates mean power across participants and shaded area indicates standard error of the mean. The grey line in the top right plot depicts the time-course for forgotten items.

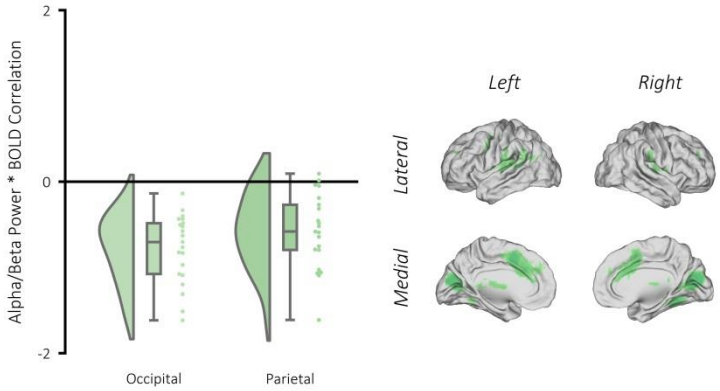

Figure 7.4. Correlation between alpha/beta power and BOLD signal during visual memory retrieval. Left: raincloud plot depicting significant clusters identified when contrasting beta weights (remembered > forgotten) for each participant. Right: brain map depicting the clusters where alpha/beta power negatively correlated with BOLD for remembered items (relative to forgotten items). A GLM was created as in Figure 2 – Figure Supplement 1 with one key exception: the binary stick functions used in the earlier GLM were replaced with parametric values dictated by alpha/beta power observed on that trial. These parametric values were calculated by convolving the source-reconstructed EEG data with a 6-cycle wavelet (-1 to 3 seconds, in steps of 25ms; 8 to 30Hz; in steps of 0.5Hz). The resulting data was z-transformed using the mean and standard deviation of power across time and trials (for each condition separately). Then, the data was restricted to the time/frequency window of interest (500-1500ms post-stimulus, 8-30Hz) and then averaged across this window and across all virtual electrodes within the brain to return a single value of alpha/beta power per trial. Trials that were removed during preprocessing due to artifact contamination were given the value 0. The statistical approach matched that of the Univariate fMRI analysis section. We uncovered two significant clusters where there was a greater negative relationship between BOLD and alpha/beta power for successfully recalled trials relative to forgotten trials: one in the occipital lobe ($pFWE < 0.001$, $k = 5183$, MNI [$x = -6$, $y = -76$, $z = 14$], Cohen's $d = 1.94$), and the other in the parietal lobe ($pFWE < 0.001$, $k = 139$, MNI [$x = 39$, $y = -40$, $z = 38$], Cohen's $d = 1.33$).

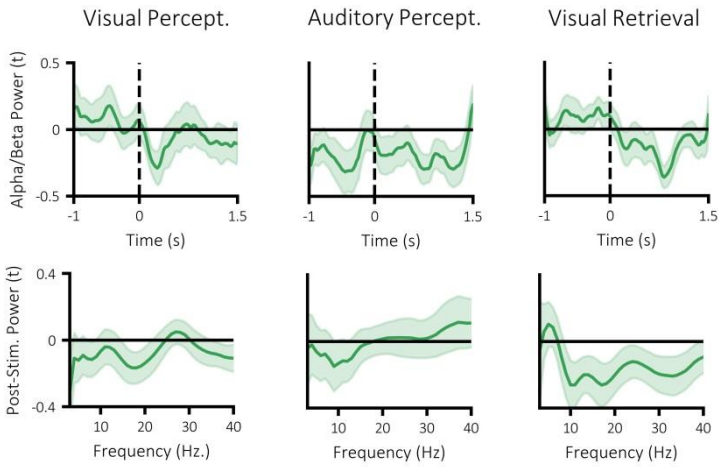

Figure 7.5. Specificity of power-similarity correlation across time (top) and frequency (bottom). Dark line indicates mean across participants and shaded area indicates standard error of the mean. A negative value indicates a negative relationship between power and stimulus-specific information. All analyses were conducted on an a priori window ranging from 8 to 30Hz, 500 to 1500ms post-stimulus.

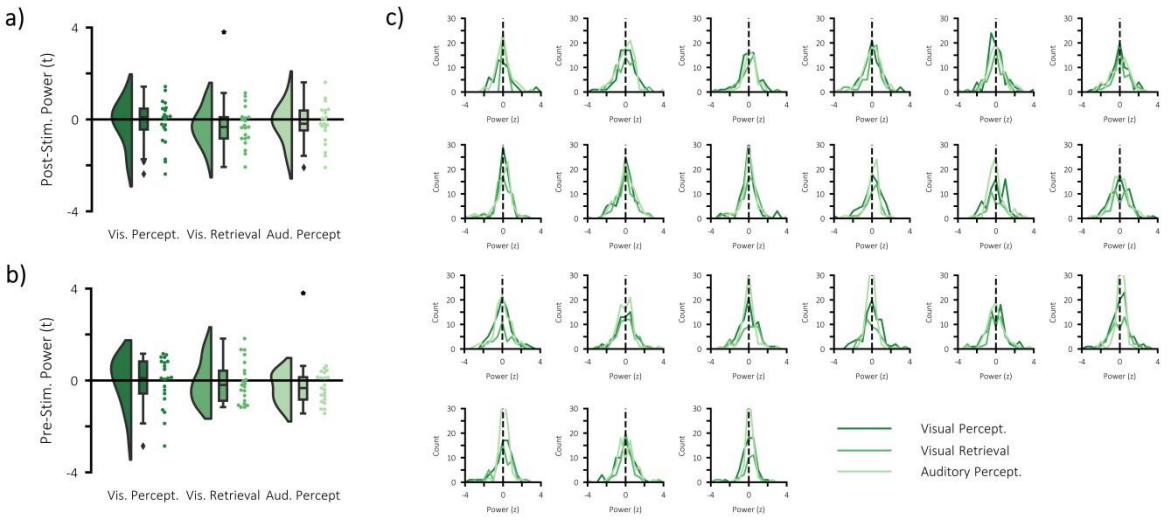

Figure 7.6. Investigating bimodal alpha power and stimulus-specific information. (a) Raincloud plot displaying the correlation between median-split post-stimulus alpha/beta power and stimulus-specific information during visual perception (each dot represents a single participant). Only during visual memory retrieval was an effect observed ($p = 0.045$, Cohen's $dz = 0.39$). Given the absence of a similar effect in the perceptual tasks, this effect may reflect an idiosyncrasy of the retrieval task such as bimodally-distributed power relating to recollection vs. familiarity. (b) Raincloud plot displaying the correlation between median-split pre-stimulus alpha/beta power and stimulus-specific information during visual perception (each dot represents a single participant). Only during auditory perception was an effect observed ($p = 0.037$, Cohen's $dz = 0.49$). (c) single participant plots of the distribution of post-stimulus alpha/beta power across trials for the three conditions. The overarching trend is a singular peak around zero, indicating a unimodal distribution.

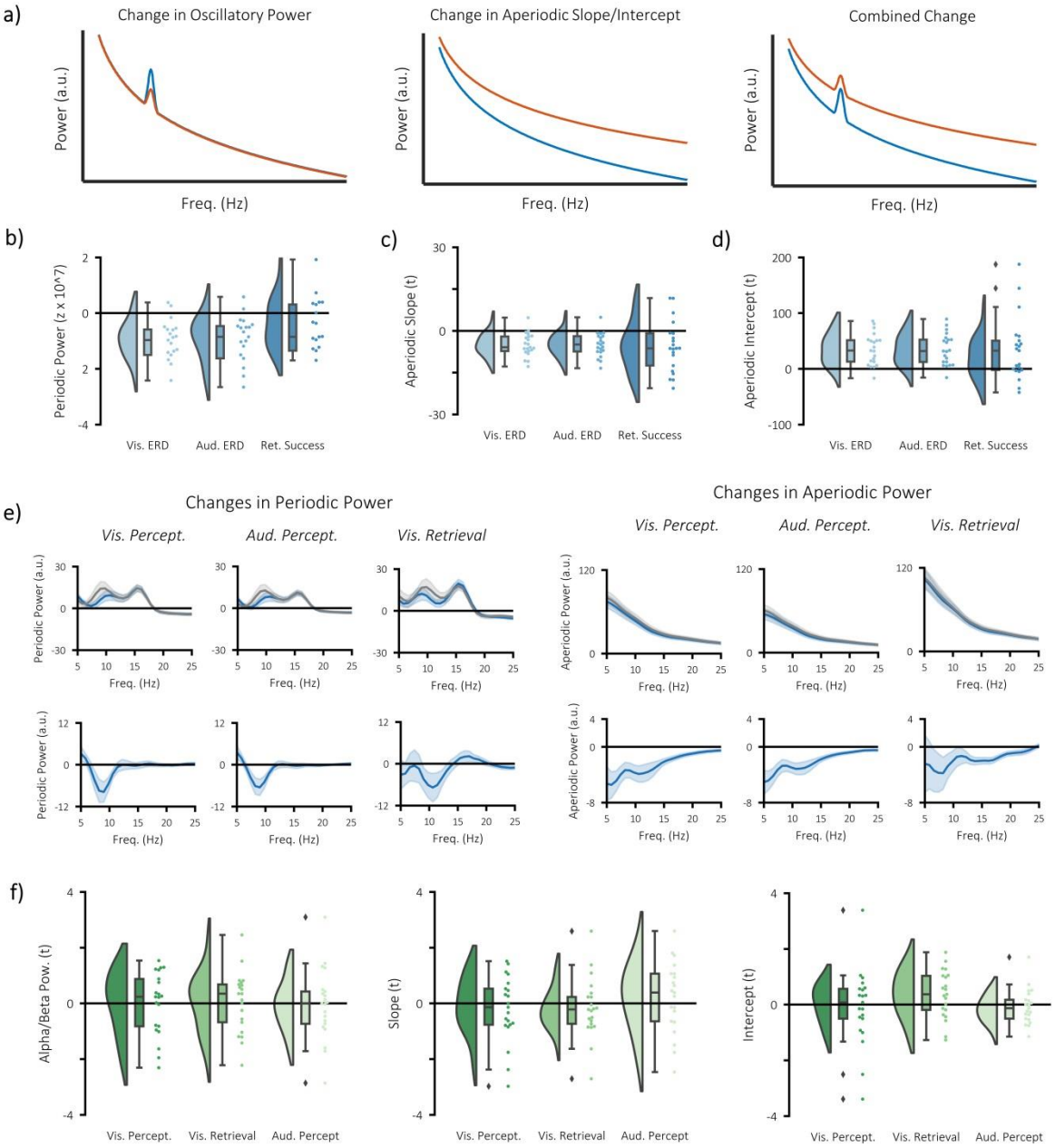

Figure 7.7. Separate contributions of periodic and aperiodic signal to event-related decreases in power. (a) wavelet-based time-frequency analytical approaches can detect changes in power that are oscillatory (left), aperiodic (middle), or a combination of the two (right). As a consequence, it becomes difficult to infer what a change in power reflects on a neural level. Methods such as the irregular-resampling auto-spectral analysis (IRASA) separates the power spectrum into periodic components (which reflects oscillatory activity) and aperiodic components (which reflect dynamics of the 1/.f phenomenon). By separating these components, we can identify whether changes in power are a result of changes in oscillatory activity or the 1/f characteristic. (b) significant decreases in periodic alpha/beta power (8-25Hz) were observed during visual perception ($p < 0.001$, Cohen's $dz = 0.55$), auditory perception ($p < 0.001$, Cohen's $dz = 0.46$), and visual memory retrieval ($p < 0.001$, Cohen's $dz = 0.48$). (c) significant decreases in the slope of the aperiodic signal (i.e. a flattening of the 1/f curve) were observed during visual perception ($p = 0.002$, Cohen's $dz = 0.68$), auditory perception ($p = 0.011$, Cohen's $dz = 0.67$), but not during visual memory retrieval ($p = 0.123$, Cohen's $dz = 0.52$).

(d) significant increases in the intercept of the aperiodic signal were observed during visual perception ($p = 0.002$, Cohen's $d_z = 0.73$) and auditory perception ($p = 0.049$, Cohen's $d_z = 0.61$), but not during visual memory retrieval ($p = 0.356$, Cohen's $d_z = 0.54$). (e) frequency spectra for periodic (left) and aperiodic (right) signals. Plots on the top compare post-stimulus (blue) power with pre-stimulus (grey) power during visual/auditory perception and hits (blue) with misses (grey) during visual retrieval. Plots on the bottom depict the difference between the blue and the grey bars. Note that the ~16Hz peak in the oscillatory signal is mostly likely produced by the MRI scanner, which collected a new slice 16 times a second. The peak could not be filtered out as done so with the wavelet data because the filtering impairs the fractal fit. (f) correlation between stimulus-specific information and periodic (left) and aperiodic (middle/right) measures of power. No significant relationship was observed in any of the measures or any of the tasks.

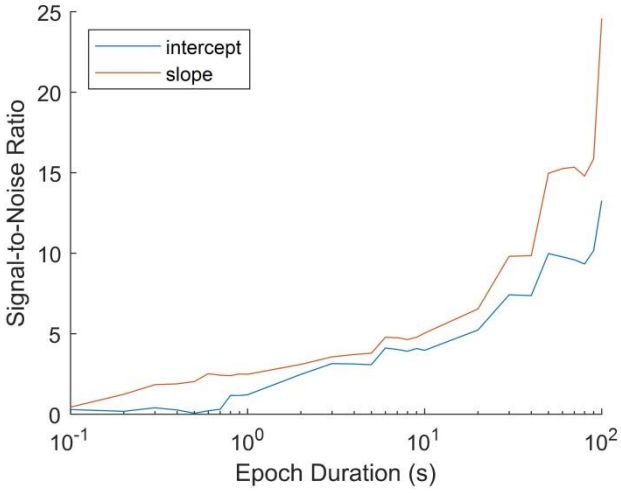

Figure 7.8. The simulated impact of epoch duration on the estimate of the 1/f curve. Fractal signal was generated using the Neuro Digital Signal Processing Toolbox (Cole et al., 2019; https://github.com/neurodsp-tools/neurodsp) for epochs with a duration of 0.1 seconds to 100s (this was repeated 1000 times for each time bin). IRASA was used to convert the resulting time-series into their fractal power spectrum. The intercept and slope of the fractal curve was then estimated as described in the methods section. Signal-to-noise was calculated for each epoch duration by dividing the mean slope estimate (across 1000 repetitions) by the standard deviation across estimates. A low signal-to-noise ratio indicates that estimates were not consistent across repetitions, while a high signal-to-noise ratio indicates high consistency across repetitions. The simulation demonstrates that short epochs (<1s) produce highly unreliable estimates of the slope. Longer epochs (>30s) produce a more reliable estimate. While long epochs are infeasible in event-related designs, averaging over trials (as in the EEG analysis of Figure 4 – Figure Supplement 4) may help approximate the estimates of longer epochs.

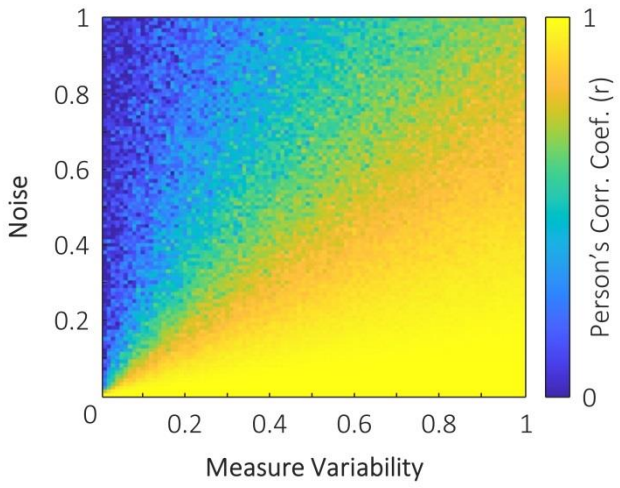

Figure 7.9. The simulated impact of measure variability and noise on the correlation between two variables. One variable with 100 samples was generated with values between zero and i, where i denotes the measure variability. When measure variability was small, the range of values across the 100 samples was small. This variable was then duplicated to provide two perfectly correlated variables with variability i. One of these variables was then distorted by noise (that is, each sample of the variable was summed with a random number between 0 and j, where j denotes the noise). These two variables were then correlated. Simulations show that when there is little variability in the measured variables (left side of plot), only a small amount of noise is required to attenuate the correlation between variables. In contrast, when there is high variability in the measured signals, substantially greater noise is required to attenuate the correlation. This may explain the small correlation observed in the visual perception task, relative to the visual retrieval and auditory perception tasks, reported in the main text. As all data was acquired within participants in the same session, we can assume that noise (physiological or non-physiological) is relatively constant across all three tasks. Measure variability however, will vary across tasks. The memory retrieval task is likely to provide highly variable stimulus representations based on memory strength and retroactive interference. The auditory perception task is likely to provide highly variable stimulus representations due to the distracting sounds of the MRI scanner. The visual perception task, however, suffers neither of these issues, and is hence likely to have less measure variability than the other two tasks. With noise constant across conditions, and measure variability smaller in the visual perception task, our simulation would predict that correlation strength would be noticeably weaker in the visual perception task.

Table 7.1. fMRI cluster-based statistics with standard thresholding compared to more conservative thresholding.

Analysis	p<.001, min 10 voxels				p<.0001, min 50 voxels			
	Cluster	p_{FWE}	*k*	*MNI*	*Cluster*	p_{FWE}	*k*	*MNI*
Visual Perception RSA	Occip.	p<.001	9911	[-30,-67,-2]	Occip.	p<.001	6072	[-30,-67,-2]
	Temp.	p=.003	64	[-48,-1,18]	*No cluster formed*			
	Cingulate	p<.001	113	[12,-16,50]	*No cluster formed*			
Audio Perception RSA	L. Temp.	p<.001	698	[-57,-37,10]	*No cluster formed*			
	R. Temp.	p<.001	859	[60,-25,10]	R. Temp.	p<.001	425	[60,-25,10]
Retrieval RSA	L. Fusi.	p<.001	472	[-45,-37,-6]	L. Fusi.	p<.001	214	[-45,-37,-6]
	R. Fusi.	p<.001	270	[27,-52,-10]	R. Fusi.	p<.001	55	[27,-52,-10]
Encoding Vis > Aud.	Occip.	p<.001	975	[42,-70,10]	R. Occip.	p<.001	367	[42,-70,10]
					L. Occip.	p<.001	322	[-24,-88,10]
	L. Temp.	p=.008	67	[-48,2,-10]	*No cluster formed*			
	R.Temp.	p=.005	72	[48,5,-14]	*No cluster formed*			
Retrieval Vis. > Aud.	L. Fusi.	p=.001	89	[-30,-46,-6]	*No cluster formed*			
	R Fusi.	p=.001	99	[21,-37,-14]	*No cluster formed*			
Retrieval Hit > Miss	Occip.	p<.001	1178	[12,-52,-14]	Occip.	p<.001	543	[12,-52,-14]
	Limbic	p<.001	1447	[-21,-16,2]	L. Limbic	p<.001	360	[-21,-16,2]
					R. Limbic	p<.001	54	[27,5,10]
Power * BOLD Hit > Miss	Occip.	p<.001	5183	[-6,-76,14]	Occip.	P<.001	715	[-6,-76,14]
	Parietal	p<.001	139	[39,-40,38]	Parietal	p<.001	51	[39,-40, 38]

APPENDIX B: SUPPLEMENTARY MATERIALS FOR INTRACRANIAL DATASET

8.1. Neocortical alpha/beta power decreases track the successful formation and retrieval of episodic memories

We investigated whether neocortical alpha/beta power decreases accompany the successful encoding and retrieval of episodic memories. Peak alpha/beta power was computed across a 1500ms window commencing at stimulus onset. As in chapter 3, the 1/f characteristic was subtracted, attenuating broadband noise. The alpha/beta power was z-transformed across the entire session for each electrode-frequency pair separately, smoothed to attenuate trial-by-trial variability in temporal/spectral responses (see methods of chapter 3), and split into "hits" and "misses" for contrasting. A group level, non-parametric permutation test revealed a significant decrease in anterior temporal lobe (ATL) alpha/beta power during encoding (p_{fdr} = 0.035, d = 0.858; 400-600ms after stimulus onset, figure 8.1) for remembered stimuli relative to forgotten stimuli. During retrieval, a group level, permutation test revealed a significant decrease in ATL alpha/beta power (800-1000ms, p_{fdr} = 0.042, d = 0.777; 1000-1200ms, p_{fdr} = 0.039, d = 0.849; figure 8.1) for remembered stimuli relative to forgotten stimuli. These results reproduce earlier findings of neocortical alpha/beta power decreases during the encoding and retrieval of human episodic memories.

8.2. Event-related potentials

Measures of low-frequency oscillatory power (<10Hz) can be distorted by event-related potentials (ERPs). To rule out the concern that the observed memory-related power effects are driven by ERPs, the ERPs themselves were examined. The data was epoched from 500ms pre-stimulus to 1000ms post-stimulus and high frequency activity was filtered out using a Butterworth low-pass filter of 20Hz. Baseline correction was computed as the difference in amplitude from a pre-stimulus window (-250 to 0ms). Trials were split based on whether the stimulus pairs were remembered or forgotten, and the data was then averaged across contacts of the same region of interest. Remembered trials were contrasted with forgotten items in a non-parametric, group-level t-test. At encoding, no memory-related difference in ERPs was observed in the ATL (p_{fdr} = 0.178) or hippocampus (p_{fdr} = 0.368).

Similarly during retrieval, no memory-related difference in ERPs was observed in the ATL (p_{fdr} = 0.291) or hippocampus (p_{fdr} = 0.279).

8.3. The influence of reference on cross-correlation results

The choice of reference can have a drastic impact on cross-regional analysis such as the cross-correlation result reported in the main text. Indeed, it is possible that as neocortical and hippocampal electrodes on the same shaft shared a common (white matter) reference, an artificial correlation between two regions may arise as a result of shared reference activity. However, such a correlation for power can only be positive and zero centred which is in stark contrast to the negative non-zero centred correlation reported in the main text. In the main text, this potential confound was tackled by contrasting hits with misses to subtract out any reference-related confound (as both conditions should fall foul to the issue) while preserving statistical power. Here, we complimented the subtraction approach by reproducing the cross-correlation analysis using different references for hippocampal and neocortical electrodes. The analytical approach is identical to that reported in the main text with one key exception: when creating hippocampal-neocortical electrode pairs, any pair from the same shaft (i.e. shared the same white matter reference) was excluded from analysis (leaving only electrode pairs with different white matter reference). Notably, one participant had only a single shaft where the hippocampus and ATL was recorded from, meaning that all hippocampal and ATL recordings in this participant shared a white matter reference. This participant was therefore excluded from this analysis. This approach yielded near identical results to those reported in the main text. ATL alpha/beta power decreases preceded hippocampal fast gamma power increases during successful memory formation (p_{fdr} = 0.026, d = 0.954), while hippocampal slow gamma power increases preceded ATL alpha/beta power decreases during successful memory retrieval (p_{fdr} = 0.035, d = 0.741). Similarly, the 2 x 2 (gamma frequency x encoding/retrieval) was replicated (p = 0.013, partial eta squared = 0.136). These findings suggest that the cross-correlation results are not due to spurious correlations owing to the choice of referencing.

8.4. The influence of interictal discharges on cross-correlation results

Notably, epileptic activity such as IEDs (Inter-Epileptical Discharges) can travel between the neocortex and the hippocampus, and these discharges can influence whether a memory is encoded/retrieved or not. While the data was cleaned of these discharges, a control analysis was run where any electrodes near the seizure foci (as described in supplementary table 4) were excluded. It is important to note that only seven subjects maintained electrodes in both the ATL and the hippocampus, and therefore were included in this control analysis.

For this approach, the memory-related alpha-gamma contrast in the ATL at encoding and at retrieval continued to demonstrate a statistically significant effect (p_{fdr} = 0.041, Cohen's d = 0.485, and p_{fdr} = 0.036, Cohen's d = 1.302). Similarly, the encoding-retrieval contrast within the ATL matched those reported in the main text (-100 to -200ms, $p_{fdr} < 0.001$, Cohen's d = 1.104; 200 to 300ms, $p_{fdr} < 0.001$, Cohen's d = 1.647). Lastly, the 2 x 2 (gamma frequency x encoding/retrieval) continued to reveal a significant interaction (p = 0.036, partial eta squared = 0.234). Together, these results analytically demonstrate that interictal discharges cannot explain the observed results.

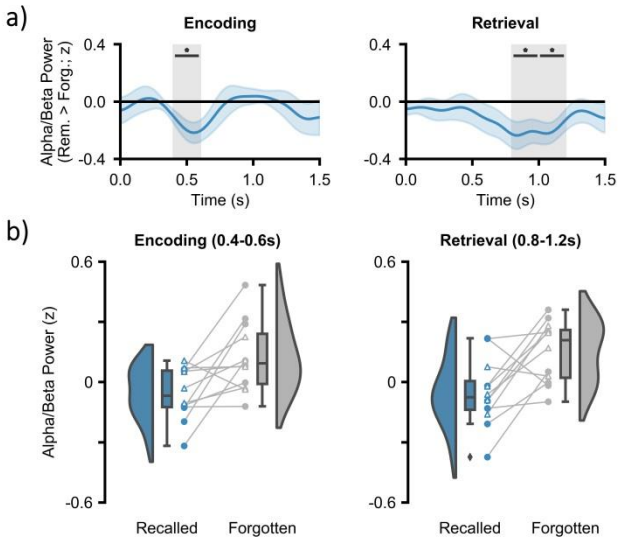

Figure 8.1. ATL alpha/beta activity during encoding and retrieval. (a) time-series of memory-related alpha/beta power for encoding and retrieval. In both cases, decreases in alpha/beta power relate to greater memory (*pfdr < 0.05). (b) raincloud plots depicting the difference in alpha/beta power between remembered and forgotten items. Coloured circles represent participants who took part in experiment 1. Uncoloured triangles represent participants who took part in experiment 2.

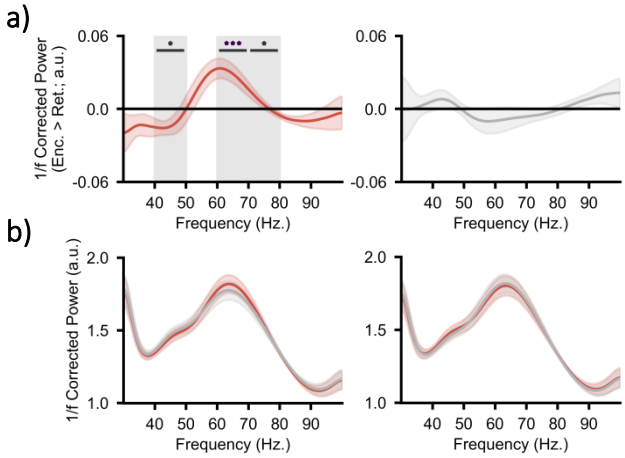

Figure 8.2. Encoding-retrieval differences in hippocampal gamma. (a) the difference in encoding hippocampal gamma power and retrieval hippocampal gamma power for remembered items (left) and forgotten items (right). (b) the power spectra for encoding and retrieval hippocampal gamma power for remembered items (left) and forgotten items (right). A clear "fast" gamma peak can be seen between 60 and 70Hz. A second notch can be seen between 40 and 50Hz, reflecting "slow" gamma activity.

Table 8.1. Resonating frequencies of each patient.

	Neocort. Alpha/Beta	Hipp. "Slow" Gamma	Hipp. "Fast" Gamma
Patient 1	12.5	39.5	64.5
Patient 2	10.0	38.0	56.0
Patient 3	11.5	49.0	63.0
Patient 4	12.0	44.5	66.0
Patient 5	14.5	44.5	67.0
Patient 6	16.0	46.5	68.0
Patient 7	10.0	45.5	70.0
Patient 8	10.5	47.5	71.0
Patient 9	10.0	40.0	56.0
Patient 10	10.5	44.5	63.5
Patient 11	10.5	47.0	60.5
Patient 12	10.0	38.5	64.5
Mean	**11.5**	**43.8**	**64.2**

Table 8.2. Number of electrodes in each region of interest per participant.

	Hippocampus	Anterior Temporal Lobe	Total
Patient 1	3	3	6
Patient 2	3	3	6
Patient 3	1	4	5
Patient 4	4	3	7
Patient 5	1	3	4
Patient 6	2	3	5
Patient 7	2	3	5
Patient 8	3	2	5
Patient 9	2	2	4
Patient 10	2	3	5
Patient 11	2	7	9
Patient 12	2	3	5
Total	**27**	**39**	**66**
Median	**2**	**3**	**5**

Table 8.3. Number of trials per condition, per participant following artefact rejection.

	Encoding			Retrieval		
	Remembered	**Forgotten**	**Total**	**Remembered**	**Forgotten**	**Total**
Patient 1	14	48	62	15	62	77
Patient 2	19	19	38	22	26	48
Patient 3	30	18	48	35	21	56
Patient 4	31	26	57	37	24	61
Patient 5	31	29	60	36	31	67
Patient 6	90	52	142	91	51	142
Patient 7	21	12	33	21	16	37
Mean	**33.7**	**29.1**	**62.9**	**36.7**	**33.0**	**69.7**
Patient 8	63	94	157	69	93	162
Patient 9	28	22	50	45	28	73
Patient 10	113	32	165	144	40	184
Patient 11	173	48	221	186	18	204
Patient 12	147	70	217	145	69	214
Mean	**104.8**	**53.2**	**162.0**	**117.8**	**49.6**	**167.4**

Table 8.4. Additional patient demographics.

Patient No.	Years of Seizures	Dominant Hand	Epileptic Foci
Patient 1	17	Right	Left hippocampus
Patient 2	3-5	Right	Bilateral medial temporal lobe
Patient 3	34	Unknown	Left frontal lobe
Patient 4	9-12	Right	Bilateral medial temporal lobe
Patient 5	8	Right	Right neocortical temporal lobe
Patient 6	10-12	Left	Right medial parietotemporal lobe
Patient 7	26	Right	Right medial temporal lobe
Patient 8	Unknown	Right	Unknown
Patient 9	26	Right	Right medial temporal lobe
Patient 10	Unknown	Right	Unknown
Patient 11	Unknown	Left	Left frontal lobe
Patient 12	22	Right	Left medial temporal lobe

APPENDIX C: SUPPLEMENTARY MATERIALS FOR MEG DATASET

9.1. Summary of pre-registration

For full pre-registration, see https://osf.io/4nt23/.

Research question	Episodic memory hinges upon our ability to process incoming information and bind these details into a coherent representation of a personally-experienced event. On an oscillatory level, these processes are thought to be supported by neocortical alpha/beta desynchronisation and hippocampal theta/gamma synchronisation respectively (Hanslmayr, Staresina & Bowman, Trends in Neuroscience, 2016). Here, we ask whether the ability to recall a greater number of elements of an event is reflected in an increase neocortical alpha/beta desynchronisation at retrieval (i.e. reflecting an increase in information processing) and an increase of hippocampal theta/gamma synchronisation at encoding (i.e. reflecting an increase in representational binding).
Hypotheses	1) The 'complete' recalling of a memory will lead to greater alpha/beta (8-30Hz) power decreases during the presentation of the retrieval cue relative to the power decreases induced by the recalling of a 'partial' memory. Similarly, the 'partial' recalling of a memory will lead to greater alpha/beta (8-30Hz) power decreases during the presentation of the retrieval cue relative to the power decreases observed during unsuccessful retrieval. 2) The 'complete' recalling of a memory will be reflected in greater theta/gamma (2-7Hz/30-100Hz) power increases and phase-amplitude coupling during mental imagery relative to the same changes induced by the recalling of a 'partial' memory. Similarly, the 'partial' recalling of a memory will be reflected in greater theta/gamma (2-7Hz/40-100Hz) power increases and phase-amplitude coupling during mental imagery relative to the same changes induced by the unsuccessful encoding of the memory.
Data collection procedures	Participants will be recruited through the University of Birmingham Research Participation Scheme and advertisements disseminated across the university via e-mail. Participants will receive financial compensation for their time (£7.50 per hour) or course credit (1 credit per hour). Participants must be between 18 and 35 years of age. Participants must not suffer any neurological illness or engaged in recent recreational drug use (>1 source of caffeine in the last hour, >3 units of alcohol in the last 24 hours, no other recreational drug use in the last 24 hours). Participants must be safe to enter an MRI scanner and MEG suite.
Sample size	24 human participants. The sample size is representative of the number of participants included in similar studies.
Stopping rule	Data collection will cease once 24 datasets have been collected that meet the "data quality check" described in the data collection procedures subsection.
Manipulated variables	We manipulate no variables. Rather, we will split the data based on observed responses (see 'measured variables').
Measured variables	We will measure behavioural performance and ongoing electrophysiological activity with magnetoencephalography (MEG). Behavioural performance on each trial will be classed as "hit" (where two aspects of the memory are recalled following the cue), "miss" (where no aspects of the memory are recalled following

	the cue), and "partial" (where one element of the memory is recalled following the cue). Any trials were participants report that they guessed their response will be marked as a miss.
Indices	Behavioural performance will be mean-averaged for each condition (hit vs. partial vs. miss) within participants to provide a measure of mean memory performance for each condition. Oscillatory power and phase-amplitude coupling will be mean-averaged across each condition (hit vs. partial vs. miss) separately prior to contrasts.
Study type	Experiment - A researcher randomly assigns treatments to study subjects, this includes field or lab experiments. This is also known as an intervention experiment and includes randomized controlled trials.
Blinding	No blinding is involved in this study.
Study design	We have a within-subjects design with 3 (hit vs. partial vs. miss) levels. For statistical analysis, the three conditions will be contrasted in a univariate repeated measures ANOVA, with three follow-up repeated measures t-tests (hit > partial; hit > miss; partial > miss).
Randomisation	Participants will be shown pseudo-randomised object-feature-scene conjunctions. The conjunctions will be randomised such that every permutation of subcategory combination (animate vs. inanimate; polka dot vs. chequered; indoor vs. outdoor) occurs equally often.
Statistical models	All contrasts of oscillatory power and phase-amplitude coupling will be assessed using a repeated measures ANOVA. In the repeated measures ANOVA, the measured categorical variable will be “memory” (hit vs. partial vs. miss) and the dependent variable will be oscillatory power/phase-amplitude coupling. Oscillatory power contrasts will be restricted to four frequency bands: theta (2-7Hz), alpha/beta (8-30Hz), “slow” gamma (30-50Hz), and “fast” gamma (60-100Hz). Contrasts will be restricted to a neocortical and medial temporal ROI. Contrasts will be restricted to 500-2500ms post-stimulus at encoding and retrieval. The alpha/beta band will only be analysed in the neocortical ROI, while only the theta and gamma bands will be analysed in the medial temporal ROI. Phase-amplitude coupling contrasts will use the “peak” theta phase (as defined by the low-frequency peak in the medial temporal power spectrum) and power in the gamma frequency band (30-100Hz). Contrasts will be restricted to the medial temporal lobe. Contrasts will be restricted to 500-2500ms post-stimulus at encoding and retrieval.
Transformations	Behavioural performance on each trial will be coded as "hit", "miss", and "partial". MEG data will be z-transformed by first mean-averaging across each epoch, and then calculating the mean and standard deviation of each channel-frequency pair across trials. MEG data will be transferred from sensor level to source space using a linearly-constrained minimum variance (LCMV) beamformer.
Inference criteria	We will use the standard $p < 0.05$ criteria for determining whether the ANOVAs reveal any differences between conditions.
Data exclusion	1) Participants with fewer than 15 hits, 15 partials and 15 misses in each condition will be excluded from further analysis. 2) Participants with "noisy" MEG data that leads to severe trial rejection (>50%)

	will be excluded from the sample. 3) Participants who move their heads more than 2 standard deviations above the mean will be excluded from the sample.
Missing data	Participants who failed to complete the experiment will be excluded from all analysis.

9.2. Deviations from protocol

Research question	None
Hypotheses	The third hypothesis will be addressed in a separate publication.
Data collection procedures	None
Sample size	Substantially more participants met the criteria for exclusion than expected. This was primarily due to underestimating the memory performance of the participants (n=6 excluded due to extreme memory performance). Due to time and financial constraints, we were unable to gather additional participants to reach the target sample size.
Stopping rule	None
Manipulated variables	None
Measured variables	None
Indices	None
Study type	None
Blinding	None
Study design	None
Randomisation	None
Statistical models	The original analysis approach involved an ANOVA and three follow-up t-tests. Statistically speaking, this is a suboptimal approach to addressing our pre-registered hypotheses. As we had hypothesised a linear relationship between the number of items recalled and spectral power/phase-amplitude coupling, a linear regression would address this in a single test, rather than the four tests originally proposed. We elected to use the more statistical valid approach (i.e. the linear regression) as opposed to the preregistered approach as it is a more elegant approach to address the questions of interest. If one considers this change in analysis approach a “implicit multiple comparison” (i.e. there have been two statistical tests [the ANOVA and the regression] rather than a single statistical test [i.e. the regression]), this can be addressed by correcting the Bonferroni-correcting the alpha threshold. This would change the statistical threshold from $\alpha = 0.05$ (for one comparison) to $\alpha = 0.025$ (for two comparisons). Such a change in statistical thresholding does not impact the interpretation of the results. The original analysis approach involved going straight into source space to analyse spectral power. In the main text, however, we first analysed the data on sensor

	level to provide a more transparent view of the data. We then reconstructed the observed effects on source level to get an idea of the origin of the effect. Indeed, this proved important as, had we used the original approach, we would have missed the alpha/beta power increase observed during the binding window as the effect was localised to regions outside of the sensory neocortex. The perceptual and retrieval effects produce equivalent results using the preregistered approach (perception: $p = 0.016$; retrieval: $p = 0.053$).
Transformations	None
Inference criteria	None
Data exclusion	None
Missing data	None

REFERENCES

Aru, J., Priesemann, V., Wibral, M., Lana, L., Pipa, G., Singer, W., & Vicente, R. (2014). Untangling cross-frequency coupling in neuroscience. *Current Opinion in Neurobiology*, *31*(September 2014), 51–61. https://doi.org/10.1101/005926

Averbeck, B. B., Latham, P. E., & Pouget, A. (2006). Neural correlations, population coding and computation. *Nature Reviews Neuroscience*, *7*(5), 358–366. https://doi.org/10.1038/nrn1888

Axmacher, N., Mormann, F., Fernández, G., Elger, C. E., & Fell, J. (2006). Memory formation by neuronal synchronization. *Brain Research Reviews*, *52*(1), 170–182. https://doi.org/10.1016/j.brainresrev.2006.01.007

Bahramisharif, A., Jensen, O., Jacobs, J., & Lisman, J. (2018). Serial representation of items during working memory maintenance at letter-selective cortical sites. *PLoS Biology*, 171660. https://doi.org/10.1101/171660

Baldassano, C., Chen, J., Zadbood, A., Pillow, J. W., Hasson, U., & Norman, K. A. (2017). Discovering event structure in continuous narrative perception and memory. *Neuron*, *95*(3), 709-721.e5. https://doi.org/10.1016/j.neuron.2017.06.041

Barker, A. T., Jalinous, R., & Freeston, I. L. (1985). Non-invasive magnetic stimulation of human motor cortex. *The Lancet*, 1106–1107. https://doi.org/10.1515/eng-2018-0022

Benjamini, Y., & Hochberg, Y. (1995). Controlling the false discovery rate: A practical and powerful approach to multiple testing. *Journal of the Royal Statistical Society. Series B (Methodological)*, *57*(1), 289–300.

Benwell, C. S. Y., London, R. E., Tagliabue, C. F., Veniero, D., Gross, J., Keitel, C., & Thut, G. (2018). Frequency and power of human alpha oscillations drift systematically and independently with time-on-task. *BioRxiv*, 1–34. https://doi.org/10.1101/263103

Benwell, C. S. Y., Tagliabue, C. F., Veniero, D., Cecere, R., Savazzi, S., & Thut, G. (2017). Prestimulus EEG power predicts conscious awareness but not objective visual performance. *ENeuro*, *4*(6), ENEURO.0182-17.2017. https://doi.org/10.1523/eneuro.0182-17.2017

Berger, H., & Gloor, P. (1969). *Hans Berger on the electroencephalogram of man: The fourteen original reports on the human electroencephalogram*. Elsevier.

Bi, G., & Poo, M. (1998). Synaptic modifications in cultured hippocampal neurons: Dependence on spike timing, synaptic strength, and postsynaptic cell type. *Journal of Neuroscience*, *18*(24), 1–9. https://doi.org/10.1038/25665

Bosch, S. E., Jehee, J. F. M., Fernández, G., & Doeller, C. F. (2014). Reinstatement of associative memories in early visual cortex is signaled by the hippocampus. *Journal of Neuroscience*, *34*(22), 7493–7500. https://doi.org/10.1523/JNEUROSCI.0805-14.2014

Bouchard, M., & Quednau, S. (2000). Multichannel recursive-least-square algorithms and fast-transversal-filter algorithms for active noise control and sound reproduction systems. *IEEE Transactions on Speech and Audio Processing*, *8*(5), 606–618. https://doi.org/10.1109/89.861382

Bragin, A., Jandó, G., Nádasdy, Z., Hetke, J., Wise, K., & Buzsáki, G. (1995). Gamma (40-100 Hz) oscillation in the hippocampus of the behaving rat. *Journal of Neuroscience*, *15*(1 Pt 1), 47–60. https://doi.org/10.1523/jneurosci.4104-10.2010

Braun, V., Sokoliuk, R., & Hanslmayr, S. (2017). On the effectiveness of event-related beta tACS on episodic memory formation and motor cortex excitability. *Brain Stimulation*, *10*(5), 910–918. https://doi.org/10.1016/j.brs.2017.04.129

Burgess, A. P., & Gruzelier, J. H. (2000). Short duration power changes in the EEG during recognition memory for words and faces. *Psychophysiology*, *37*(5), 596–606. https://doi.org/10.1111/1469-8986.3750596

Burke, J. F., Long, N. M., Zaghloul, K. A., Sharan, A. D., Sperling, M. R., & Kahana, M. J. (2014). Human intracranial high-frequency activity maps episodic memory formation in space and time. *NeuroImage*, *85*, 834–843. https://doi.org/10.1016/j.neuroimage.2013.06.067

Burke, J. F., Zaghloul, K. a., Jacobs, J., Williams, R. B., Sperling, M. R., Sharan, a. D., & Kahana, M. J. (2013). Synchronous and asynchronous theta and gamma activity during episodic memory formation. *Journal of Neuroscience*, *33*(1), 292–304. https://doi.org/10.1523/JNEUROSCI.2057-12.2013

Busch, N. A., Dubois, J., & VanRullen, R. (2009). The phase of ongoing EEG oscillations predicts visual perception. *Journal of Neuroscience*, *29*(24), 7869–7876. https://doi.org/10.1523/jneurosci.0113-09.2009

Buzsáki, G., Anastassiou, C. A., & Koch, C. (2012). The origin of extracellular fields and currents-EEG, ECoG, LFP and spikes. *Nature Reviews Neuroscience*, *13*(6), 407–420. https://doi.org/10.1038/nrn3241

Buzsaki, G., & Draguhn, A. (2004). Neuronal oscillations in cortical networks. *Science*, *304*(5679), 1926–1938.

Chatila, M., Milleret, C., Buser, P., & Rougeul, A. (1992). A 10 Hz “alpha-like” rhythm in the visual cortex of the waking cat. *Electroencephalography and Clinical Neurophysiology*, *83*(3), 217–222. https://doi.org/10.1016/0013-4694(92)90147-A

Chen, Janice, Leong, Y. C., Honey, C. J., Yong, C. H., Norman, K. A., & Hasson, U. (2016). Shared memories reveal shared structure in neural activity across individuals. *Nature Neuroscience*, *advance on*(1). https://doi.org/10.1038/nn.4450

Chen, Jianjun, Zhou, C., Wu, B., Wang, Y., Li, Q., Wei, Y., … Xie, P. (2013). Left versus right repetitive transcranial magnetic stimulation in treating major depression: A meta-analysis of randomised controlled trials. *Psychiatry Research*, *210*(3), 1260–1264. https://doi.org/10.1016/j.psychres.2013.09.007

Churchland, M. M., Yu, B. M., Cunningham, J. P., Sugrue, L. P., Cohen, M. R., Corrado, G. S., … Shenoy, K. V. (2010). Stimulus onset quenches neural variability: a widespread cortical phenomenon. *Nature Neuroscience*, *13*(3), 369–378. https://doi.org/10.1038/nn.2501

Clouter, A., Shapiro, K. L., & Hanslmayr, S. (2017). Theta phase synchronization is the glue that binds human associative memory. *Current Biology*, 1–6. https://doi.org/10.1016/j.cub.2017.09.001

Cohen, J. (1988). *Statistical power analysis for the behavioral sciences*. New York, NY: Routledge Academic.

Cohen, M. R., & Kohn, A. (2011). Measuring and interpreting neuronal correlations. *Nature Neuroscience*, *14*(7), 811–819. https://doi.org/10.1038/nn.2842

Colgin, L. L. (2015a). Do slow and fast gamma rhythms correspond to distinct functional states in the hippocampal network? *Brain Research*, *1621*, 309–315. https://doi.org/10.1016/j.brainres.2015.01.005

Colgin, L. L. (2015b). Theta-gamma coupling in the entorhinal-hippocampal system. *Current Opinion in Neurobiology*, *31*, 45–50. https://doi.org/10.1016/j.conb.2014.08.001

Colgin, L. L. (2016). Rhythms of the hippocampal network. *Nature Reviews Neuroscience*, *17*(4), 239–249. https://doi.org/10.1038/nrn.2016.21

Colgin, L. L., Denninger, T., Fyhn, M., Hafting, T., Bonnevie, T., Jensen, O., … Moser, E. I. (2009). Frequency of gamma oscillations routes flow of information in the hippocampus. *Nature*, *462*(7271), 353–357. https://doi.org/10.1038/nature08573

Colgin, L. L., & Moser, E. I. (2010). Gamma oscillations in the hippocampus. *Physiology*, *25*(5), 319–329. https://doi.org/10.1152/physiol.00021.2010

Conway, M. A. (2009). Episodic memories. *Neuropsychologia*, *47*(11), 2305–2313. https://doi.org/10.1016/j.neuropsychologia.2009.02.003

Crone, N., Miglioretti, D. L., Gordon, B., Sieracki, J. M., Wilson, M. T., Uematsu, S., & Lesser, R. P. (1998). Functional mapping of human sensorimotor cortex with electrocorticographic spectral analysis. I. Alpha and beta event- related desynchronization. *Brain*, *121*(12), 2271–2299. https://doi.org/10.1093/brain/121.12.2271

Cui, Y., Liu, L. D., McFarland, J. M., Pack, C. C., & Butts, D. A. (2016). Inferring cortical variability from local field potentials. *Journal of Neuroscience*, *36*(14), 4121–4135. https://doi.org/10.1523/jneurosci.2502-15.2016

Daniel, A. J., Smith, J. A., Spencer, G. S., Jorge, J., Bowtell, R., & Mullinger, K. J. (2019). Exploring the relative efficacy of motion artefact correction techniques for EEG data acquired during simultaneous fMRI. *Human Brain Mapping*, *40*(2), 578–596. https://doi.org/10.1002/hbm.24396

Davachi, L. (2006). Item, context and relational episodic encoding in humans. *Current Opinion in Neurobiology*, *16*(6), 693–700. https://doi.org/10.1016/j.conb.2006.10.012

De Almeida, L., Idiart, M., & Lisman, J. E. (2007). Memory retrieval time and memory capacity of the CA3 network: Role of gamma frequency oscillations. *Learning and Memory*, *14*(11), 795–806. https://doi.org/10.1101/lm.730207

Dijkstra, N., Bosch, S. E., & van Gerven, M. A. J. (2019). Shared neural mechanisms of visual perception and imagery. *Trends in Cognitive Sciences*, *23*(5), 423–434. https://doi.org/10.1016/j.tics.2019.02.004

Dujardin, K., Bourriez, J. L., & Guieu, J. D. (1994). Event-Related Desynchronization (ERD) patterns during verbal memory tasks: effect of age. *International Journal of Psychophysiology*, *16*(1), 17–27. https://doi.org/10.1016/0167-8760(94)90038-8

Duvernoy, H. M. (2005). *The Human Hippocampus: Functional Anatomy, Vascularization, and Serial Sections with MRI*. New York: Springer.

Eklund, A., Nichols, T. E., & Knutsson, H. (2016). Cluster failure: Why fMRI inferences for spatial extent have inflated false-positive rates. *Proceedings of the National Academy of Sciences*, *113*(28), 7900–7905. https://doi.org/10.1073/pnas.1602413113

Fell, J., Ludowig, E., Rosburg, T., Axmacher, N., & Elger, C. E. (2008). Phase-locking within human mediotemporal lobe

predicts memory formation. *NeuroImage*, *43*(2), 410–419. https://doi.org/10.1016/j.neuroimage.2008.07.021

Fellner, M.-C., Bäuml, K.-H. T., & Hanslmayr, S. (2013). Brain oscillatory subsequent memory effects differ in power and long-range synchronization between semantic and survival processing. *NeuroImage*, *79*, 361–370. https://doi.org/10.1016/j.neuroimage.2013.04.121

Fellner, M.-C., Gollwitzer, S., Rampp, S., Kreiselmeyr, G., Bush, D., Diehl, B., … Hanslmayr, S. (2019). Spectral fingerprints or spectral tilt? Evidence for distinct oscillatory signatures of memory formation. *PLOS Biology*, *17*(7), e3000403. https://doi.org/10.1371/journal.pbio.3000403

Fellner, M.-C., Volberg, G., Mullinger, K. J., Goldhacker, M., Wimber, M., Greenlee, M. W., & Hanslmayr, S. (2016). Spurious correlations in simultaneous EEG-fMRI driven by in-scanner movement. *NeuroImage*, *133*(March), 354–366. https://doi.org/10.1016/j.neuroimage.2016.03.031

Freyer, F., Aquino, K., Robinson, P. A., Ritter, P., & Breakspear, M. (2009). Bistability and non-gaussian fluctuations in spontaneous cortical activity. *Journal of Neuroscience*, *29*(26), 8512–8524. https://doi.org/10.1523/jneurosci.0754-09.2009

Friedman, D., & Johnson, R. (2000). Event-related potential (ERP) studies of memory encoding and retrieval: A selective review. *Microscopy Research and Technique*, *51*, 6–28. https://doi.org/10.1002/1097-0029(20001001)51

Fries, P. (2015). Rhythms for cognition: Communication through coherence. *Neuron*, *88*(1), 220–235. https://doi.org/10.1016/j.neuron.2015.09.034

Gagnon, G., Schneider, C., Grondin, S., & Blanchet, S. (2011). Enhancement of episodic memory in young and healthy adults: A paired-pulse TMS study on encoding and retrieval performance. *Neuroscience Letters*, *488*(2), 138–142. https://doi.org/10.1016/j.neulet.2010.11.016

Goard, M., & Dan, Y. (2009). Basal forebrain activation enhances cortical coding of natural scenes. *Nature Neuroscience*, *12*(11), 1444–1449. https://doi.org/10.1038/nn.2402

Green, D. M., & Swets, J. A. (1966). *Signal detection theory and psychophysics*. New York: Wiley.

Greenberg, J. A., Burke, J. F., Haque, R., Kahana, M. J., & Zaghloul, K. A. (2015). Decreases in theta and increases in high frequency activity underlie associative memory encoding. *NeuroImage*, *114*, 257–263. https://doi.org/10.1016/j.neuroimage.2015.03.077

Griffiths, B. J., & Fuentemilla, L. (2019). Event conjunction: How the hippocampus integrates episodic memories across event boundaries. *Hippocampus*, 1–15. https://doi.org/10.1002/hipo.23161

Griffiths, B. J., Mazaheri, A., Debener, S., & Hanslmayr, S. (2016). Brain oscillations track the formation of episodic memories in the real world. *NeuroImage*, *143*, 256–266. https://doi.org/10.1101/042929

Griffiths, B. J., Parish, G., Roux, F., Michelmann, S., Plas, M. Van Der, Kolibius, D., … Hanslmayr, S. (2019). Directional coupling of slow and fast hippocampal gamma with neocortical alpha / beta oscillations in human episodic memory. *Proceedings of the National Academy of Sciences*, 1–9. https://doi.org/10.1073/pnas.1914180116

Grossman, N., Bono, D., Dedic, N., Kodandaramaiah, S. B., Rudenko, A., Suk, H. J., … Boyden, E. S. (2017). Noninvasive Deep Brain Stimulation via Temporally Interfering Electric Fields. *Cell*, *169*(6), 1029-1041.e16. https://doi.org/10.1016/j.cell.2017.05.024

Guderian, S., Schott, B. H., Richardson-Klavehn, a., & Duzel, E. (2009). Medial temporal theta state before an event predicts episodic encoding success in humans. *Proceedings of the National Academy of Sciences*, *106*(13), 5365–5370. https://doi.org/10.1073/pnas.0900289106

Haegens, S., Nacher, V., Luna, R., Romo, R., & Jensen, O. (2011). α-Oscillations in the monkey sensorimotor network influence discrimination performance by rhythmical inhibition of neuronal spiking. *Proceedings of the National Academy of Sciences*, *108*(48), 19377–19382. https://doi.org/10.1073/pnas.1117190108

Haller, M., Donoghue, T., Peterson, E., Varma, P., Sebastian, P., Gao, R., … Voytek, B. (2018). Parameterizing neural power spectra. *BioRxiv*, 299859. https://doi.org/10.1101/299859

Hanslmayr, S., Aslan, A., Staudigl, T., Klimesch, W., Herrmann, C. S., & Bäuml, K. H. (2007). Prestimulus oscillations predict visual perception performance between and within subjects. *NeuroImage*, *37*(4), 1465–1473. https://doi.org/10.1016/j.neuroimage.2007.07.011

Hanslmayr, S., Axmacher, N., & Inman, C. S. (2019). Modulating Human Memory via Entrainment of Brain Oscillations. *Trends in Neurosciences*, *42*(7), 485–499. https://doi.org/10.1016/j.tins.2019.04.004

Hanslmayr, S., Matuschek, J., & Fellner, M.-C. (2014). Entrainment of prefrontal beta oscillations induces an endogenous echo and impairs memory formation. *Current Biology*, *24*(8), 904–909. https://doi.org/10.1016/j.cub.2014.03.007

Hanslmayr, S., Spitzer, B., & Bauml, K.-H. (2009). Brain oscillations dissociate between semantic and nonsemantic encoding

of episodic memories. *Cerebral Cortex*, *19*(7), 1631–1640. https://doi.org/10.1093/cercor/bhn197

Hanslmayr, S., Staresina, B. P., & Bowman, H. (2016). Oscillations and episodic memory – Addressing the synchronization/desynchronization conundrum. *Trends in Neurosciences*, *39*(1), 16–25. https://doi.org/10.1016/j.tins.2015.11.004

Hanslmayr, S., & Staudigl, T. (2014). How brain oscillations form memories--a processing based perspective on oscillatory subsequent memory effects. *NeuroImage*, *85 Pt 2*, 648–655. https://doi.org/10.1016/j.neuroimage.2013.05.121

Hanslmayr, S., Staudigl, T., & Fellner, M.-C. (2012). Oscillatory power decreases and long-term memory: the information via desynchronization hypothesis. *Frontiers in Human Neuroscience*, *6*(74), 1–12. https://doi.org/10.3389/fnhum.2012.00074

Hanslmayr, S., Volberg, G., Wimber, M., Raabe, M., Greenlee, M. W., & Bauml, K.-H. T. (2011). The relationship between brain oscillations and BOLD signal during memory formation: A combined EEG-fMRI study. *Journal of Neuroscience*, *31*(44), 15674–15680. https://doi.org/10.1523/JNEUROSCI.3140-11.2011

Harris, K. D., & Thiele, A. (2011). Cortical state and attention. *Nature Reviews Neuroscience*, *12*(9), 509–523. https://doi.org/10.1038/nrn3084

Hasselmo, M. E. (2005). What is the function of hippocampal theta rhythm? - Linking behavioral data to phasic properties of field potential and unit recording data. *Hippocampus*, *15*(7), 936–949. https://doi.org/10.1002/hipo.20116

Hasselmo, M. E., Bodelón, C., & Wyble, B. P. (2002). A proposed function for hippocampal theta rhythm: Separate phases of encoding and retrieval enhance reversal of prior learning. *Neural Computation*, *14*(4), 793–817. https://doi.org/10.1162/089976602317318965

Haynes, J. D. (2015). A primer on pattern-based approaches to fMRI: Principles, pitfalls, and perspectives. *Neuron*, *87*(2), 257–270. https://doi.org/10.1016/j.neuron.2015.05.025

Herrmann, C. S., Rach, S., Neuling, T., & Strüber, D. (2013). Transcranial alternating current stimulation: A review of the underlying mechanisms and modulation of cognitive processes. *Frontiers in Human Neuroscience*, *7*(MAY), 1–13. https://doi.org/10.3389/fnhum.2013.00279

Heusser, A. C., Poeppel, D., Ezzyat, Y., & Davachi, L. (2016). Episodic sequence memory is supported by a theta-gamma phase code. *Nature Neuroscience*, *19*(August). https://doi.org/10.1038/nn.4374

Holroyd, C. B., Ribas-Fernandes, J. J. F., Shahnazian, D., Silvetti, M., & Verguts, T. (2018). Human midcingulate cortex encodes distributed representations of task progress. *Proceedings of the National Academy of Sciences of the United States of America*, *115*(25), 6398–6403. https://doi.org/10.1073/pnas.1803650115

Huerta, P. T., & Lisman, J. E. (1995). Bidirectional synaptic plasticity induced by a single burst during cholinergic theta oscillation in CA1 in vitro. *Neuron*, *15*(5), 1053–1063. https://doi.org/10.1016/0896-6273(95)90094-2

Hyman, J. M., Wyble, B. P., Goyal, V., Rossi, C. A., & Hasselmo, M. E. (2003). Stimulation in hippocampal region CA1 in behaving rats yields long-term potentiation when delivered to the peak of theta and long-term depression when delivered to the trough. *Journal of Neuroscience*, *23*(37), 11725–11731. https://doi.org/23/37/11725 [pii]

Iannetti, G. D., Niazy, R. K., Wise, R. G., Jezzard, P., Brooks, J. C. W., Zambreanu, L., … Tracey, I. (2005). Simultaneous recording of laser-evoked brain potentials and continuous, high-field functional magnetic resonance imaging in humans. *NeuroImage*, *28*(3), 708–719. https://doi.org/10.1016/j.neuroimage.2005.06.060

Iemi, L., Chaumon, M., Crouzet, S. M., & Busch, N. A. (2017). Spontaneous neural oscillations bias perception by modulating baseline excitability. *The Journal of Neuroscience*, *37*(4), 807–819. https://doi.org/10.1523/jneurosci.1432-16.2017

JASP-Team. (2018). JASP (Version 0.9). Cambridge University Press.

Jensen, O., & Mazaheri, A. (2010). Shaping functional architecture by oscillatory alpha activity: Gating by inhibition. *Frontiers in Human Neuroscience*, *4*(November), 1–8. https://doi.org/10.3389/fnhum.2010.00186

Johnson, J. D., McDuff, S. G. R., Rugg, M. D., & Norman, K. A. (2009). Recollection, familiarity, and cortical reinstatement: A multivoxel pattern analysis. *Neuron*, *63*(5), 697–708. https://doi.org/10.1016/j.neuron.2009.08.011

Johnson, J. D., & Rugg, M. D. (2007). Recollection and the reinstatement of encoding-related cortical activity. *Cerebral Cortex*, *17*(11), 2507–2515. https://doi.org/10.1093/cercor/bhl156

Jorge, J., Grouiller, F., Gruetter, R., van der Zwaag, W., & Figueiredo, P. (2015). Towards high-quality simultaneous EEG-fMRI at 7T: Detection and reduction of EEG artifacts due to head motion. *NeuroImage*, *120*, 143–153. https://doi.org/10.1016/j.neuroimage.2015.07.020

Jutras, M. J., Fries, P., & Buffalo, E. A. (2009). Gamma-Band Synchronization in the Macaque Hippocampus and Memory Formation. *Journal of Neuroscience*, *29*(40), 12521–12531. https://doi.org/10.1523/JNEUROSCI.0640-09.2009

Karsen, E. F., Watts, B. V., & Holtzheimer, P. E. (2014). Review of the effectiveness of transcranial magnetic stimulation for post-traumatic stress disorder. *Brain Stimulation*, *7*(2), 151–157. https://doi.org/10.1016/j.brs.2013.10.006

Kemere, C., Carr, M. F., Karlsson, M. P., & Frank, L. M. (2013). Rapid and Continuous Modulation of Hippocampal Network State during Exploration of New Places. *PLoS ONE*, *8*(9), e73114. https://doi.org/10.1371/journal.pone.0073114

Kerrén, C., Linde-Domingo, J., Hanslmayr, S., & Wimber, M. (2018). An optimal oscillatory phase for pattern reactivation during memory retrieval. *Current Biology*, *28*(21), 3383-3392.e6. https://doi.org/10.1016/j.cub.2018.08.065

Khader, P. H., & Rösler, F. (2011). EEG power changes reflect distinct mechanisms during long-term memory retrieval. *Psychophysiology*, *48*(3), 362–369. https://doi.org/10.1111/j.1469-8986.2010.01063.x

Kim, H. (2011). Neural activity that predicts subsequent memory and forgetting: A meta-analysis of 74 fMRI studies. *NeuroImage*, *54*(3), 2446–2461. https://doi.org/10.1016/j.neuroimage.2010.09.045

Klimesch, W., Sauseng, P., & Hanslmayr, S. (2007). EEG alpha oscillations: the inhibition-timing hypothesis. *Brain Research Reviews*, *53*(1), 63–88. https://doi.org/10.1016/j.brainresrev.2006.06.003

Konkel, A., & Cohen, N. J. (2009). Relational memory and the hippocampus: Representations and methods. *Frontiers in Neuroscience*, *3*(SEP), 166–174. https://doi.org/10.3389/neuro.01.023.2009

Koster, R., Chadwick, M. J., Chen, Y., Berron, D., Banino, A., Düzel, E., … Kumaran, D. (2018). Big-loop recurrence within the hippocampal system supports integration of information across episodes. *Neuron*, *99*(6), 1342-1354.e6. https://doi.org/10.1016/j.neuron.2018.08.009

Krause, C. M., Lang, H. A., Laine, M., Helle, S. I., Kuusisto, M., & Pörn, B. (1994). Event-related desynchronization evoked by auditory stimuli. *Brain Topography*, *7*(2), 107–112.

Kriegeskorte, N., Formisano, E., Sorger, B., & Goebel, R. (2007). Individual faces elicit distinct response patterns in human anterior temporal cortex. *PNAS*, *104*(51), 20600–20605. https://doi.org/0705654104 [pii] 10.1073/pnas.0705654104 ET - 2007/12/14

Kriegeskorte, N., Simmons, W. K., Bellgowan, P. S. F., & Baker, C. I. (2009). Circular analysis in systems neuroscience: the dangers of double dipping. *Nature Neuroscience*, *12*(5), 535–540. https://doi.org/10.1167/8.6.88

Lafon, B., Henin, S., Huang, Y., Friedman, D., Melloni, L., Thesen, T., … Liu, A. A. (2017). Low frequency transcranial electrical stimulation does not entrain sleep rhythms measured by human intracranial recordings. *Nature Communications*, *8*(1), 1–14. https://doi.org/10.1038/s41467-017-01045-x

Lange, J., Oostenveld, R., & Fries, P. (2013). Reduced occipital alpha power indexes enhanced excitability rather than improved visual perception. *Journal of Neuroscience*, *33*(7), 3212–3220. https://doi.org/10.1523/jneurosci.3755-12.2013

Ledoit, O., & Wolf, M. (2004). Honey, I Shrunk the Sample Covariance Matrix. *The Journal of Portfolio Management*, *30*(4), 110–119. https://doi.org/10.3905/jpm.2004.110

Lee, M. D., & Wagenmakers, E. J. (2013). *Bayesian data analysis for cognitive science: A practical course*.

Lega, B., Germi, J., & Rugg, M. D. (2017). Modulation of oscillatory power and connectivity in the human posterior cingulate cortex supports the encoding and retrieval of episodic memories. *Journal of Cognitive Neuroscience*, *29*(8), 1415–1432. https://doi.org/10.1162/jocn

Limbach, K., & Corballis, P. M. (2016). Prestimulus alpha power influences response criterion in a detection task. *Psychophysiology*, *53*(8), 1154–1164. https://doi.org/10.1111/psyp.12666

Linde-Domingo, J., Treder, M. S., Kerrén, C., & Wimber, M. (2019). Evidence that neural information flow is reversed between object perception and object reconstruction from memory. *Nature Communications*, *10*(1). https://doi.org/10.1038/s41467-018-08080-2

Lisman, J. E., & Jensen, O. (2013). The theta-gamma neural code. *Neuron*, *77*(6), 1002–1016. https://doi.org/10.1016/j.neuron.2013.03.007

Long, N. M., & Kahana, M. J. (2015). Successful memory formation is driven by contextual encoding in the core memory network. *NeuroImage*, *119*, 332–337. https://doi.org/10.1016/j.neuroimage.2015.06.073

Lubenov, E. V., & Siapas, A. G. (2009). Hippocampal theta oscillations are travelling waves. *Nature*, *459*(7246), 534–539. https://doi.org/10.1038/nature08010

Maldjian, J. A., Laurienti, P. J., Kraft, R. A., & Burdette, J. H. (2003). An automated method for neuroanatomic and cytoarchitectonic atlas-based interrogation of fMRI data sets. *NeuroImage*, *19*(3), 1233–1239. https://doi.org/10.1016/S1053-8119(03)00169-1

Manning, J. R., Jacobs, J., Fried, I., & Kahana, M. J. (2009). Broadband shifts in local field potential power spectra are

correlated with single-neuron spiking in humans. *Journal of Neuroscience*, *29*(43), 13613–13620. https://doi.org/10.1523/JNEUROSCI.2041-09.2009

Maris, E., & Oostenveld, R. (2007). Nonparametric statistical testing of EEG- and MEG-data. *Journal of Neuroscience Methods*, *164*(1), 177–190. https://doi.org/10.1016/j.jneumeth.2007.03.024

Marr, D. (1971). Simple memory: A theory for archicortex. *Philosophical Transactions of the Royal Society B: Biological Sciences*, *262*(841), 23–81. https://doi.org/10.1098/rstb.1971.0078

Martín-Buro, M. C., Wimber, M., Henson, R. N., & Staresina, B. P. (2019). Alpha rhythms reveal when, where and how memories are retrieved. *BioRxiv*, 708602. https://doi.org/10.1101/708602

Masterton, R. A. J., Abbott, D. F., Fleming, S. W., & Jackson, G. D. (2007). Measurement and reduction of motion and ballistocardiogram artefacts from simultaneous EEG and fMRI recordings. *NeuroImage*, *37*(1), 202–211. https://doi.org/10.1016/j.neuroimage.2007.02.060

McClelland, J. L., McNaughton, B. L., & O'Reilly, R. C. (1995). Why there are complementary learning systems in the hippocampus and neocortex: Insights from the successes and failures of connectionist models of learning and memory. *Psychological Review*, *102*(3), 419–457. https://doi.org/10.1037/0033-295X.102.3.419

Meeuwissen, E. B., Takashima, A., Fernandez, G., & Jensen, O. (2011). Evidence for human Fronto-Central gamma activity during long-term memory encoding of word sequences. *PLoS ONE*, *6*(6). https://doi.org/10.1371/journal.pone.0021356

Michelmann, S., Bowman, H., & Hanslmayr, S. (2016). The temporal signature of memories: Identification of a general mechanism for dynamic memory replay in humans. *PLOS Biology*, *14*(8), e1002528. https://doi.org/10.1371/journal.pbio.1002528

Miller, K. J., Sorensen, L. B., Ojemann, J. G., & Den Nijs, M. (2009). Power-law scaling in the brain surface electric potential. *PLoS Computational Biology*, *5*(12). https://doi.org/10.1371/journal.pcbi.1000609

Mitchell, J. F., Sundberg, K. A., & Reynolds, J. H. (2009). Spatial attention decorrelates intrinsic activity fluctuations in macaque area V4. *Neuron*, *63*(6), 879–888. https://doi.org/10.1016/j.neuron.2009.09.013

Montgomery, S., & Buzsáki, G. (2007). Gamma oscillations dynamically couple hippocampal CA3 and CA1 regions during memory task performance. *Proceedings of the National Academy of Sciences*, *104*(36), 14495–14500.

Ng, B. S. W., Logothetis, N. K., & Kayser, C. (2013). EEG phase patterns reflect the selectivity of neural firing. *Cerebral Cortex*, *23*(2), 389–398. https://doi.org/10.1093/cercor/bhs031

Niazy, R. K., Beckmann, C. F., Iannetti, G. D., Brady, J. M., & Smith, S. M. (2005). Removal of FMRI environment artifacts from EEG data using optimal basis sets. *NeuroImage*, *28*(3), 720–737. https://doi.org/10.1016/j.neuroimage.2005.06.067

Nili, H., Wingfield, C., Walther, A., Su, L., Marslen-Wilson, W., & Kriegeskorte, N. (2014). A toolbox for representational similarity analysis. *PLoS Computational Biology*, *10*(4). https://doi.org/10.1371/journal.pcbi.1003553

Nitsche, M. A., Cohen, L. G., Wassermann, E. M., Priori, A., Lang, N., Antal, A., … Pascual-Leone, A. (2008). Transcranial direct current stimulation: State of the art 2008. *Brain Stimulation*, *1*(3), 206–223. https://doi.org/10.1016/j.brs.2008.06.004

Noh, E., Herzmann, G., Curran, T., & De Sa, V. R. (2014). Using single-trial EEG to predict and analyze subsequent memory. *NeuroImage*, *84*, 712–723. https://doi.org/10.1016/j.neuroimage.2013.09.028

Nyberg, L., Habib, R., McIntosh, A. R., & Tulving, E. (2000). Reactivation of encoding-related brain activity during memory retrieval. *Proceedings of the National Academy of Sciences*, *97*, 11120–11124. https://doi.org/10.1073/pnas.97.20.11120

Nyberg, L., Petersson, K. M., Nilsson, L. G., Sandblom, J., Åberg, C., & Ingvar, M. (2001). Reactivation of motor brain areas during explicit memory for actions. *NeuroImage*, *14*(2), 521–528. https://doi.org/10.1006/nimg.2001.0801

Nyhus, E., & Curran, T. (2010). Functional role of gamma and theta oscillations in episodic memory. *Neuroscience and Biobehavioral Reviews*, *34*(7), 1023–1035. https://doi.org/10.1016/j.neubiorev.2009.12.014

Obleser, J., & Weisz, N. (2012). Suppressed alpha oscillations predict intelligibility of speech and its acoustic details. *Cerebral Cortex*, *22*(11), 2466–2477. https://doi.org/10.1093/cercor/bhr325

Olsen, R. K., Moses, S. N., Riggs, L., & Ryan, J. D. (2012). The hippocampus supports multiple cognitive processes through relational binding and comparison. *Frontiers in Human Neuroscience*, *6*(May), 146. https://doi.org/10.3389/fnhum.2012.00146

Oostenveld, R., Fries, P., Maris, E., & Schoffelen, J.-M. (2011). FieldTrip: Open source software for advanced analysis of MEG, EEG, and invasive electrophysiological data. *Computational Intelligence and Neuroscience*, *2011*, 1–9.

https://doi.org/10.1155/2011/156869

Osipova, D., Takashima, A., Oostenveld, R., Fernandez, G., Maris, E., & Jensen, O. (2006). Theta and gamma oscillations predict encoding and retrieval of declarative memory. *Journal of Neuroscience*, *26*(28), 7523–7531. https://doi.org/10.1523/JNEUROSCI.1948-06.2006

Parish, G., Hanslmayr, S., & Bowman, H. (2018). The sync/desync model: How a synchronized hippocampus and a desynchronized neocortex code memories. *Journal of Neuroscience*, *38*(14), 3428–3440. https://doi.org/10.1523/JNEUROSCI.2561-17.2018

Pavlides, C., Greenstein, Y. J., Grudman, M., & Winson, J. (1988). Long-term potentiation in the dentate gyrus is induced preferentially on the positive phase of θ-rhythm. *Brain Research*, *439*(1–2), 383–387. https://doi.org/10.1016/0006-8993(88)91499-0

Pfurtscheller, G., Neuper, C., & Mohl, W. (1994). Event-related desynchronization (ERD) during visual processing. *International Journal of Psychophysiology*, *16*(2–3), 147–153. https://doi.org/10.1016/0167-8760(89)90041-X

Pfurtscheller, G., Stancák, A., & Neuper, C. (1996). Event-related synchronization (ERS) in the alpha band - An electrophysiological correlate of cortical idling: A review. *International Journal of Psychophysiology*, *24*(1–2), 39–46. https://doi.org/10.1016/S0167-8760(96)00066-9

Popov, T., & Szyszka, P. (2019). Alpha oscillations govern interhemispheric spike timing coordination in the honey bee brain. *BioRxiv*, 1–10. https://doi.org/10.1101/628867

Poppenk, J., & Moscovitch, M. (2011). A hippocampal marker of recollection memory ability among healthy young adults: Contributions of posterior and anterior segments. *Neuron*, *72*(6), 931–937. https://doi.org/10.1016/j.neuron.2011.10.014

Poulet, J. F. A., & Petersen, C. C. H. (2008). Internal brain state regulates membrane potential synchrony in barrel cortex of behaving mice. *Nature*, *454*(7206), 881–885. https://doi.org/10.1038/nature07150

Rice, G. E., Ralph, M. A. L., & Hoffman, P. (2015). The roles of left versus right anterior temporal lobes in conceptual knowledge: An ALE meta-analysis of 97 functional neuroimaging studies. *Cerebral Cortex*, *25*(11), 4374–4391. https://doi.org/10.1093/cercor/bhv024

Rolls, E. T. (2007). An attractor network in the hippocampus. *Learning & Memory*, *14*(11), 714–731. https://doi.org/10.1101/lm.631207.lesions.

Rolls, E. T. (2013). The mechanisms for pattern completion and pattern separation in the hippocampus. *Frontiers in Systems Neuroscience*, *7*(October), 1–21. https://doi.org/10.3389/fnsys.2013.00074

Rugg, M. D., Johnson, J. D., Park, H., & Uncapher, M. R. (2008). Encoding-retrieval overlap in human episodic memory: A functional neuroimaging perspective. *Progress in Brain Research*, *169*, 339–352. https://doi.org/10.1016/S0079-6123(07)00021-0

Rugg, M. D., & Vilberg, K. L. (2014). Brain networks underlying episodic memory retrieval. *Current Opinion in Neurobiology*, *23*(2), 255–260. https://doi.org/10.1016/j.conb.2012.11.005.Brain

Ruzich, E., Crespo-García, M., Dalal, S. S., & Schneiderman, J. F. (2019). Characterizing hippocampal dynamics with MEG: A systematic review and evidence-based guidelines. *Human Brain Mapping*, *40*(4), 1353–1375. https://doi.org/10.1002/hbm.24445

Samaha, J., Iemi, L., & Postle, B. R. (2017). Prestimulus alpha-band power biases visual discrimination confidence, but not accuracy. *Consciousness and Cognition*, *54*, 47–55. https://doi.org/10.1016/j.concog.2017.02.005

Santarnecchi, E., Brem, A. K., Levenbaum, E., Thompson, T., Kadosh, R. C., & Pascual-Leone, A. (2015). Enhancing cognition using transcranial electrical stimulation. *Current Opinion in Behavioral Sciences*, *4*, 171–178. https://doi.org/10.1016/j.cobeha.2015.06.003

Schapiro, A. C., Turk-Browne, N. B., Botvinick, M. M., & Norman, K. A. (2017). Complementary learning systems within the hippocampus: A neural network modeling approach to recomciling episodic memory with statistical learning. *Philosophical Transactions of the Royal Society B*, *372*. https://doi.org/10.1098/rstb.2016.0049

Sederberg, P. B., Schulze-Bonhage, A., Madsen, J. R., Bromfield, E. B., McCarthy, D. C., Brandt, A., … Kahana, M. J. (2007). Hippocampal and neocortical gamma oscillations predict memory formation in humans. *Cerebral Cortex*, *17*(5), 1190–1196. https://doi.org/10.1093/cercor/bhl030

Shannon, C. E., & Weaver, W. (1949). *A mathematical theory of communication*. Urbana, IL: University of Illinois Press.

Spitzer, B., Hanslmayr, S., Opitz, B., Mecklinger, A., & Bäuml, K.-H. (2009). Oscillatory correlates of retrieval-induced forgetting in recognition memory. *Journal of Cognitive Neuroscience*, *21*(5), 976–990. https://doi.org/10.1162/jocn.2009.21072

Staresina, B. P., Henson, R. N. A., Kriegeskorte, N., & Alink, A. (2012). Episodic reinstatement in the medial temporal lobe. *Journal of Neuroscience*, *32*(50), 18150–18156. https://doi.org/10.1523/JNEUROSCI.4156-12.2012

Staresina, B. P., Michelmann, S., Bonnefond, M., Jensen, O., Axmacher, N., & Fell, J. (2016). Hippocampal pattern completion is linked to gamma power increases and alpha power decreases during recollection. *ELife*, *5*(AUGUST), 1–18. https://doi.org/10.7554/eLife.17397.001

Staudigl, T., & Hanslmayr, S. (2013). Theta oscillations at encoding mediate the context-dependent nature of human episodic memory. *Current Biology*, *23*(12), 1101–1106.

Tamura, Y., Hoshiyama, M., Nakata, H., Hiroe, N., Inui, K., Kaneoke, Y., … Kakigi, R. (2005). Functional relationship between human rolandic oscillations and motor cortical excitability: An MEG study. *European Journal of Neuroscience*, *21*(9), 2555–2562. https://doi.org/10.1111/j.1460-9568.2005.04096.x

Teyler, T. J., & Rudy, J. W. (2007). The hippocampal indexing theory and episodic memory: Updating the index. *Hippocampus*, *17*, 1158–1169. https://doi.org/10.1002/hipo

Tort, A. B. L., Komorowski, R., Eichenbaum, H., & Kopell, N. (2010). Measuring phase-amplitude coupling between neuronal oscillations of different frequencies. *Journal of Neurophysiology*, *104*(2), 1195–1210. https://doi.org/10.1152/jn.00106.2010

Tort, A. B. L., Komorowski, R. W., Manns, J. R., Kopell, N. J., & Eichenbaum, H. (2009). Theta-gamma coupling increases during the learning of item-context associations. *Proceedings of the National Academy of Sciences*, *106*(49), 20942–20947. https://doi.org/10.1073/pnas.0911331106

Tuladhar, A. M., Ter Huurne, N., Schoffelen, J. M., Maris, E., Oostenveld, R., & Jensen, O. (2007). Parieto-occipital sources account for the increase in alpha activity with working memory load. *Human Brain Mapping*, *28*(8), 785–792. https://doi.org/10.1002/hbm.20306

Tulving, E. (1972). Episodic and semantic memory. In *Organization of Memory* (pp. 381–403).

Tulving, E. (2002). Episodic memory: from mind to brain. *Annual Review of Psychology*, *53*, 1–25. https://doi.org/10.1146/annurev.psych.53.100901.135114

Tulving, E., & Thomson, D. (1973). Encoding specificity and retrieval processes in episodic memory. *Psychological Review*, *80*(5), 352–373. https://doi.org/10.1037/h0020071

van Dijk, H., Schoffelen, J.-M., Oostenveld, R., & Jensen, O. (2008). Prestimulus oscillatory activity in the alpha band predicts visual discrimination ability. *Journal of Neuroscience*, *28*(8), 1816–1823. https://doi.org/10.1523/jneurosci.1853-07.2008

van Veen, B., van Drongelen, W., Yuchtman, M., & Suzuki, A. (1997). Localization of brain electrical activity via linearly constrained minimum variance spatial filtering. *IEEE Transactions on Biomedical Engineering*, *44*(9), 867–880. https://doi.org/10.1109/10.623056

Visser, M., Jefferies, E., & Lambon Ralph, M. (2010). Semantic processing in the anterior temporal lobes: a meta-analysis of the functional neuroimaging literature. *Journal of Cognitive Neuroscience*, *22*(6), 1083–1094. https://doi.org/10.1162/jocn.2009.21309

Waldhauser, G. T., Braun, V., & Hanslmayr, S. (2016). Episodic memory retrieval functionally relies on very rapid reactivation of sensory information. *Journal of Neuroscience*, *36*(1), 251–260. https://doi.org/10.1523/JNEUROSCI.2101-15.2016

Wallenstein, G. V, Eichenbaum, H., & Hasselmo, M. E. (1998). The hippocampus as an associator of discontiguous events. *Trends in Neurosciences*, *21*(8), 317–323.

Walsh, V., & Cowey, A. (2000). Transcranial magnetic stimulation and cognitive neuroscience. *Nature Reviews Neuroscience*, *1*(1), 73–80. https://doi.org/10.1038/35036239

Walther, A., Nili, H., Ejaz, N., Alink, A., Kriegeskorte, N., & Diedrichsen, J. (2015). Reliability of dissimilarity measures for multi-voxel pattern analysis. *NeuroImage*, *137*, 188–200. https://doi.org/10.1016/j.neuroimage.2015.12.012

Weiss, S., & Rappelsberger, P. (2000). Long-range EEG synchronization during word encoding correlates with successful memory performance. *Cognitive Brain Research*, *9*(3), 299–312. https://doi.org/10.1016/S0926-6410(00)00011-2

Wen, H., & Liu, Z. (2016). Separating fractal and oscillatory components in the power spectrum of neurophysiological signal. *Brain Topography*, *29*(1), 13–26. https://doi.org/10.1007/s10548-015-0448-0

Wheeler, M. E., Petersen, S. E., & Buckner, R. L. (2000). Memory's echo: Vivid remembering reactivates sensory-specific cortex. *Proceedings of the National Academy of Sciences*, *97*(20), 11125–11129.

Whitmarsh, S., Oostenveld, R., Almeida, R., & Lundqvist, D. (2017). Metacognition of attention during tactile discrimination. *NeuroImage*, *147*(November 2016), 121–129. https://doi.org/10.1016/j.neuroimage.2016.11.070

Wianda, E., & Ross, B. (2019). The roles of alpha oscillation in working memory retention. *Brain and Behavior*, *9*(4), 1–21. https://doi.org/10.1002/brb3.1263

Wiest, M. C., & Nicolelis, M. A. L. (2003). Behavioral detection of tactile stimuli during 7-12 Hz cortical oscillations in awake rats. *Nature Neuroscience*, *6*(9), 913–914. https://doi.org/10.1038/nn1107

Woodruff, C. C., Johnson, J. D., Uncapher, M. R., & Rugg, M. D. (2005). Content-specificity of the neural correlates of recollection. *Neuropsychologia*, *43*(7), 1022–1032. https://doi.org/10.1016/j.neuropsychologia.2004.10.013

Wöstmann, M., Waschke, L., & Obleser, J. (2019). Prestimulus neural alpha power predicts confidence in discriminating identical auditory stimuli. *European Journal of Neuroscience*, *49*(1), 94–105. https://doi.org/10.1111/ejn.14226

Zhang, H., & Jacobs, J. (2015). Traveling theta waves in the human hippocampus. *Journal of Neuroscience*, *35*(36), 12477–12487. https://doi.org/10.1523/JNEUROSCI.5102-14.2015

Zion-Golumbic, E., Kutas, M., & Bentin, S. (2010). Neural dynamics associated with semantic and episodic memory for faces: evidence from multiple frequency bands. *Journal of Cognitive Neuroscience*, *22*(2), 263–277. https://doi.org/10.1162/jocn.2009.21251

Zohary, E., Shadlen, M. N., & Newsome, W. T. (1994). Correlated neuronal discharge rate and its implications for psychophysical performance. *Nature*, *370*(14), 140–143.